Technical Report Documentation Page

1. Report No.	2. Government Accession No.	3. Recipient's Catalog No.
FHWA/TX-92+1210-4		

4. Title and Subtitle	5. Report Date
BEHAVIOR OF STATICALLY LOADED PRETENSIONED CONCRETE BEAMS WITH 0.5-INCH DIAMETER DEBONDED STRANDS	January 1992
	6. Performing Organization Code
7. Author(s) Leslie G. Zumbrunnen, Bruce W. Russell, and Ned H. Burns	8. Performing Organization Report No. Research Report 1210-4
9. Performing Organization Name and Address Center for Transportation Research The University of Texas at Austin Austin, Texas 78712-1075	10. Work Unit No. (TRAIS)
	11. Contract or Grant No. Research Study 3-5-89/2-1210
12. Sponsoring Agency Name and Address Texas Department of Transportation Transportation Planning Division P. O. Box 5051 Austin, Texas 78763-5051	13. Type of Report and Period Covered Interim
	14. Sponsoring Agency Code

15. Supplementary Notes

Study conducted in cooperation with the U. S. Department of Transportation, Federal Highway Administration. Research Study Title: "Influence of Debonding of Strands on Behavior of Composite Prestressed Concrete Bridge Girders"

16. Abstract

One of the primary objectives of this research project is to develop design guidelines for the use of debonded, or blanketed, strand. The debonding of pretensioned strand is an alternative to draping strands in order to control the maximum tensile and compressive stresses in pretensioned beams. Debonding strands can simplify girder construction; draping strands is more difficult and more dangerous. Likewise, straight debonded strands enjoy economical advantages to draped strands in the total cost of girders.

Static flexural tests were performed on specimens with debonded strand. An analytical rationale, The Bond Failure Prediction Model, was used to predict cracking and subsequent bond failure for these tests. The agreement between test results and the prediction model was outstanding, demonstrating that a rational design method can be developed for beams with debonded strands. This research also shows that the currently required multiplier of 2.0 for the development length of debonded strand may be significantly reduced, or, more appropriately, the provisions for debonded strand may be changed. Conversely, some dangerous and unsafe designs may be allowed by the current code.

Beams tested in this report were I-shaped and made to resemble an AASHTO section complete with a composite deck. Altogether, ten (10) tests were performed. The beams were loaded statically in flexure until failure. For each test, two types of failure were possible, flexural failure or bond failure. Results from these tests are shown to be accurately predicted by the prediction model.

17. Key Words	18. Distribution Statement
debonded strand, blanketed strand, pretensioned, draping, tensile stresses, compressive stresses, girder, specimens, bond failure, cracking, beams, design	No restrictions. This document is available to the public through the National Technical Information Service, Springfield, Virginia 22161.

19. Security Classif. (of this report)	20. Security Classif. (of this page)	21. No. of Pages	22. Price
Unclassified	Unclassified	138	

Form DOT F 1700.7 (8-72) Reproduction of completed page authorized

BEHAVIOR OF STATICALLY LOADED PRETENSIONED CONCRETE BEAMS WITH 0.5-INCH DIAMETER DEBONDED STRANDS

by

Leslie G. Zumbrunnen
Bruce W. Russell
Ned H. Burns

Research Report Number 1210-4

Research Project 3-5-89/2-1210

Influence of Debonding of Strands on Behavior of Composite Prestressed Concrete Bridge Girders

conducted for

Texas Department of Transportation

in cooperation with the

U. S. Department of Transportation
Federal Highway Administration

by the

CENTER FOR TRANSPORTATION RESEARCH
Bureau of Engineering Research
THE UNIVERSITY OF TEXAS AT AUSTIN

January 1992

NOT INTENDED FOR CONSTRUCTION, PERMIT, OR BIDDING PURPOSES

Ned H. Burns, P.E., *Research Supervisor*

The contents of this report reflect the views of the authors, who are responsible for the facts and the accuracy of the data presented herein. The contents do not necessarily reflect the official views or policies of the Federal Highway Administration or the Texas Department of Transportation. This report does not constitute a standard, specification, or regulation.

PREFACE

This is the fourth report in a series of four reports which discuss the transfer and development length of 0.5 inch and 0.6 inch diameter prestressing strand. This report focuses on the behavior of pretensioned concrete beams with debonded strand. Experimental procedures, data collection, previous research and possible conclusions are discussed in detail.

The first report dealt mainly with transfer length. The second report discussed the effects of transverse post-tensioning on strand development. The third report focused on development length testing for 0.5 inch and 0.6 inch diameter strands. Later reports are expected to focus on fatigue testing and more comprehensive design guidelines as a summary of results from the entire project. This work is part of Research Project 3-5-89-1210, entitled **Influence of Debonding of Strands on Behavior of Composite Prestressed Concrete Bridge Girders.** This project was modified in March 1989 to include transfer and development length testing for 0.6 inch strand. The work performed under the modification is reported primarily in the first three reports. The principles learned in the research done under the modification contribute directly to the primary research objectives for debonded strands.

The research is being conducted at the Phil M. Ferguson Structural Engineering Laboratory as part of the overall research program for the Center for Transportation Research of The University of Texas at Austin. The work is sponsored jointly by the Texas Department of Transportation (TxDOT) and the Federal Highway Administration (FHWA). Liaison with TxDOT is maintained through Mr. David P. Hohmann, the contact representative. Ms. Susan N. Lane of the FHWA has also been quite active in her support and consultation on the research.

The project is directed by Dr. Ned H. Burns, the Zarrow Centennial Professor in Civil Engineering and the Associate Dean of Engineering for Academic Affairs. Dr. Michael E. Kreger, Associate Professor of Civil Engineering has assisted the project by reviewing the efforts. Graduate Research Assistants who have made significant contributions to this portion of the research are Mr. Asit Baxi, Mr. Leslie ZumBrunnen, Mr. Riyad Aboutaha, Mr. Bruce Lutz and Mr. Bruce Russell. Thanks also go to Mr. Andy Linseisen and Mr. "Rusty" Barnhill, Undergraduate Research Assistants.

SUMMARY

One of the primary objectives of this research project is to develop design guidelines for the use of debonded, or blanketed, strand. The debonding of pretensioned strand is an alternative to draping strands in order to control the maximum tensile and compressive stresses in pretensioned beams. Debonding strands can simplify girder construction; draping strands is more difficult and more dangerous. Likewise, straight debonded strands enjoy economical advantages to draped strands in the total cost of girders.

Static flexural tests were performed on specimens with debonded strand. An analytical rationale, The Bond Failure Prediction Model was used to predict cracking and subsequent bond failure for these tests. The agreement between the prediction model was outstanding, demonstrating that a rational design method can be developed for beams with debonded strands. This research also shows that the currently required multiplier of 2.0 for the development length of debonded strand may be significantly reduced; or more appropriately, changed to reflect a greater understanding of the behavior. Conversely, some dangerous and unsafe designs may be allowed by the current code.

Beams tested in this report were I-shaped and made to resemble an AASHTO section complete with a composite deck. Altogether, ten (10) tests were performed. The beams were loaded statically in flexure until failure. For each test, two types of failure were possible, flexural failure or bond failure. Flexural failures typically developed their ultimate flexural capacity, then experienced large deformations (ductility) before failing by yielding of the strands and crushing of the concrete. Bond failures were characterized by general slip of the strand through the specimen and gross displacements of the strand relative to the concrete (end slip). In general, bond failures were not able to develop the ultimate flexural capacity of the section.

Simply stated, the Bond Failure Prediction Model says that a strand is likely to experience bond failure where a crack propagates into the transfer zone of the strand. For fully bonded strands, the transfer zone is located at the ends of a beam and web shear cracking is the only typical cracking that can cause bond failure. However, in debonded beams, the transfer zones of debonded strands extend into the mid regions of the beam where flexural cracking is more likely to occur. In this case, either web shear cracking or flexural cracking can cause bond failure. Furthermore, in debonded beams, the potential for cracking is exacerbated because the effective prestress force has been decreased through the region of debonding. Reducing the prestress force increases the likelihood of cracking in the debond/transfer zone.

Fortunately, cracking in concrete can be predicted reasonably well. Consequently, bond failure and subsequent collapse of the pretensioned member can be predicted and avoided.

IMPLEMENTATION

The testing program discussed in this report clearly demonstrates the ability to accurately predict the behavior of beams with debonded strands. However, these data represent a relatively small test sample that makes it difficult to draw any far reaching conclusions. Further testing is currently underway to help substantiate (or discount) these findings. Additionally, some more analytical work is required to refine the Bond Failure Prediction Model.

In the very least, however, this report and the findings it contains, represent a very large step forward towards determining the effects that debonded strands have on beams and the development of sound, rational design guidelines.

TABLE OF CONTENTS

LIST OF FIGURES

LIST OF TABLES

CHAPTER ONE

INTRODUCTION

1.1 Background

As more competitors enter the prestress market, the need for efficient and economical members becomes crucial. In order to improve the efficiency of pretensioned girders, design dictates that at midspan, the eccentricity of the prestressing force be as large as possible. However, if the force and eccentricity remain constant over the full length, the allowable design stresses may be exceeded at the ends of the beams. This can result in too much tension in the top fibers or too much compression in the bottom fibers.

The typical method of controlling the end stresses is to reduce the eccentricity of the prestressing at the ends of the girder. Common practice has been to 'drape' a portion of the strands, beginning at or near third points in the beam. These strands usually extend to a point above the neutral axis and offset the effect of the prestressing moment produced by the remaining strands.

The main disadvantage of draping is the high cost of fabrication. Draping requires time and specialized equipment to stress and depress the inclined strands. Also, because a draped strand is stressed horizontally and then pulled down into position, the actual level of prestress obtained throughout the length of the strand is questionable.

A second method of controlling the end stresses is to use straight tendons and limit the level of force transferred to the concrete. By preventing the concrete from bonding to a portion of the strands, the effect is to lower the prestress force at the beam ends. The procedure is called blanketing, or debonding, and is accomplished by greasing the strand, coating it with retarder, or covering it with plastic tubing.

Although grease and retarders are methods of debonding, their use is avoided because careless application to the specified tendons can affect the other strands. Also, ease of application and inspection make the plastic tubing the preferred choice.

1.2 Overview of Experimental Project

This thesis is part four of a larger investigation studying the influence of bond between prestressing strand and concrete on the behavior of prestressed concrete bridge girders. The first two reports dealt with the transfer of prestressing force of 0.5 inch and 0.6 inch diameter strand into rectangular concrete members. The variables studied were the effects of sudden versus gradual release, single versus multi-strand specimens, strand spacing

in multi-strand specimens, and the effect of debonding on the transfer length of both single and multi-strand specimens [12,17].

The third portion of the investigation explored the code requirements for development length of 0.5 inch and 0.6 inch diameter prestressing strand. The girders measured 22 inches in depth and contained either five 0.5 inch or four 0.6 inch diameter fully bonded strands. From the data obtained, the conclusions were that the ACI/AASHTO code requirements for development length were adequate [11].

The continuing research focuses on the behavior of fully bonded and debonded specimens under fatigue conditions. The testing involves specimens similar to girders in the third and fourth phases of the investigation and also includes full-size AASHTO bridge girders.

1.3 Objective and Scope

1.3.1 Objective. The objective of this thesis is to investigate the behavior of prestressed concrete beams containing debonded strands. Because of the possibilities of many variables, this thesis focuses on the following areas:

a) The embedment length necessary to develop the flexural capacity of the cross section.

b) The effect of sudden versus gradual termination of debonding.

c) The role that flexural and web shear cracking play in the behavior of specimens containing debonded strands.

To guide the investigation, an analytical model was developed in the design stage. It considers the previously mentioned variables and predicts the failure mode. The model will be compared to the data obtained in this study to determine its validity.

1.3.2 Scope. The scope of the test program for this thesis consisted of planning, construction and testing of six beams. The first four beams tested were 40 feet in length, 23.5 inches deep and contained eight 0.5 inch diameter prestressing strands. Four of the strands were debonded to a maximum of 78 inches at both ends. Two of the beams had gradually debonded strands while the other two contained suddenly debonded strands.

The last two beams tested consisted of the same cross section as the first four. However, these beams were 27.5 feet in length and had strand with a maximum debond length of 36 inches at both ends. Three ends contained strands that were gradually debonded while the fourth end had suddenly debonded strands.

Gradual debonding meant that the termination of debonding occurred in two different locations. Two of the strands were debonded to half the maximum debond length

while the other two strands were debonded to the full desired length. Termination of debonding of all four strands at the maximum length was defined as sudden debonding.

Fabrication and testing occurred at the Phil M. Ferguson Structural Engineering Laboratory at the University of Texas at Austin's Balcones Research Center. The Texas State Department of Highways and Public Transportation and the University of Texas at Austin's Graduate School Fellowship Program provided funding.

CHAPTER TWO

LITERATURE REVIEW

2.1 General

The behavior of pretensioned girders with debonded strands is dependent on a number of variables common to all prestressed members. To better understand members with blanketed strands, important variables such as bond, transfer length and development length need examining.

The total force of prestressing is transferred to the concrete by the bonding of the tendon to the concrete surrounding it. The bonding mechanism consists of two parts: transfer bond and flexural bond. Activation of the transfer bond occurs due to the initial tensioning and release of the prestressing strand in pretensioned, precast concrete specimens. It uses a portion of the available tensile force in the strand to establish compression in the concrete. The distance in which the prestressing stress, f_{se}, is transferred by bond to the concrete is the transfer bond length, L_t (Figure 2.1).

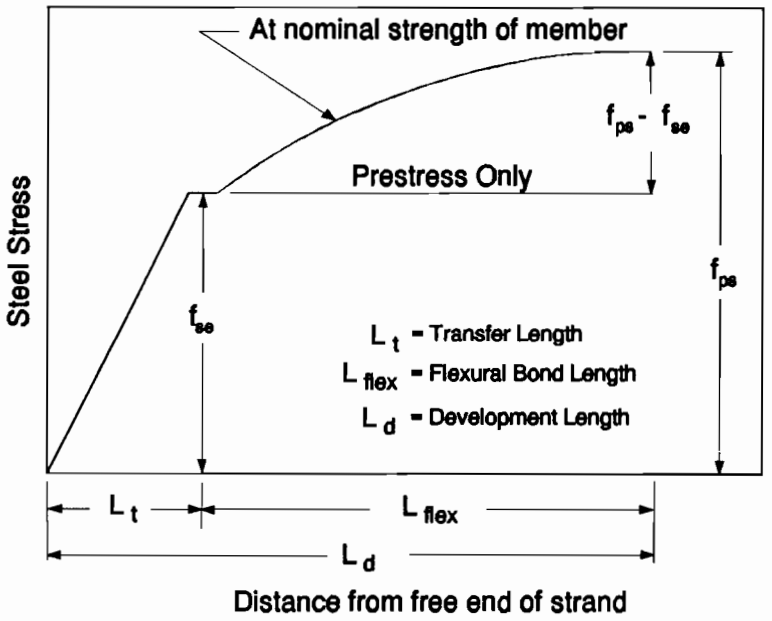

Figure 2.1 - Variation of Steel Stress [3]

Flexural bond is mobilized as the member responds to externally applied loads that cause bending. As the loads increase, the level of stress in the strand also increases. The additional bond length required to develop from the effective prestressing stress to the new level of stress is the flexural bond length.

As the load reaches the ultimate capacity, the length of strand required to transfer the total strand stress to the concrete is the development length, L_d. It is the sum of the transfer and the flexural bond lengths.

There are many variables that can affect transfer and flexural bond lengths. For a review of literature discussing transfer and development length variables, refer to the theses of Raheel Malik [12] and Ozgur Unay [17].

2.2 Presentation of ACI/AASHTO Provisions

Section 12.9 of ACI 318-83 contains the current provisions for development length of prestressing strand. The provisions are based on tests performed on specimens fabricated using normal weight concrete with a minimum cover of two inches. They read as follows:

> **Section 12.9.1** - Three- or seven-wire pretensioning strand shall be bonded beyond the critical section for a development length, in inches, not less than where
>
> $$(f_{ps} - 2/3\, f_{se})\, d_b \qquad (1)$$
>
> d_b = nominal strand diameter in inches
>
> f_{ps} = stress in prestressed reinforcement at nominal strength in kips per square inch
>
> f_{se} = effective stress in prestressed reinforcement (after allowance for all losses) in ksi.
>
> **Section 12.9.2** - Investigation may be limited to cross sections nearest each end of the member that are required to develop full design strength under specified factored loads.
>
> **Section 12.9.3** - Where bonding of strand does not extend to end of member, and design includes tension at service load in precompressed tensile zone and permitted by Section 18.4.2, development length specified in Section 12.9.1 shall be doubled.

The Commentary to the ACI Code considers the equation in Section 12.9.1 and suggests the equation be rewritten as:

$$L_d = \frac{f_{se}}{3} d_b + (f_{ps} - f_{se}) d_b \qquad (2)$$

The first term represents the transfer length while the second term symbolizes the flexural bond length. These expressions are based on tests of members prestressed with clean, 1/4, 3/8, and 1/2 inch diameter strands in which the maximum value of f_{ps} was 275 ksi [3]. The variation of strand stress along the development length at maximum load is also displayed by Figure 2.1. The code expressions are derived in large part from tests performed with Grade 250 ksi strand, whereas commonly used strand today is Grade 270 ksi.

Section 12.9.3 is based on experimental evidence that girders with debonded tendons designed for twice the required development length closely matched the performance of draped specimens. Specimens in the same investigation with a normal development length, as defined by equation (1), failed in bond fatigue. A full review of this study by Kaar and Magura [9] is presented in Section 2.3.2.

The ACI Commentary also provides an additional option to the requirements of Section 12.9.3. It proposes that pretensioned members designed for zero tension in the concrete under service load conditions may disregard Section 12.9.3 requirements. A review of the investigation by Rabbat, Kaar, Russell and Bruce [14] that led to this exception is presented in Section 2.3.4.

The calculated values for development length contained in this report are consistent with 1989 ACI and 1990 AASHTO revisions. ACI (1989) was used to calculate the development lengths which corresponds to the latest edition of AASHTO (1990). The 1989 AASHTO specification contained a different formula for calculating f_{su}^* that in turn affects the calculation for development length.

2.3 Review of Literature Pertaining to Debonded Strands

2.3.1 Introduction. Although debonding of strands seems like a viable alternative to draping, very little research has been done to date. Currently, only three major investigations have been completed on the behavior of girders containing blanketed strands. They were performed by Kaar and Magura[9], Dane and Bruce [5], and Rabbat, Kaar, Russell, and Bruce [14]. A complete review of their objectives and conclusions are presented in Sections 2.3.2, 2.3.3 and 2.3.4, respectively.

2.3.2 Kaar and Magura. In 1965, Kaar and Magura [9] experimentally studied the effect of strand blanketing on the performance of pretensioned girders. The investigation evaluated the effect of strand debonding on flexural behavior and shear capacity.

Three half-scale AASHTO-PCI Type III girders with 3/8 inch diameter strand were designed and tested for flexural behavior. Girder 1 was fabricated as a control specimen and was fully bonded. Girder 2, which was partially blanketed, was fabricated to have strands debonded to a point that was twice the required embedment length from the cross section in question. Girder 3 was designed to have strands blanketed to a point that was one embedment length from the point of consideration. The girders' cross sectional properties, loading arrangement and strand blanketing are shown in Figure 2.2.

The testing procedure consisted of subjecting all three girders to 5 million cycles of the design live load before static testing to failure. Under the fatigue loading, all three beams exhibited no detrimental effects due to strand debonding. However, there was a reported difference once static loading began and cracking occurred. Girders 1 and 2 behaved similarly while Girder 3 failed in a much different manner. In Girders 1 and 2, extensive yielding of the strand occurred before rupture at the ultimate applied load. In the test of Girder 3, the specimen failed at a much lower moment at a section under the outside loading point. At the failure location, only ten of the twelve strands were contributing to the flexural capacity due to strand debonding.

The shear investigation consisted of the static testing to destruction of two girders. Girders 4 and 5 were identical to Girders 1 and 2 in the flexural study except they contained fewer stirrups. The reduction in stirrups provided a means to examine the effects of debonding on the shear capacity. After completion of testing, determination was that both girders performed satisfactorily. The conclusion was that the debonding of strands had no detrimental effects on the shear capacity of the girders.

Based on the flexural investigation, the conclusion was that the ACI code requirement for development length of prestressing strand could not be directly applied to debonded strands. However, it was noted that the behavior of blanketed strand girders with double the required development lengths closely matched the performance of the draped girder. Section 12.9.3 of the ACI code was based on this single observation.

2.3.3 Dane and Bruce. In tests conducted at Tulane University in 1975, Dane and Bruce [5] looked at the elimination of draping by using straight strands having certain debonded lengths. The objective of the investigation was to determine the influence of the debonded strands on the flexural strength and behavior of prestressed concrete girders. Consideration of shear and fatigue effects was not involved.

The scope of the project involved six half-scale Type III AASHTO-PCI girders and three full size Type II AASHTO-PCI girders. Designed in pairs, the six half-scale girders' major variable was the method of strand anchorage. Fabricated with conventional draped strands, the first two girders served as reference specimens. The second pair of girders was designed with 17% of their strands blanketed to a length of 9.22 feet at each end of the beam. A mild reinforcing cage was provided at the point where the blanketing stopped and the transfer zone began.

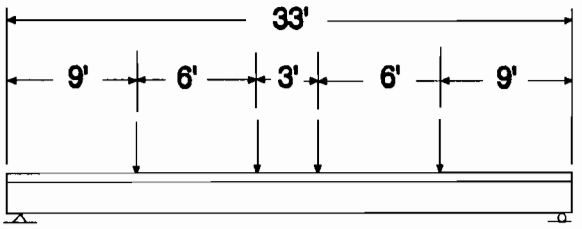

Girder Loading Diagram

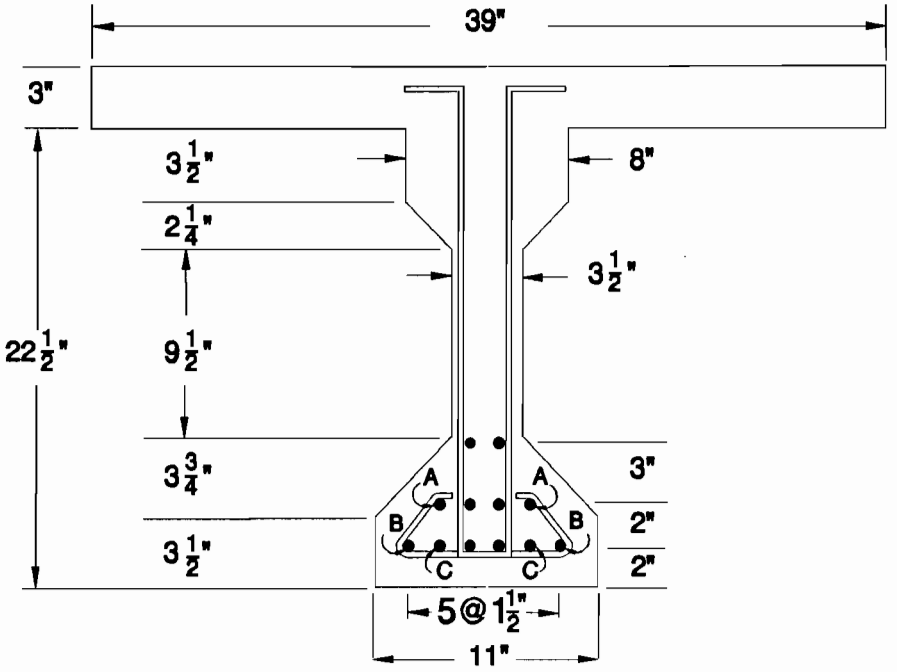

Blanket Lengths

	Strand A	Strand B	Strand C
Girder 3	3' - 11"	6' - 11"	10' - 11"
Girder 2, 5		2' - 4"	6' - 4"

Figure 2.2 - Girder Cross-Section and Load Arrangement [9]

In the third pair, the design was identical except that internal mechanical anchors were provided instead of the rebar cage. The mechanical anchors consisted of a steel plate and a strand chuck. Upon transfer, the debonded strand slip was resisted by the chuck which bore directly against the embedded steel plate. The specimens were all 34 feet long and contained 3/8 inch diameter prestressing strand.

With the full scale specimens, the first girder served as a reference and had conventionally draped strands. The other two specimens were designed as duplicates with 17% of the strands being debonded for a length of 11 feet at each end. The beams were 50 feet in length and used 7/16 inch diameter prestressing strand as the main reinforcement. Both beams contained reinforcing cages at the termination points of the strand blanketing.

To determine the number and length of strands to blanket, the authors used the following steps and Figure 2.3:

a) An appropriate moment diagram was generated for the applied loads as shown in Figure 2.3(a).

b) The amount and location of the main reinforcement was determined to provide sufficient flexural capacity.

c) To meet code requirements for allowable stresses, a portion of the strands was debonded.

d) The moment capacity for the cross section containing blanketed strands was calculated. Construction of a moment capacity diagram for the specimen was then completed (Figure 2.3(b)).

e) The two diagrams were then superimposed such that point C was the point of intersection between both moment diagrams as shown in Figure 2.3(c).

f) To determine the length of debonding, the length from point C to the support was first calculated (L_r). The embedment length was then calculated from the required code provisions using a development length of one. The length of strand blanketing was the difference between the two lengths (Figure 2.3(c)).

This design insures that the ultimate moment capacity provided at one development length from the termination point of the debonded strands is always greater than or equal to the moment applied.

The test procedure was to load each specimen at third points until failure occurred. Definition of failure was a concrete compression failure or the point where the deflection

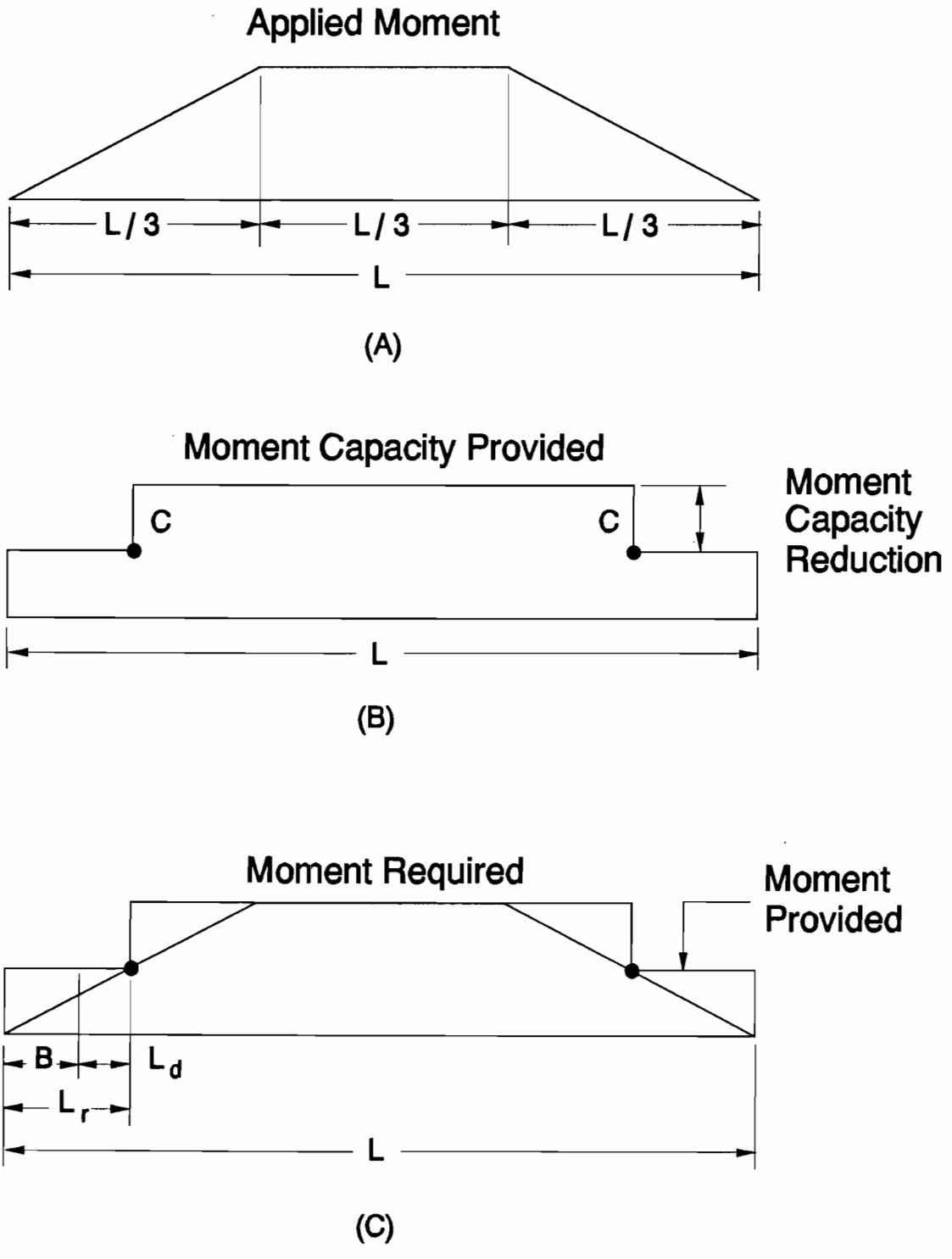

Figure 2.3 - Moment Capacity for Girders with Blanketed Strand [5]

continued to increase without increasing the load. During testing, all girders failed in the region of maximum moment without any significant difference in behavior being observed.

Although all girders displayed movement of the blanketed strands relative to the end of the girder, conclusions were that the girders behaved satisfactorily when compared to the draped specimens. Furthermore, it was shown that the development length equations found in the ACI code were acceptable and that the additional requirement of doubling the development length for debonded strands was unnecessary.

2.3.4 Rabbat, Kaar, Russell, and Bruce. In 1978, Rabbat, Kaar, Russell, and Bruce [14] carried out fatigue tests on pretensioned girders with blanketed and draped strands. The purpose of the investigation was threefold. The first was to determine if tension in the concrete under service load conditions affects the development length of the prestressing strand. The second objective was to determine whether one or two development lengths were required for debonded strands. The final objective was to determine if confining the concrete in the stress transfer region of the debonded strands was beneficial.

The scope of the investigation involved six full-sized, 50 feet long, Type II AASHTO-PCI girders. As the tests were an extension of the tests by Dane and Bruce, the girders contained the same number, size and grade of strands. Two girders contained draped strands while the other four contained four blanketed tendons. The strands were 7/16 inch diameter and were Grade 250, stress relieved.

Designed in groups of three, the first set of girders had no tension in the concrete under service load. The set contained one draped specimen, a blanketed specimen with a development length of one, and a blanketed specimen that had a development length of twice the required embedment length.

The second set contained a draped specimen, and two blanketed girders with a development length of one. One of the debonded specimens contained additional confinement reinforcement in the area of the stress transfer zone of the debonded strands. This group of girders was designed for a tension stress in the bottom fiber of $6\sqrt{f_c'}$

The test program called for 5 million cycles of loading between dead load and dead plus live load. Static tests of full dead load plus live load were performed before cycling and after 1, 2.5, and 5 million cycles, respectively. After completion of the 5 million cycles, the girders were statically loaded to destruction. The following conclusions were drawn from the test results:

a) In debonded specimens designed for one development length and zero tension stress, no significant differences were noticed in behavior and strength from those of the draped specimens.

b) Debonded specimens designed for a maximum tensile stress of $6\sqrt{f_c'}$ in the concrete and having blanketed strands designed for twice the development length exhibited equal strength when compared to the draped specimen. However, those designed for one development length failed in bond fatigue.

c) Use of additional confining reinforcement in the stress transfer region of blanketed strands did not provide any substantial improvement in the behavior.

The conclusions indicated that a design for zero tension in the concrete significantly changed the behavior of the specimen. The ACI committee recognized the change and amended Section 12.9.3 of the ACI code to allow relaxation of the provision if the member was designed for zero tension in the concrete under service load conditions.

2.3.5 Pertinent Publications. For completeness, it should be mentioned that two other publications about strand debonding exist. In 1981, Horn and Preston [7] published a report for the PCI Committee on Bridges. It contained an overview of research pertaining to transfer and development length of pretensioned members. It also gave brief recommendations concerning member design and techniques for strand debonding.

In 1986, Ghosh and Fintel [6] published an edited portion of a larger report discussing the development length of prestressing strands. In one section of the publication, they presented an overview of all research applicable to the development length provisions for debonded strand in the ACI Code.

A second section contained the partial results from an industry survey in which prestressed concrete producers were asked if the development length provisions for prestressing strand presented any problems. Although most answers were negative, a couple of the positive answers posed the following questions: "Why should L_d be doubled? Does it make any difference if the strand is debonded six inches or ten feet?" The authors answered the questions by concluding that the code provision was based on reliable experimental evidence. A provision change could not be proposed until further investigation of development lengths less than two prove to be sufficient.

CHAPTER THREE

TEST PROGRAM

The purpose of this investigation was to examine the influence of strand debonding on the behavior of pretensioned girders. Because of the many different variables involved in prestressed members, careful attention was given to details involving the design, fabrication, and testing program. This chapter presents the specimen design, fabrication, material properties, testing frame, instrumentation, and test procedures used during this series of tests.

3.1 Specimen design

Under current code provisions, the development length for specimens containing debonded strands is twice the normal requirement (ACI Section 12.9.3). An exception to this stipulation is a design requiring zero tension in the concrete under service loads. The requirements are based on a series of tests in which girders exhibited bond failure when designed under the normal code provisions but performed adequately when designed for twice the requirement [9]. The provision may be too strict since research has not been completed on specimens designed for lengths greater than one but less than twice the development length provision.

To determine the development length of debonded, 0.5 inch diameter strand, a series of I-shaped girders were designed for testing. To aid in the design, an analytical model was developed which attempted to predict cracking in the debond/transfer zone of the specimen. If cracking occurred, the model also predicted a bond failure of the debonded strands. Presentations of the prediction model, specimen design, and specimen designation are presented in Sections 3.1.1, 3.1.2 and 3.1.3, respectively.

3.1.1 Model for Prediction of Cracking and Bond Failure. The prediction model was produced as a guide to behavior of the specimens in the design phase for both the static and fatigue investigations. Bruce W. Russell, a Ph. D. candidate responsible for the completion of the overall investigation, developed the model. The presentation of the prediction model is an adaptation of a technical memorandum produced by Russell to the Texas State Department of Highways and Public Transportation [16].

The model is based on the following theory: when a crack forms in the concrete, bond failure between the concrete and strand occurs for a finite distance on both sides of the crack. As a crack develops, the bond stress in the immediate vicinity of the crack increases to a limiting value. If the limiting value is exceeded, local bond slip occurs for a distance along the length of the strand. This results in dispersement of the excess stress into the areas adjacent to the crack.

As load increases, the occurrence of flexural cracking progresses from the load point along the length of the beam. This results in a wave of high bond stress moving toward the support as each new crack forms. If the wave of high bond stress reaches the transfer zone, L_t, total bond failure will occur. Appropriately, if a crack forms in the debond/transfer zone of a debonded strand, the result is a general strand slip.

The formation of cracks in the debond/transfer zone is the basis of the prediction model for bond failure of debonded strand. If cracking occurs at or near the transfer zone of a debonded strand, bond failure of that strand will occur. Since cracking in the concrete can be predicted with reasonable accuracy, the ability to predict strand slip is possible.

Figure 3.1 illustrates the consequences of debonding on the load carrying capacity of a pretensioned girder. In this example, four of the eight prestressing strands are debonded. In the middle portion of Figure 3.1, the prestressing force is plotted versus the length of the beam. At the beam end, the effective prestress force increases from 0 kips to 98 kips (4 strands x 24.5 kips/strand = 98 kips). This increase in prestress force represents the transfer zone of the four fully bonded strands. If all eight strands were fully bonded, the prestress force at the end of the transfer zone would be 196 kips.

The effective prestress force remains constant until debonding is terminated, and the debonded strands are allowed to bond to the concrete. By following the line marked "Sudden Debond", where all four of the debonded strands are debonded a distance of 78 inches, a second transfer zone occurs as these strands transfer their prestressing force into the concrete. The assumed transfer length is 25 inches, based on earlier transfer length

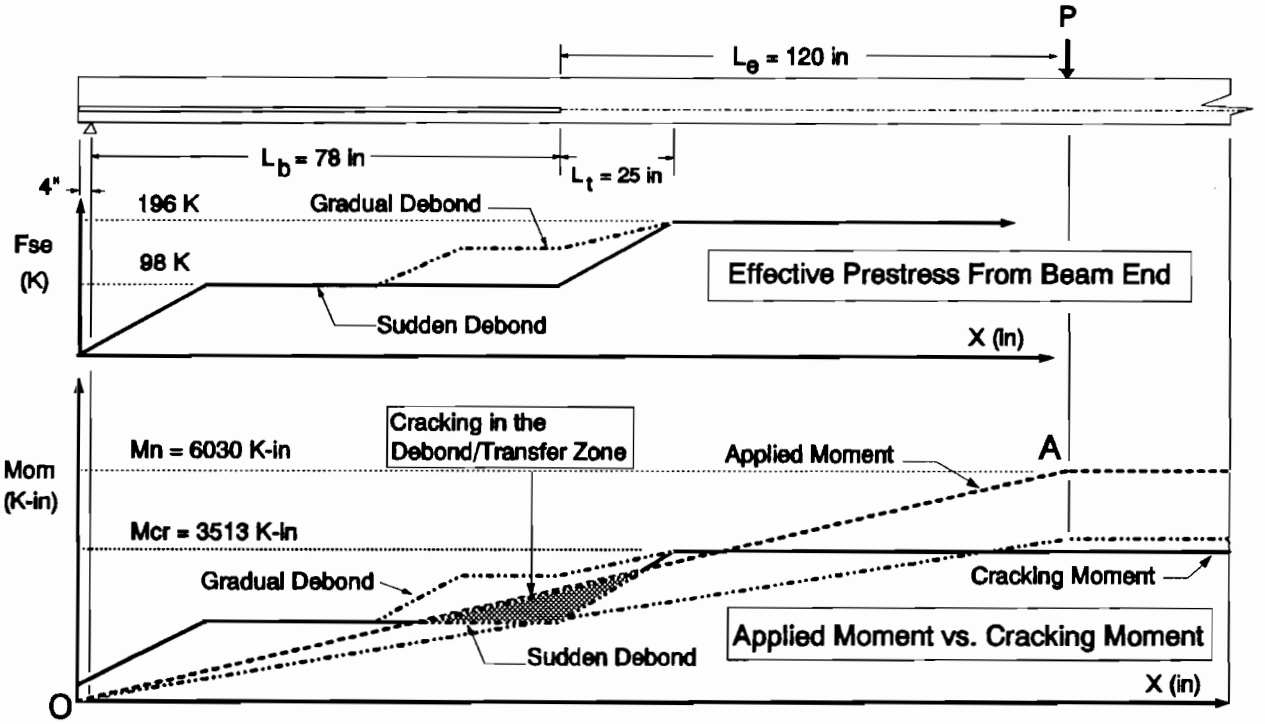

Figure 3.1 Applied Moment vs. Cracking Moment

measurements[17]. At the end of the second transfer zone, the effective prestress force is 196 kips (8 strands x 24.5 kips/strand).

By debonding strands, the effective prestress force is effectively reduced in the end regions of a beam, when compared to a fully bonded beam. In turn, the reduced prestress also reduces the beam's cracking resistance in the regions where strands are debonded, the debond/transfer zone. The effects of the reduced cracking moments are illustrated in the lower portion of Figure 3.1 where both cracking moment and applied moment are plotted versus the length of the beam. The cracking moment, shown by the solid line in the lower portion of the figure, follows the same pattern as the effective prestress force, increasing linearly in each transfer zone and remaining constant in regions where the prestress force is constant.

The consequences of debonding are dramatized by line OA which plots the applied moment as the ultimate moment is applied. Note that the applied moment, given by line OA exceeds the cracking moment in the region where strands are debonded, and where the debonded strands are transferring their prestress force. This region is termed the "debond/transfer zone." Flexural cracking that occurs in this region is distinct and separate from the flexural cracking that occurs in the vicinity of the load point.

As the flexural cracking occurs in the transfer zone of debonded strands, the crack disturbs the anchorage of these strands. The flexural cracking causes local increases in strand tension. As these strands increase in tension, their diameter is slightly reduced from Poisson's ratio and bond restraint caused by the wedging action at prestress transfer is singificantly reduced. Consequently, strand slips will occur and bond failure is likely.

Figure 3.1 also illustrates the effects of staggering the debonding terminations. By staggering the termination points of the debonded strands, the detrimental effects of debonding can be minimized. This is illustrated in Figure 3.1 by the dashed lines marked as "Gradual Debond." The positive effects of staggering debond termination points are best illustrated by the lower portion of the figure. As described above, a beam that contains strands with sudden debonding will experience cracking in the debond/transfer zone (with probable bond failure of the debonded strands). On the other hand, a beam with staggered debond terminations, but otherwise identical, will not crack in the debond/transfer zone, and will probably sustain loads through the flexural capacity of the beam with fully developed debonded strands.

Although the prediction for the suddenly debonded strands is a bond failure, Figure 3.1 also illustrates that a gradual debonding of the same four strands should result in a flexural failure. Gradual debonding is the deliberate variation of the debonding termination points along the length of the debonded zone. The result is that the effective prestress force of the debonded strands transfers to the concrete more quickly. In this example, two strands are debonded half the distance while the second pair is blanketed for the full length desired. The effective prestress force and the cracking moment are shown by the dashed lines.

Figure 3.1 shows that the achievement of the ultimate flexural moment occurs before crack formation in the debond/transfer zone. This would suggest that general bond slip of the debonded strand would not occur, thus resulting in a flexural failure.

The cracking moment is not the only variable influenced by the reduction of the effective prestress force. The resistance to web shear cracking also suffers when strands are debonded. The formation of web shear cracks occurs when the tensile strength of the concrete is exceeded on an inclined plane. As pretensioned girders derive much of their resistance to inclined tensile cracking from the effective prestress force, a reduction in force lowers the girder's resistance to web shear cracking in the debond/transfer zone.

Developed as a design guide (calculations in Appendix D), Figure 3.2 graphically illustrates the expected behavior of a specimen at any given debonded length, L_d, and embedment length, L_e. (The embedment length is the distance from the end of the longest debonded length to the point of maximum moment.) The plot is divided into several different areas. Each area represents a different prediction of behavior. Case 1 areas predict cracking will not occur in the debond/transfer zone and a flexural failure is likely.

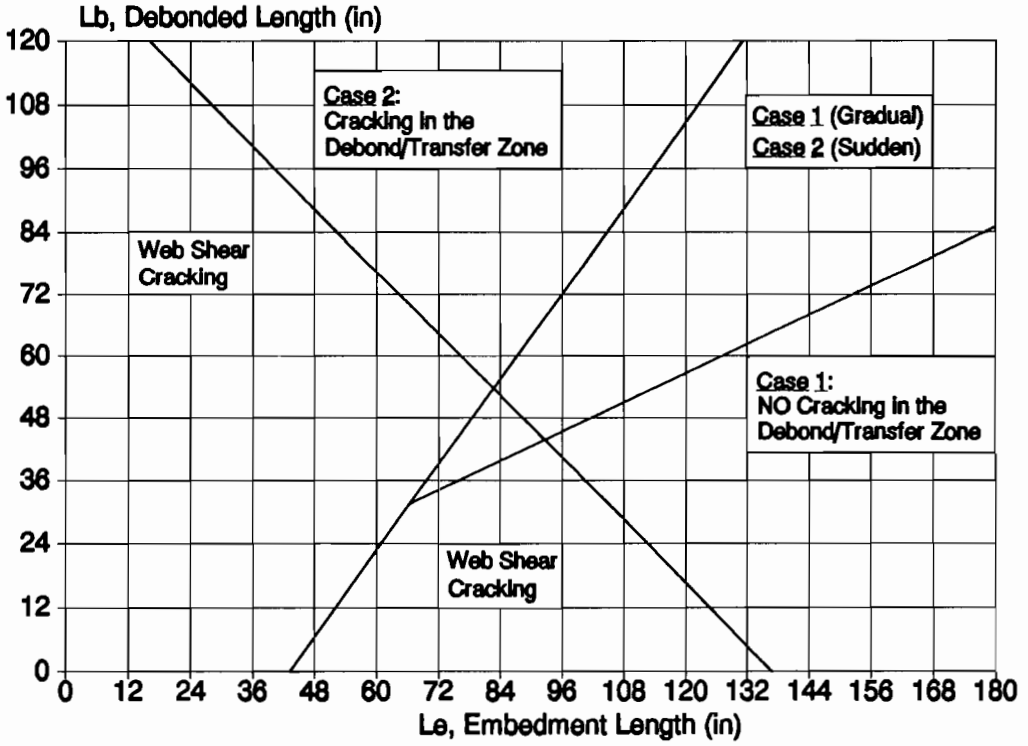

Figure 3.2 Prediction Model of Cracking and Bond Failure

Case 2 areas predict that cracking will occur in the debond/transfer zone resulting in bond failure. Areas where web shear cracking are likely to control are defined by the dashed lines.

The plot is a function of the cross sectional properties, the number and location of debonded strands, and the loading condition. It is easily generated for any combination of cross section and design conditions.

3.1.2 Specimen Design. A total of six I-shaped pretensioned concrete girders were fabricated for this study. The typical cross section is shown in Figure 3.3. Two of the specimens were 27.5 feet long while the other four were 40 feet long. Each specimen contained eight, 0.5 inch diameter prestressing strands, four of which were debonded. The decision to debond four of the strands was based on the following:

1. Debonding of four strands would allow the effects of sudden versus gradual debonding to be examined while also maintaining the symmetry of the cross section.

2. In the industry's normal size sections, only a small portion of the total number of strands would be blanketed. The determination was that debonding of half of the available strands would magnify any possible effects. Also, blanketing of more than 50 percent would be uncharacteristic of industry practice.

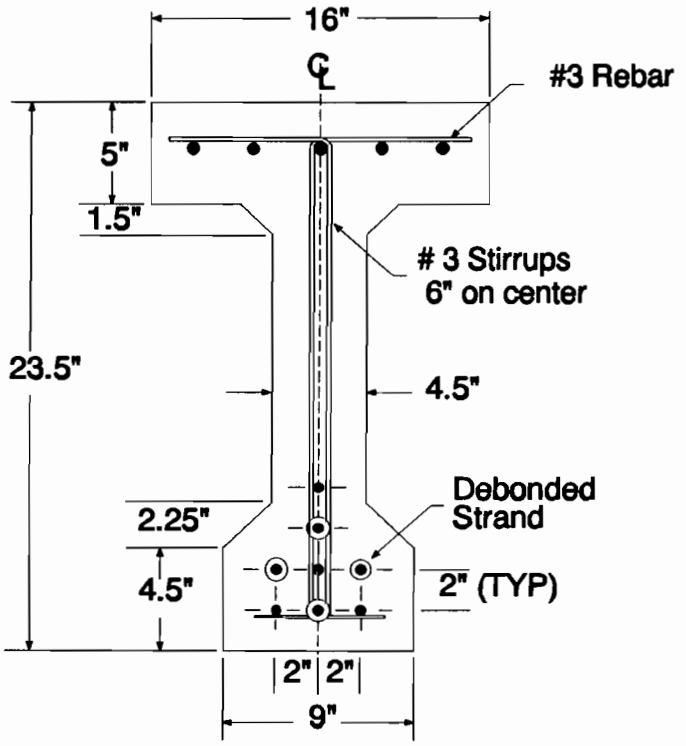

Cross-Sectional Properties

A_g	=	197.0	in^2
A_s	=	1.2	in^2
I	=	12080.0	in^4
S_b	=	921.0	in^3
S_t	=	1164.0	in^3
Y_b	=	13.1	in
e	=	9.1	in

Figure 3.3 Specimen Cross Section Details

Beams DB850-1 and DB850-2 were both 27.5 feet long and contained strands with a maximum debond length of 36 inches. Three ends contained gradually debonded strands while the fourth end was suddenly debonded.

In the 40 foot specimens, DB850-5 and DB850-6 contained suddenly debonded strands with a maximum debond length of 78 inches. Specimens DB850-3 and DB850-4 contained gradually debonded strands with two strands blanketed to 39 inches and two strands blanketed to 78 inches. Table 3.1 provides a summary of the length of debonding for each strand in each beam.

Table 3.1 Summary of Strand Debonded Lengths

Beam	End	Debonded Length in Inches			
		Strand B	Strand D	Strand F	Strand G
DB850-1	North & South	36	18	18	36
DB850-2	North, South	36,36	18, 36	18, 36	36,36
DB850-3	North & South	78	39	39	78
DB850-4	North & South	78	39	39	78
DB850-5	North & South	78	78	78	78
DB850-6	North & South	78	78	78	78

3.1.3 Specimen Numbering System. In order to keep track of all specimens throughout the investigation, a numbering scheme was devised that described the characteristics of each beam. An example of the numbering system is illustrated in Table 3.2. For ease of reference and clarity, an additional symbol of '(S)' or '(G)' will be added after the test number. The symbols show whether the specimen was suddenly or gradually debonded.

A numbering scheme was also devised for the strands to keep track of all pertinent data relating to each strand. Figure 3.4 displays the strand labeling scheme.

3.2 Material Properties

3.2.1 Prestressing Strand. The seven-wire, low-relaxation prestressing strand used in this investigation was donated by the Florida Wire and Cable Company (FWC). It had a nominal diameter of 0.5 inches (area = 0.153 square inches) and a specified ultimate

Table 3.2 - Numbering Scheme

DB850 - 1A	
D	Debonded specimen (F = Fully Bonded)
B	Type B cross section (A = Type A)
8	Number of Strands
5	Diameter of Strand (6 = 0.6 inch strand)
0	2 inch spacing grid (2 = 2.25 inch grid)
1	Specimen number in the series
A	First test of specimen (B = second test)

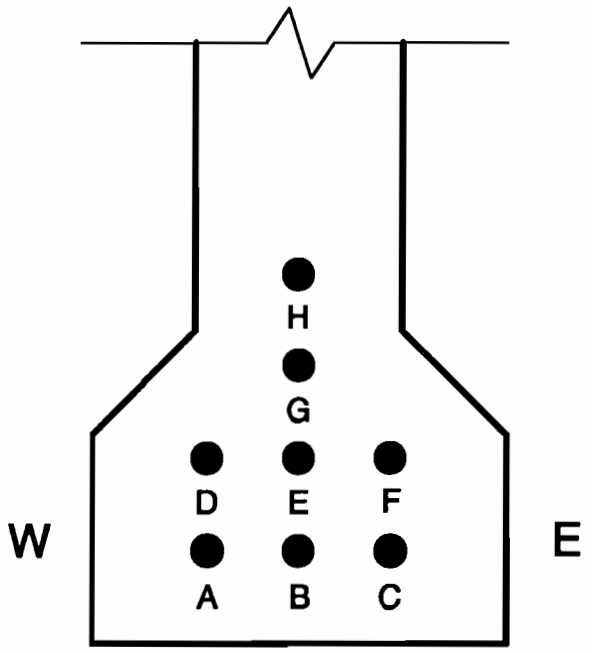

Figure 3.4 Strand Labeling Scheme

strength of 270 ksi. The manufacturer's data gave a yield stress of 276 ksi and an ultimate stress, f_{pu}, of 289.5 ksi. A graph displaying the stress-strain relationship is found in Appendix A.

The strand was examined upon arrival and found to display a clean, mill condition surface. Since industry practice is to use the strand as delivered, the prestressing strand was used directly from the spool without cleaning the surface. Also, the clean, mill condition surface presented the worst case scenario for bonding of the concrete to the steel surface.

3.2.2 Concrete Mix. The concrete mix was designed to achieve a 48 hour compressive strength of 4500 psi and a nominal 28-day strength of 6000 psi. The concrete was purchased from a local ready-mix producer and was delivered to the laboratory by truck. The concrete mix was a standard laboratory design and its mix proportions are presented in Appendix A.

As placement of the concrete occurred, sample cylinders (6 x 12 inches) were cast in accordance to ASTM C 31-87a [4]. A set of three, moist cured cylinders were tested in compression at each of the following intervals: 2 days (transfer), 7 days, 14 days, 28 days and the day the first test was conducted on each specimen. At the time of specimen testing, compression testing of a set of field cured cylinders was completed for comparison to the standard moist cured specimens. Graphs of compressive strength versus time for the specimens can be found in Appendix A. Figure 3.5 displays the average compressive strengths for the series of specimens.

3.2.3 Debond Material. The debond material used was a plastic sheathing that was split along the length of the tubing. The debonding material was donated by Austin

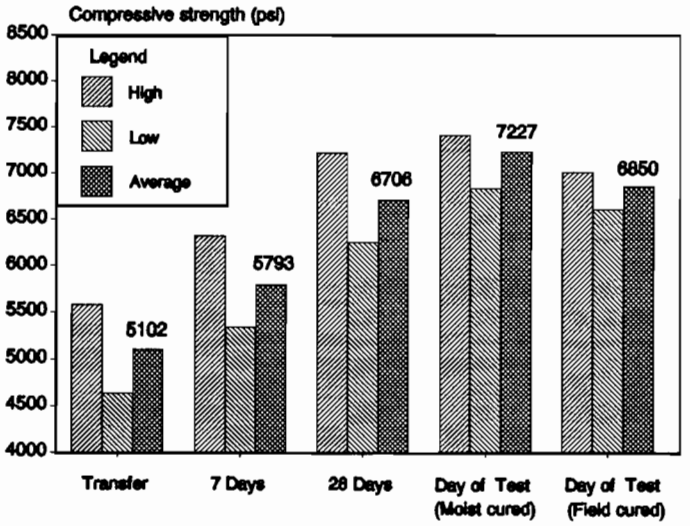

Figure 3.5 Compressive Strength of Concrete Cylinders

Prestressed Company. Application of the sheathing took place once the strands had the full prestress force applied. To prevent cement infiltration, the ends of the debond material were sealed with common duct tape.

3.2.4 Epoxy. The epoxy used in the modification of the 27.5 foot specimens was Sikadur 31, Hi Mod Gel. Before application of the epoxy to the specimen, the specimen and steel plates were cleaned to remove any substance that might interfere with the epoxy bond. The mixing and application of the epoxy then occurred in compliance with the manufacturer's specifications.

A thin layer, approximately 1/4 inch thick, was applied to the web of the specimen. The steel plates were then positioned on the web and tightly bolted. The tightening of the plates removed air pockets and produced a uniform thickness of epoxy between the specimen and the plates. An overnight curing period allowed the epoxy to gain full strength before testing of the specimen occurred.

3.3 Specimen Fabrication

All beams in this series were constructed in the Phil M. Ferguson Structural Laboratory at the University of Texas at Austin's Balcones Research Center. Fabrication consisted of construction of the reinforcement cage, stressing of the prestressing strands, placement of formwork, placement of concrete, and transfer of the pretensioning force to the concrete. The girders were then stored in the laboratory under ambient conditions to allow the fabrication of additional beams while the curing process took place.

3.3.1 Prestressing Bed. The fabrication of the girders took place in prestressing bays oriented between two steel abutments. The abutments were 71 feet apart and anchored the prestressing strand once it was tensioned. Each bay contained a table that was 2 feet wide and 56 feet long. The tables functioned as the bottom form and were topped with Plexiglass. The Plexiglass served to reduce the friction between the table and the concrete member during the transfer of the prestressing force. Figure 3.6 displays the prestressing bed.

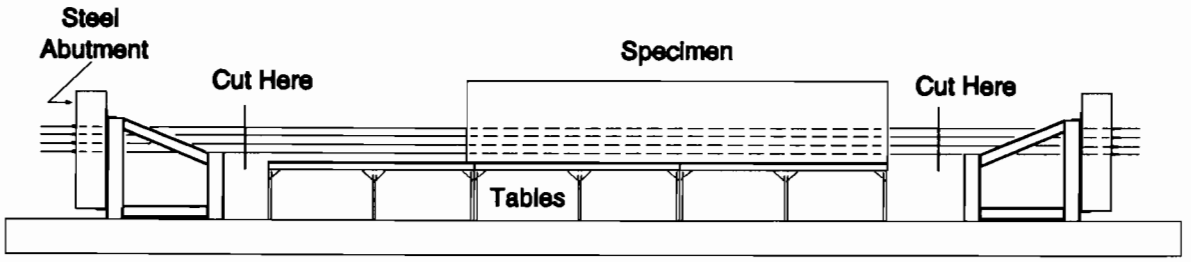

Figure 3.6 Prestressing Bed

3.3.2 Pretensioning Instrumentation . To achieve reliability and consistency in the level of stress in each pretensioned tendon, several types of instrumentation were used. They included electrical resistance strain gauges, a load cell, a hydraulic pressure indicator, a hydraulic pressure transducer, and a linear variable displacement transducer (LVDT). A data acquisition system, described in Section 3.5, scanned and obtained the data readings from the load cell, strain gauges, pressure transducer and LVDT.

Four strain gauges were applied at each end of the specimen to monitor the strain in the strands. Application of the first gauge was to strand B in the stress transfer zone. The remainder of the gauges alternated between strands B and G at an even increment of length.

During stressing, it was important to monitor the amount of force applied to the strand by the hydraulic system. A pressure indicator provided visual reference for manual control of the stressing system. An electronic pressure transducer was also used to monitor the pressure. During each scan of the electronic system, the data acquisition unit obtained the level of pressure from the transducer for future reference. As an additional check, a load cell was placed at the anchoring end of the prestressing bed to measure the actual force in strand G.

A final verification of the level of stress in the strand was the measurement of strand elongation. The elongation of strand G was measured by an LVDT which was directly monitored by the computer. To minimize danger and speed the stressing process, a steel rule was used to measure the elongation of the remaining strands (accuracy = 1/32 inch).

3.3.3 Pretensioning Procedure. Before tensioning the strands, a shear reinforcement cage was constructed consisting of stirrups fabricated from #3 reinforcing bars. Once completed, strands B and G were passed between the two abutments and temporarily stressed to approximately 10 ksi. The initial tensioning aligned the strands to accommodate the application of strain gauges and to seat the anchoring end chucks. Once the strands were instrumented, removal of the initial stress was accomplished through the displacement of the chucks at the stressing end. Care was taken not to disturb the anchoring end chucks to eliminate possible strand movement prior to tensioning.

The next phase was to pass strands A and C through the abutment and to stress all four strands. In consideration of strand spacing and convenience, the rebar cage was tied to strands A, B, and C once the four strands were stressed. The remaining strands were then threaded through the cage and abutment and were stressed. At this point, the debonding material was placed on strands B, D, F, and G.

The stressing of all strands was accomplished by using a double cylinder Velzy hydraulic ram. The ram bore directly against the stressing end chuck, which reacted against the steel abutment. Reusable chucks, using male conical wedges and a female cylindrical chuck body, anchored the stressed strand between the abutments. To accommodate the

procurement of data during stressing, the pretensioning force was applied in many increments. Predetermined stress levels of 10, 26, 104, 197.5 and 202.5 ksi were convenient points to allow the data acquisition unit to take readings. Elongation readings, measured by the steel rule, were also completed at this time. The desired level of prestress in the strands was $0.75f_{pu}$ which corresponded to 202.5 ksi.

The double cylinder Velzy hydraulic ram provided a method of physically seating the male conical wedges while also preventing the strand from slipping. After reaching the desired level of force, the ram transferred the jacking force into a seating force which drove the wedges into the female chuck body. This method of seating was very efficient and yielded an approximate loss of eight percent.

All strands were pretensioned in the same manner except for strand G. Strand G had two 1/2 inch shims placed between the stressing end chuck and the abutment. These removable shims provided an additional inch of strand in the prestressed system which would allow gradual detensioning when removed during the transfer procedure (Section 3.3.6).

3.3.4 Formwork. Wooden forms provided a reusable system that allowed the fabrication of twenty specimens. Once the pretensioning procedure had been completed, the placement of the formwork was the next step before casting. The forms were bolted to the tables and tied together at the top with all-thread rods. This allowed adjustment of the forms to achieve the desired cross-sectional dimensions throughout the length of the member. Either one 40 foot specimen or two 27.5 foot specimens were capable of being cast at one time.

Because careless application of form oil could damage the bond characteristics of the strands, no form oil was used. Instead, after each use, the forms were scraped and lacquered to extend their life and to aid in removal. The pretensioning procedure and the placement of the formwork was completed one day before casting of the specimen.

3.3.5 Concrete Placement. The placement of the concrete took an average of 45 minutes to complete once the truck arrived. It consisted of transporting the concrete from the ready mix truck to the forms by an overhead crane and a 3/4 cubic yard bucket. The concrete was placed in two lifts, with roughly half of the concrete being deposited in the first lift. Before the second lift, the concrete was consolidated by both internal vibrators and an external form vibrator. The second lift was placed and consolidated in the same manner. The top of the specimen was then screeded, floated, and troweled to provide a smooth surface.

After the concrete was cast, it cured in the forms for 48 hours. To prevent excessive moisture loss, plastic sheets covered the top of the specimen while in the forms. After 48 hours, the forms and plastic were removed.

3.3.6 Procedure for Transfer of Pretensioning Force. After 48 hours, a set of three cylinders was tested to determine the compressive strength of the concrete. Once the required strength of 4500 psi (f'_{ci}) was confirmed, transfer was completed.

To simulate the worst case scenario, all of the strands were flame cut with an acetylene torch. Unfortunately, when the strands were cut on the first girder of the series, excessive shock and dynamic forces were transferred to the tables, threatening to collapse them. On subsequent girders, one strand was partially detensioned to reduce the shock and dynamic loading. The detensioning represented only one percent of the total prestress force in the system.

To simulate industry practice, a sequence of cutting was standardized. To simplify notation, the strands will be referenced either north (n) or south (s) and by the labelling scheme described in Section 3.1.3 and Figure 3.4. The sequence started with the following nine flame cut releases: C(n), A(n), B(n), F(s), E(s), D(s), H(n), H(s), and E(n).

The partial detensioning of G(s) occurred next with the removal of the two 1/2 inch shims. The Velzy ram was used to increase the force (and the elongation) in the strand until the shims were removed and then to release the strand. The cutting sequence then resumed in the following manner: B(s), D(n), F(n), C(s), A(s) and G(n).

As a safety precaution and as an energy dissipator, each strand was fitted with a three foot segment of strand in the region where the strand was to be flame cut. The short segment was connected to the strand by two cable clamps. The purpose of the clamps was to prevent the strand from unraveling during the cutting process and to provide a mechanism to dissipate energy. As the strand failed by yielding (from loss of strength from the applied heat), the movement of the strand was damped by the mechanical clamping of the short segment around the cut area. This provided a non-violent release of energy in comparison to strands cut without the short segment. Figure 3.7 illustrates the attachment of the short segment to the strand.

The data acquisition system was used to scan the strain gauges and load cell after each cut and after partial detensioning. After completion of the transfer procedure, strand slippage, relative to the end of the beam, was measured with a steel rule.

3.4 Test Setup

3.4.1 Description of Test Setup. The test bay was located next to the fabrication bays and consisted of two floor beams and a structural steel frame. The test setup was designed to accommodate a wide variety of load cases and embedment lengths without major modifications to the arrangement. Figure 3.8 illustrates the test setup.

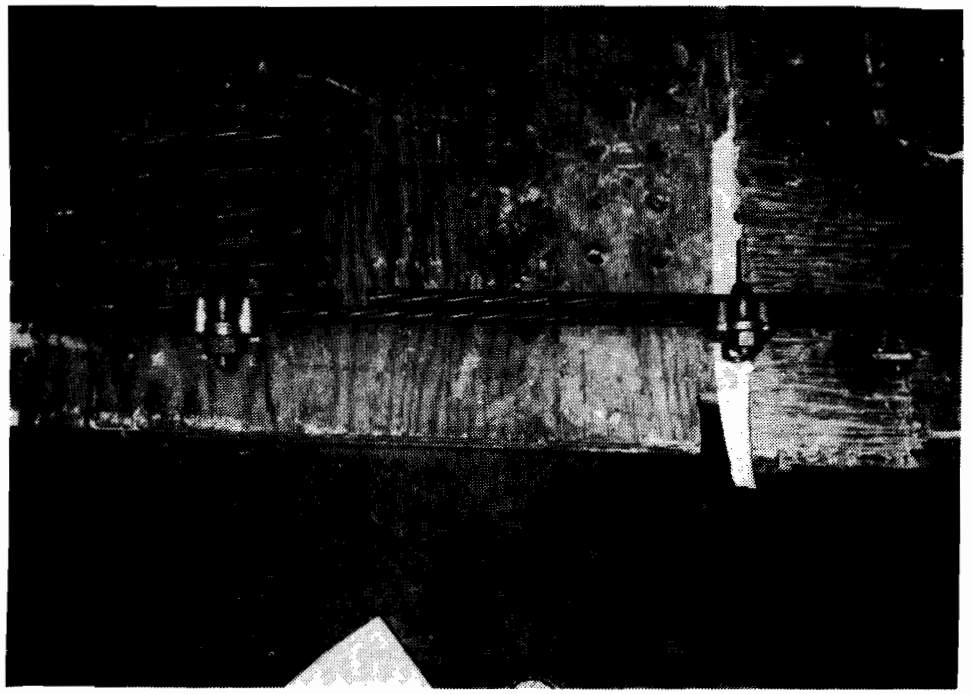

Figure 3.7 Strand Segment Serving as an Energy Dissipater

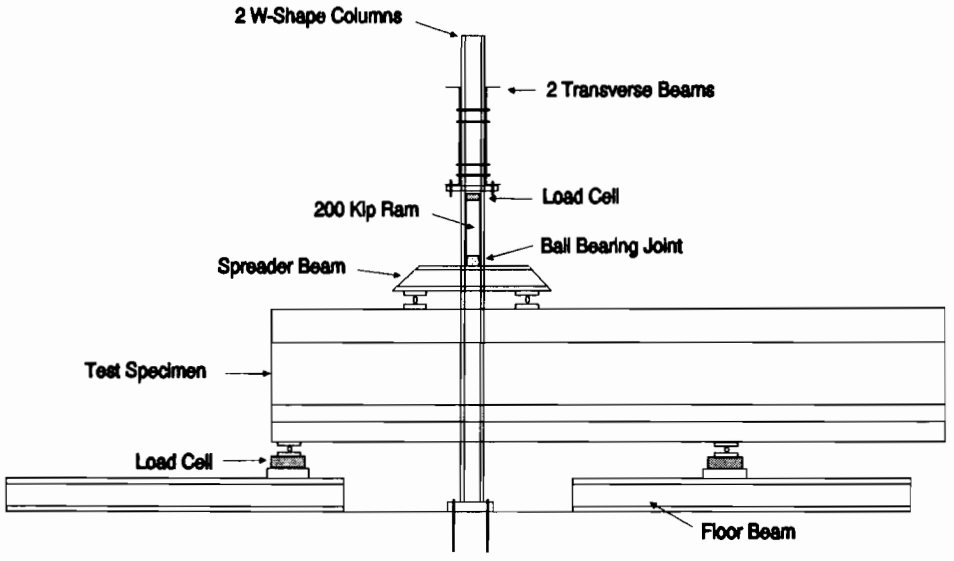

Figure 3.8 Test Setup

The two floor beams provided flexibility in the positioning of the specimen supports. To prevent movement relative to the floor and testing frame, the beams were embedded in hydrostone. Steel plates, four inches in width, were grouted into place on top of the support beams to provide a level bearing surface.

Figure 3.9 is a photograph illustrating a specimen support. In the arrangement, a load cell was sandwiched between two steel plates. The bottom plate bore directly against the floor beam and provided a complete bearing surface for the load cell. The top plate was permanently attached and had a piece of one inch diameter round stock welded to it. A second plate was positioned between the round stock and the specimen to provide a

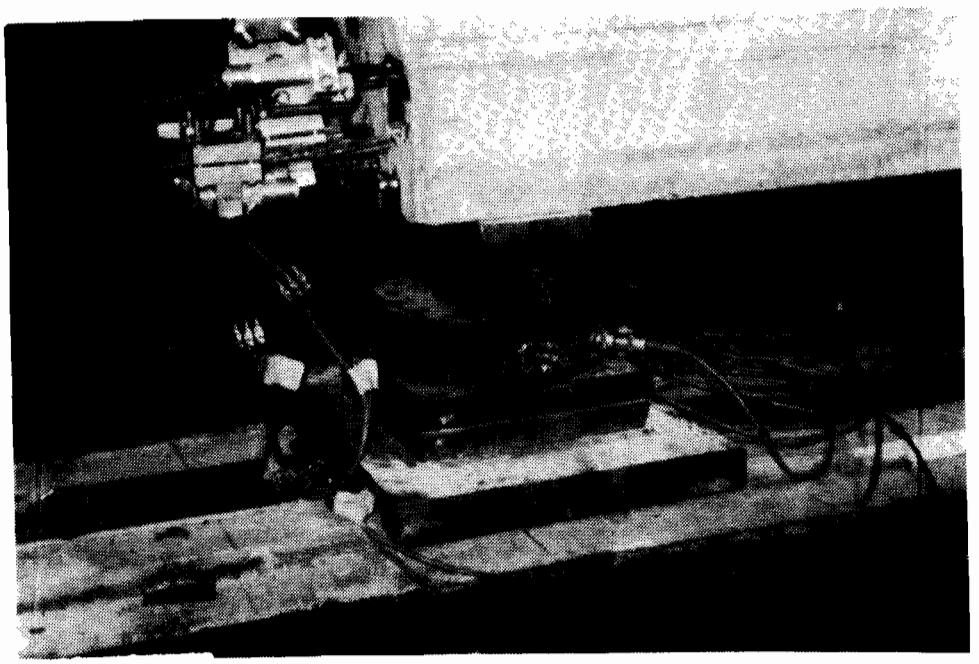

Figure 3.9 Specimen Support

bearing surface for the concrete. To reduce possible horizontal reactions in the "roller" support, common axle grease was applied to the round stock and bearing plate.

Once the specimen was in the correct position, two steel plates were positioned on top of the specimen and leveled with a two foot carpenter's level. The plates were seated in hydrostone to provide a solid bearing surface.

The load was applied to the specimen through a spreader beam consisting of a five foot length of a W10X88 steel section. The spreader beam was fitted with two pieces of one inch diameter round stock to provide point loads. Because the beam rested directly upon the hydrostoned plates, axle grease was provided to reduce the possibility of horizontal reactions at the bearing surfaces.

A 200 kip hydraulic ram was used to load the specimen. The ram rested on a ball and socket bearing assembly and reacted against the test frame. Positioned on top of the spreader beam, the ball and socket assembly was used to prevent moment transfer between the specimen and ram during testing. The test frame consisted of two W-shaped columns that were post-tensioned to the lab floor. Two transverse channel beams were bolted to the columns and provided a surface for the ram to load against.

3.4.2 Testing Instrumentation. During each test, the specimen's reaction to applied load was monitored by several types of instrumentation and recorded by the data acquisition system. The instrumentation involved load cells, a pressure gauge, a pressure transducer, linear variable displacement transducers, electrical strain gauges, and a mechanical strain gauge.

The applied load was determined from load cells positioned at each of the supports and at the point of application. The accuracy of each load cell was one percent of the registered load. Additionally, a pressure gauge and pressure transducer recorded the level of pressure in the hydraulic system for a further check on the applied load.

Deflections and strand end slips were measured by linear variable displacement transducers (LVDT). An average deflection was obtained by placing a pair of LVDT's between the load points. The LVDT's, positioned on each side of the bottom flange, could measure a maximum of six inches of deflection to the nearest thousandths of an inch before having to be repositioned.

Strand end slip was measured by clamping an LVDT to each strand on the end being tested. The LVDT's had a maximum stroke of two inches and accuracy of one thousandths of an inch. Figure 3.10 illustrates the attachment of the LVDT's to the strands.

Strain in the prestressing strand was obtained through electrical strain gauges applied before the concrete was cast. These same strain gauges measured the pretensioning forces and losses during fabrication.

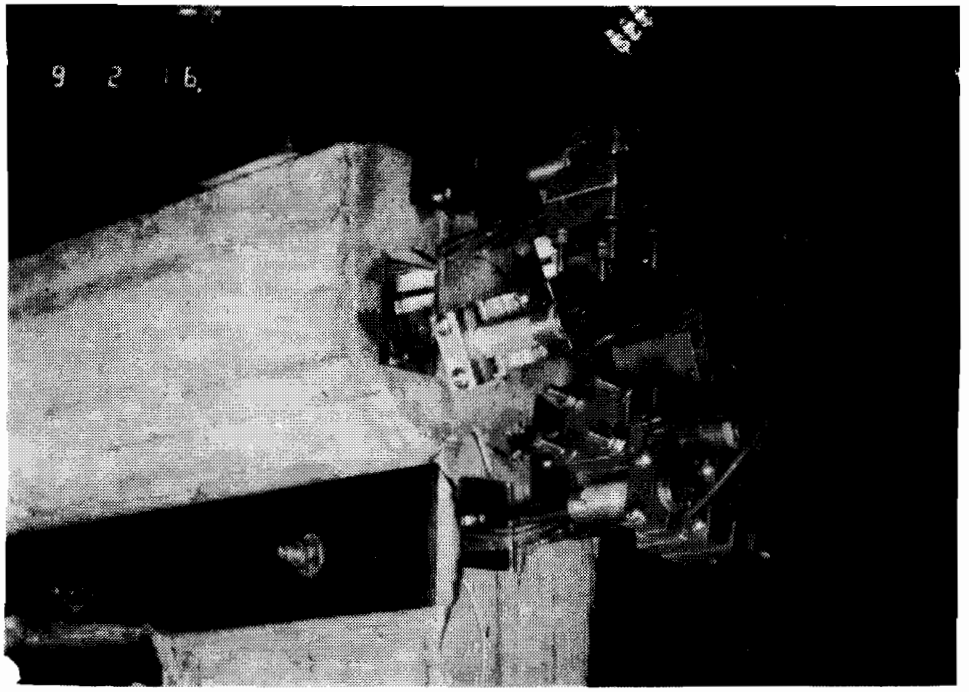

Figure 3.10 End Slip Measurement Devices

Compressive strain in the extreme fibers of the concrete flange was measured by four pairs of DEMEC gauge points. The points were positioned on the beam with a 1-1/2 inch lateral spacing and an 8 inch gauge length. The gauge points were 2 inches from the edge of the top flange on both sides of the beam. A common five-minute epoxy attached the points to the surface of the concrete. Figure 3.11 is a photograph exhibiting the position of DEMEC gauge points.

Measurements were taken by recording the distance between points using a special mechanical dial gauge. An initial set of readings, taken before testing began, served as reference points. As the load increased and caused higher compressive concrete stresses, the change in strain was determined by subtracting the distance measured under load from the reference distance. The result was then multiplied by the correct gauge calibration factor to determine the strain in the concrete. The accuracy of the DEMEC system was ± 20 microstrain (± 0.00002 in/in).

3.4.3 Test Procedure. The test procedure called for incremental loading of the specimen while taking readings at each load level. Initially, the application of load was in 5 kip increments but decreased to as little as 2 kips once flexural cracking occurred. When unanticipated behavior occurred, loading was halted for measurements and observations. At each increment of load, measurements of strand strain, applied load, end slip, hydraulic pressure, deflections, and concrete compressive strain were taken. Also, important observations about beam behavior and cracking pattern were recorded. All visible cracks

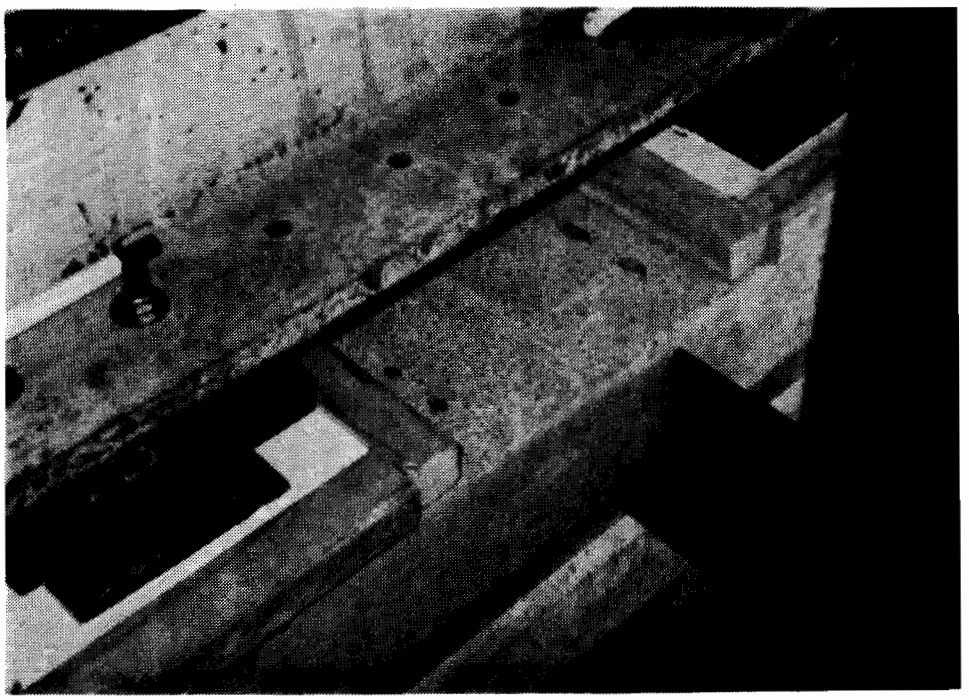

Figure 3.11 DEMEC Gauge Points

were marked with ink markers and labelled with the appropriate level of load. Loading continued until failure occurred. Typically, a complete test took approximately two hours.

3.4.4 Test Modifications on 40' Beams. During the testing procedure, modifications were made to the 40 foot specimens to prevent strand slippage during the second test. If the first test resulted in bond failure and strand slip, it was feared that additional strand slip could occur and influence the results of the second test. The modification was a physical restraint of the strands at the previously tested end.

This was accomplished by welding a set of plates to the exposed strands at the end of the specimen. The welding prevented the strands from rotating and also provided a physical anchorage to keep them from slipping. Figure 3.12 is a photograph of the completed modification.

3.4.5 Test Modifications on 27.5' Beams. Two modifications to the shorter specimens occurred during the completion of the experimental phase. The first modification addressed the problem of controlling web shear cracking. The second modification was directed toward the prevention of strand movement during the second test on a specimen.

The first modification developed after discovering that the shorter girders contained insufficient reinforcement (Section 4.2.9) to control the propagation of web shear cracks. After calculating the required amount of steel to control the cracking, steel plates were fabricated and epoxied to both sides of the web.

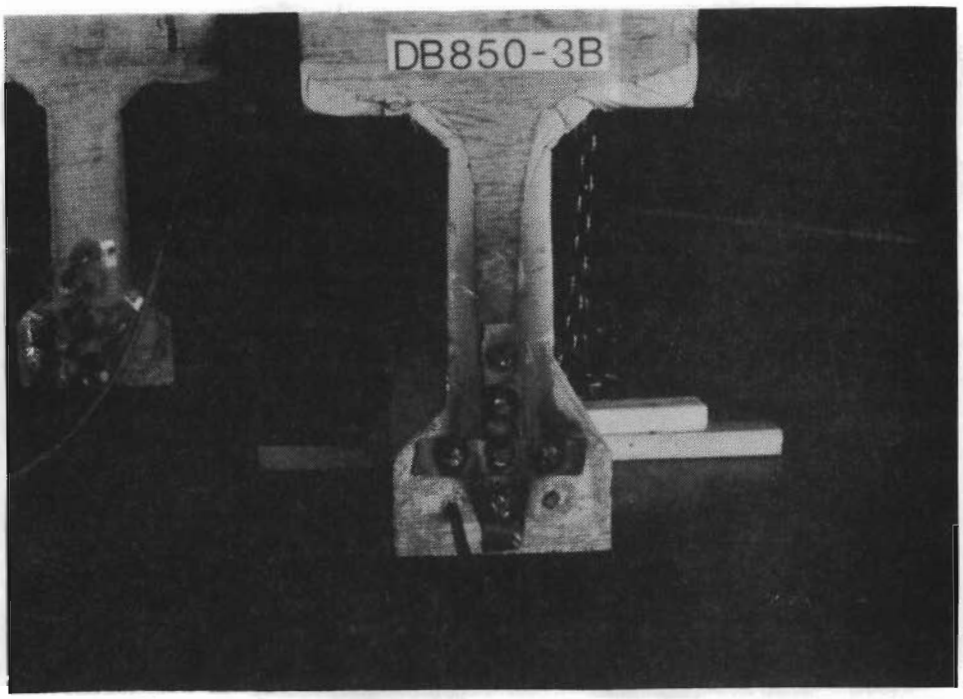

Figure 3.12 Test Modification to 40-Foot Beams

Because of a minor incompatibility of a formwork joint, a 1/8 inch difference was present in the surface of the web for tests DB850-1B(G) and DB850-2A(G). Four, three inch wide steel plates were fabricated for each side of the specimens to account for the surface flaw. Welding of the plates into a unit was to occur before testing took place. For DB850-2B(S) only two plates per side were necessary since the sides of the web were smooth.

The plates were attached to the south end of DB850-1 in the following manner:

1. Holes were drilled into the web to a depth of one inch to facilitate the placement of anchor bolts. The bolts provided a mechanical means of attaching the plates tightly to the web while the epoxy cured.

2. The steel plates were fabricated to match the anchor bolt pattern and were polished to provide a clean bonding surface for the epoxy.

3. The epoxy was mixed and applied to the web of the specimen.

4. The steel plates were slipped over the bolts and positioned into place on the web against the epoxy.

4. The anchor bolts were tightened down in order to provide a thin layer of epoxy between the concrete and the plates.

5. The plates were to be welded after 24 hours of curing.

Unfortunately, it was discovered that the epoxy was flammable in its solid state so welding was abandoned for test DB850-1B (G). For tests' DB850-2A (G) and DB850-2B (S), the welding occurred before the plates were epoxied to the sides of the web. Figure 3.13 is a photograph illustrating the location and application of the plates to the web of the beam.

The second adjustment needed was similar to the modification completed on the 40 foot specimens. However, because of the amount of damage and strand slip recorded, it was necessary to provide an additional mechanism to repair the cross section and to prevent further slip. A decision to utilize post-tensioned, external reinforcement to provide an external clamping force was based on related research completed by Riyad Aboutaha [1]. Because the extent of damage was different, the repair of each beam was unique.

In the repair of the beam for test DB850-1B (G), five sets of post-tensioning rods (5/8 inch Dywidag prestressing bars) were used to clamp the strand at the damaged end. Three sets were placed across the failed zone at a distance of 24, 32, and 44 inches from the end of the beam and were stressed to a load of 7 kips per rod. Two additional sets of rods were provided at 84 and 96 inches from the beam's end. The force in those rods reached the maximum design capacity of 29 kips per rod.

In the beam repair for test DB850-2B(S), the damage to the cross section and resulting end slip was minor in comparison to the first repair. Only two sets of post-tensioning rods were necessary. Their position was at 36 and 72 inches from the beam end and each rod was stressed to the desired force of 20 kips.

In both cases, strain gauge readings and behavior of the beams under loading suggested that the repair was successful in controlling further end slip. Figure 3.14 is a photograph illustrating the repairs completed to beam DB850-1.

3.5 Data Acquisition System

In order to obtain and store the data, an IBM personal computer was used in conjunction with a Hewlett Packard scanner to scan the electrical instrumentation. For convenience, the instrumentation (load cells, LVDT's, pressure transducer, and strand strain gauges) fed into a centralized circuit panel which was wired directly into the scanner. A program, written by Alex Tahmassebi (HPDAS2), scanned each of the channels on the panel and recorded the change in voltage for each instrument. The data was later converted from voltages to engineering units by another program, CPROF7. This program conveniently formatted the data for use in a spread sheet.

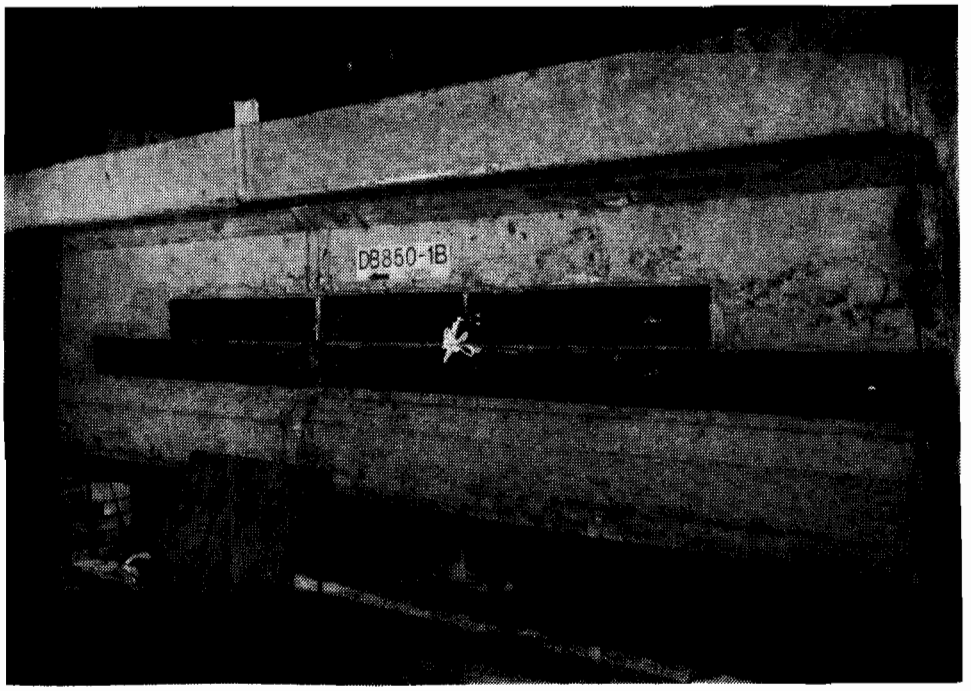

Figure 3.13 Steel Plate Cladding, Test DB850-1B(G)

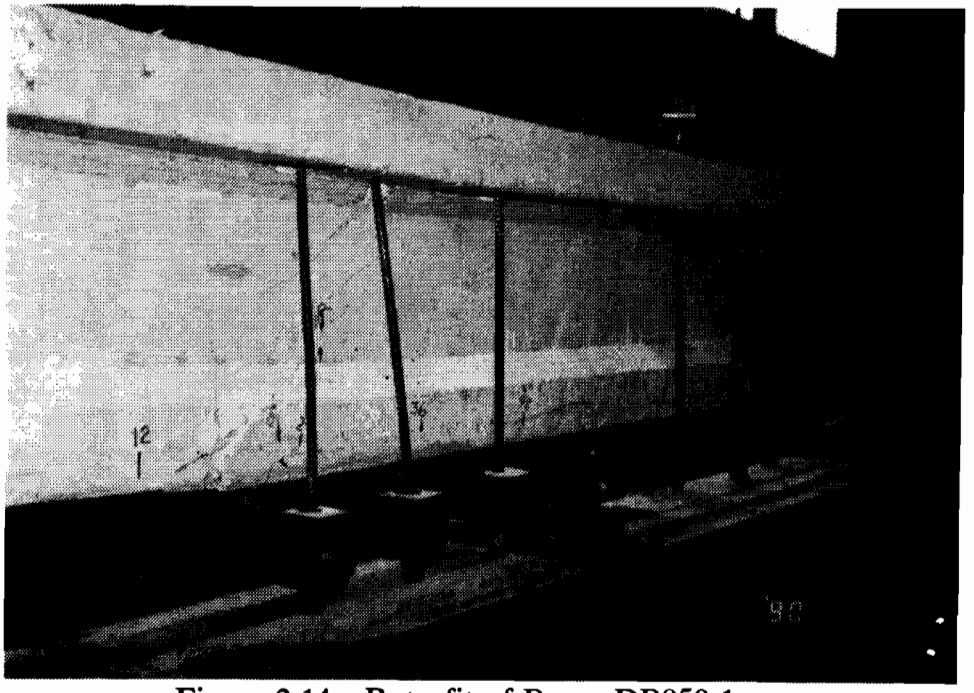

Figure 3.14 Retrofit of Beam DB850-1

CHAPTER FOUR

PRESENTATION OF TEST RESULTS

This chapter presents the data gathered in the production and testing of the six specimens in this investigation. Section 4.1 is dedicated to displaying the data obtained in the fabrication of the specimens. Section 4.2 presents a detailed description of each of the eleven tests completed on the six specimens. Section 4.3 is a summary of the test results presented in Section 4.2.

4.1 Specimen Fabrication Results

4.1.1 Initial Pretensioning. During girder fabrication, it was important that the force in each strand was approximately equal. To achieve the necessary consistency, the pressure in the hydraulic stressing system was closely monitored by a pressure indicator and a pressure transducer to manually regulate the amount of force applied to each strand.

To determine the actual level of stress in each strand after seating losses, a steel rule and a LVDT was used to measure the elastic elongation of each strand during stressing. For strands B and G, the data acquisition system gathered additional data from the strain gauges applied to the two strands before stressing.

Figure 4.1 displays the level of stress in strands B and G as registered by the strain gauges for each beam. The average value of stress in the strands after seating losses was 192 ksi.

As an additional source of data, a LVDT and a steel rule measured the elastic elongation of each strand after completion of the stressing process. Initial measurements were taken after the application of 200 psi to the hydraulic system. The 200 psi corresponds to a stress of 10.5 ksi in the strand. In Figure 4.2, the left side illustrates the amount of strand elongation registered for each strand of DB850-6. The right side corresponds to the value of stress in each strand including the initial 10.5 ksi. The average value of stress for DB850-6 was 199 ksi which is higher than the overall specimen average of 197 ksi.

4.1.2 Losses from Transfer. During the transfer procedure, a portion of initial force was lost due to elastic shortening of the specimen. The loss of force was registered as a change in strain by the strain gauges mounted on the strand. Figure 4.3 presents the amount of stress in strands B and G after transfer occurred. The average loss of stress due to elastic shortening at transfer was approximately 14 ksi. This resulted in an initial prestress force, f_{si}, of approximately 178 ksi per strand.

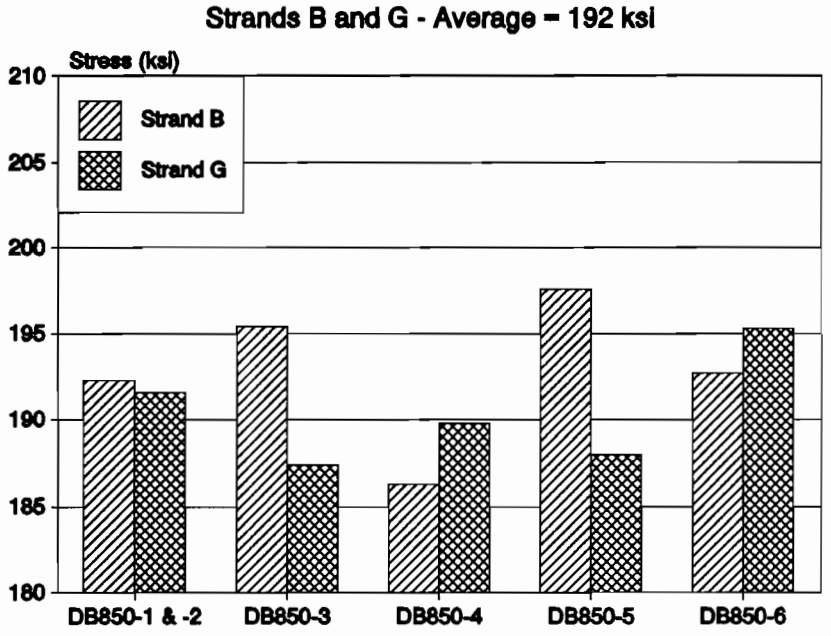

Figure 4.1 Level of Stress in Strands B and G Before Transfer

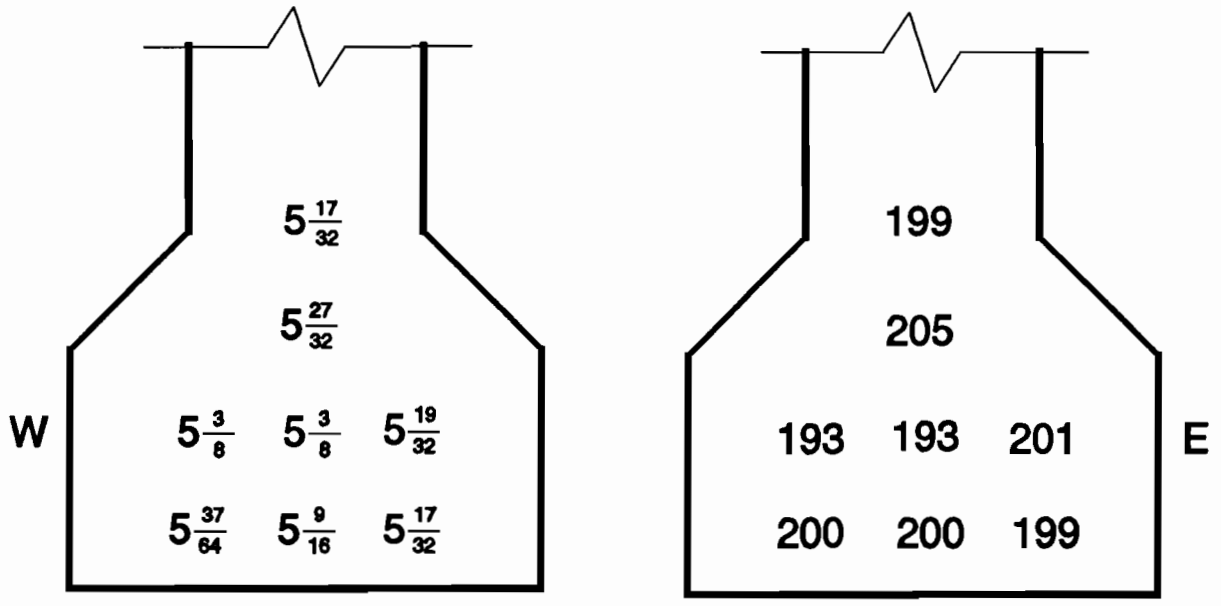

Figure 4.2 Strand Elongation and Stress for DB850-6

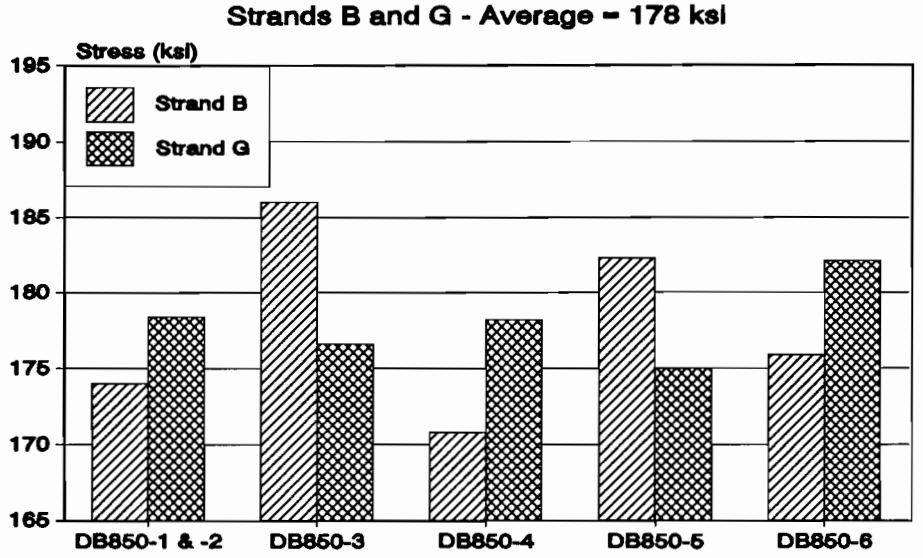

Figure 4.3 Level of Stress in Strands B and G After Transfer

4.1.3 Effective Prestress Force at Time of Testing. From the time of initial stressing until the specimen was actually tested, a period of 50 to 70 days occurred. In this time, the stress in the strand was reduced by a series of losses including transfer, creep and shrinkage. These losses were estimated using the general method described by the PCI Committee for calculating prestress losses [10,15]. The losses were estimated using the value of stress calculated from the elongation measurements and are included in Appendix C.

The calculations determined that the value of stress after transfer was 179 ksi which correlated well with the value of 178 ksi obtained from the strain gauges. For the average time period of 60 days, the effective prestress was estimated at 160 ksi per strand.

4.2 Test Results

The specimens in this study were tested to determine the validity of the prediction model. A total of eleven tests were completed according to the test procedure outlined in Section 3.4.3. Although the failure modes could be classified as either a flexural failure or a bond failure, each test presented insight into the behavior of girders with debonded strands. A full description of each test is presented in the order of testing.

4.2.1 Failure Criteria. During testing of the specimens, two types of failures were possible: bond failure and flexural failure. Bond failure was the mode of failure that prevented the specimen from achieving adequate flexural strength and ductility. A typical bond failure included strand slip, resulting in a loss of prestress. A dramatic decrease in load

carrying capacity of the test specimen normally followed. Depending on the amount of prestress lost, the failure could be catastrophic.

A flexural failure was the mode of failure that allowed the cross section to achieve the calculated ultimate flexural strength and ductility. Typically, a flexural failure included yielding of the strands and eventual crushing of the concrete in the extreme compression fibers without perceivable strand slip.

A flexural failure could also occur with a slight amount of end slip. This was possible if the specimen was at, or near, the calculated capacity when the strands began to slip. For the failure to be considered a flexural failure, the specimen must have continued to allow additional deformation to occur while maintaining (or increasing) the load carrying capacity. Strand yielding and a compressive failure of the concrete was also necessary to classify the failure as flexural.

4.2.2 Calculation of Flexural Capacity and Deflections. A strain compatibility analysis was used to determine the moment- curvature relationship for the cross section of the specimens. The values calculated were then used to estimate the amount of deflection under the applied loading. The calculations for generating the moment curvature relationship are found in Appendix C.

During the testing procedure, an estimated load versus deflection plot was generated for each test and used to identify possible changes in behavior. To develop the 'calculated' load versus deflection curve, three points of immediate interest were chosen. The points corresponded to first cracking, yield ($f_{ps} = 0.9f_{pu}$), and the ultimate load. The calculated curves are illustrated on the actual load versus deflection plots for each test.

4.2.3 Test DB850-3A (G). Test DB850-3A (G) was performed on the north end of specimen DB850-3 which contained gradually debonded strands. The setup tested an embedment length of 80 inches, corresponding to a development length of 1.0 L_d (defined by equation (1) in Section 2.2). An overview of the test layout is presented in Figure 4.4.

As displayed by Figure 4.5, the deformations were linearly proportional to the load until flexural cracking occurred at a load of 44 kips, directly beneath the load points. At 63.5 kips, strand G registered the first end slip of 0.065 inches.

At a load of 66 kips, flexural cracks were observed in the debond/transfer zone at a distance of 88 and 96 inches from the end of the beam. Although no major end slip was registered at that level, significant end slip occurred in strands B and G as the load was increased. Figure 4.6 illustrates the measured strand end slip.

Under additional loading, the specimen continued to exhibit increased load carrying capacity. However, at a load of 69.6 kips, the specimen experienced a sudden reduction in load capacity and exhibited a compression failure of the top flange.

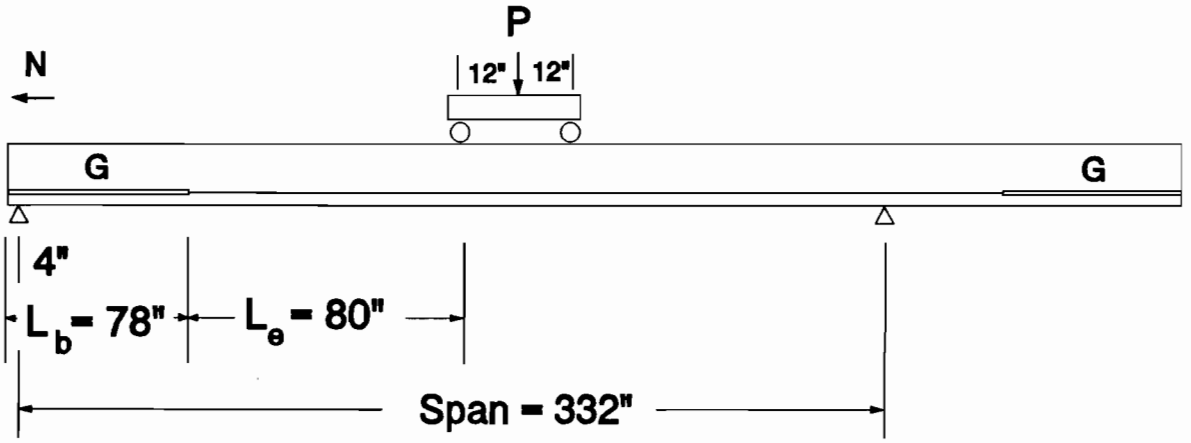

Figure 4.4 Test Setup for DB850-3A (G)

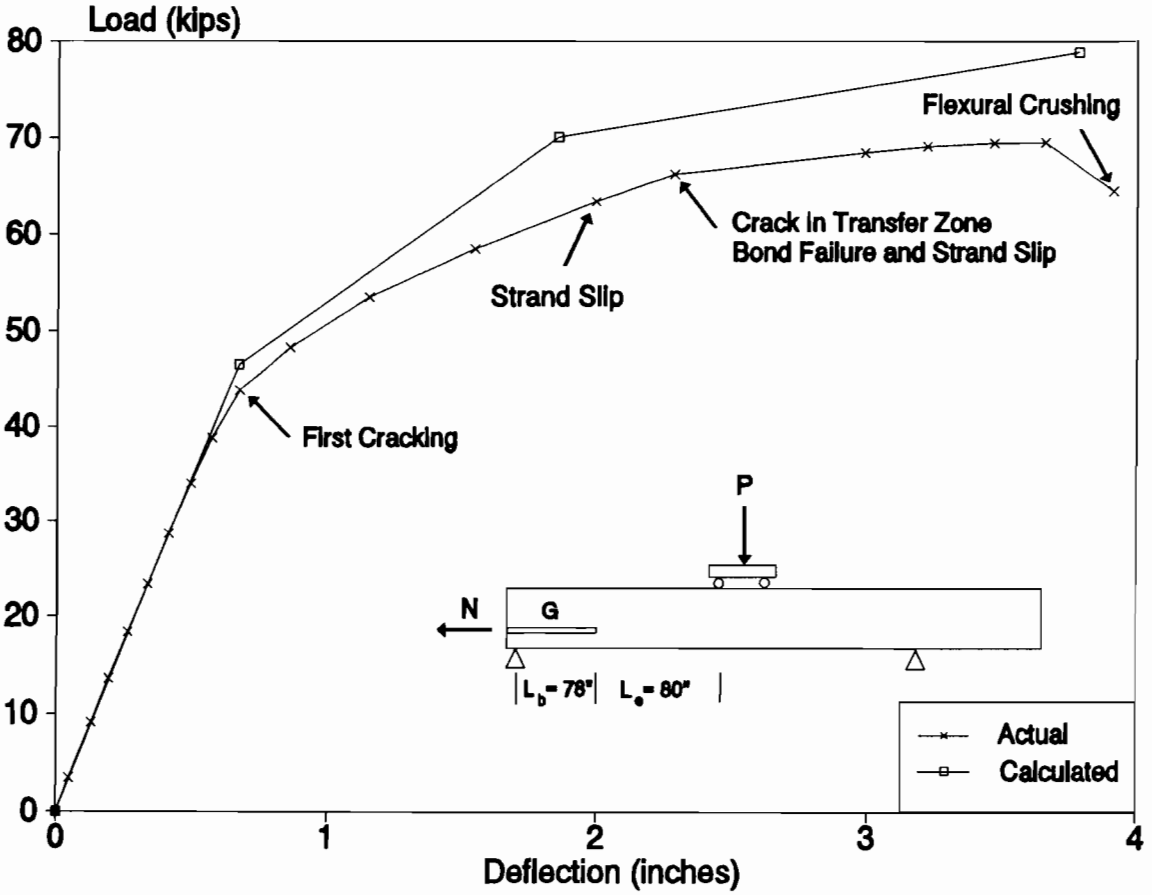

Figure 4.5 Load vs. Deflection, DB850-3A (G)

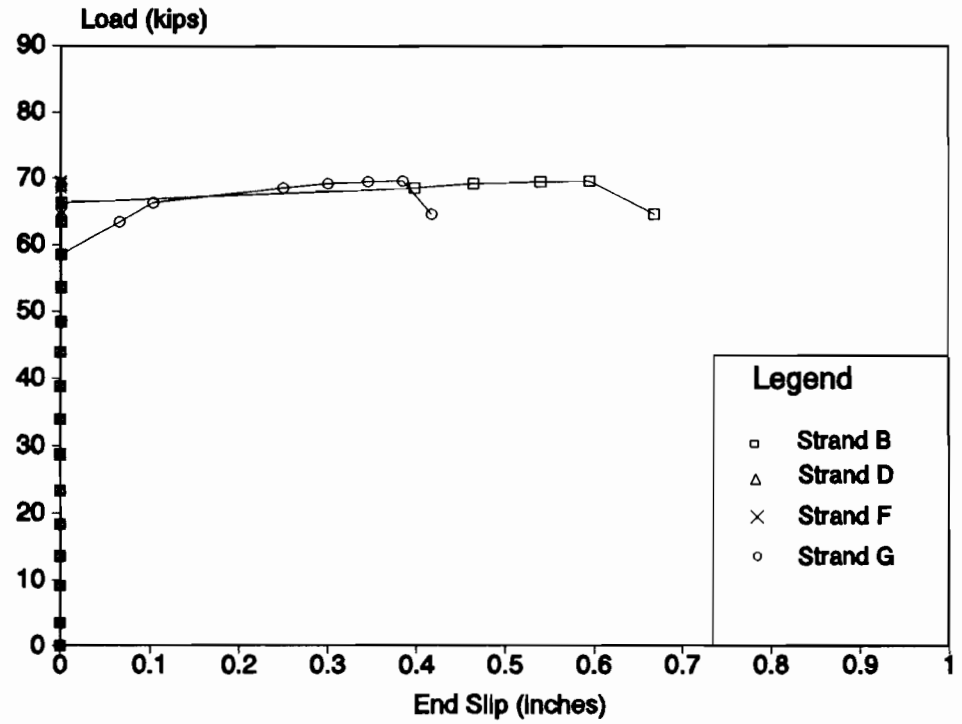

Figure 4.6 Load vs. End Slip, DB850-3A (G)

Although a concrete compression failure occurred, the specimen did not achieve the calculated ultimate flexural capacity. Furthermore, the specimen experienced significant amounts of slip in strands B and G resulting in an average end slip of 0.542 inches. These factors classified test DB850-3A (G) as a bond failure.

4.2.4 Test DB850-3B (G). Test DB850-3B (G) was conducted on the south end of specimen DB850-3. The test was set up with an embedment length of 108 inches corresponding to a development length of 1.35 L_d. The test layout is shown in Figure 4.7.

As portrayed by the load versus deflection plot (Figure 4.8), the girder behaved elastically until the first flexural cracking occurred at 39.5 kips. Under additional loading, deformations increased more rapidly than expected. Upon close examination of the specimen, it was determined that the flexural cracks formed during test DB850-3A (G) were reopening and allowing greater deflection to occur.

At a load of 66 kips, the first end slip of 0.101 inches was recorded in strand B (Figure 4.9). Under further loading, increased deformations resulted only in a small

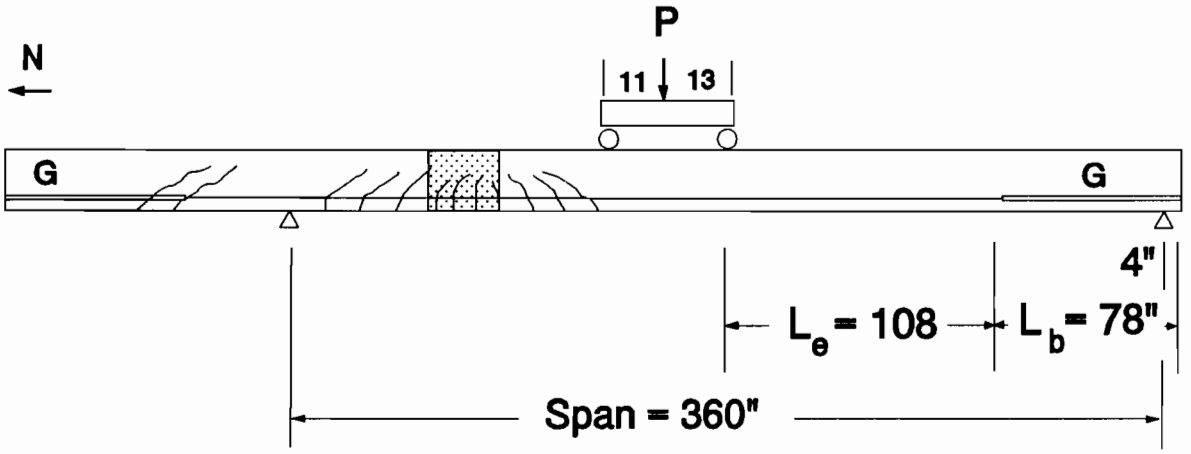

Figure 4.7 Test Setup for DB850-3B (G)

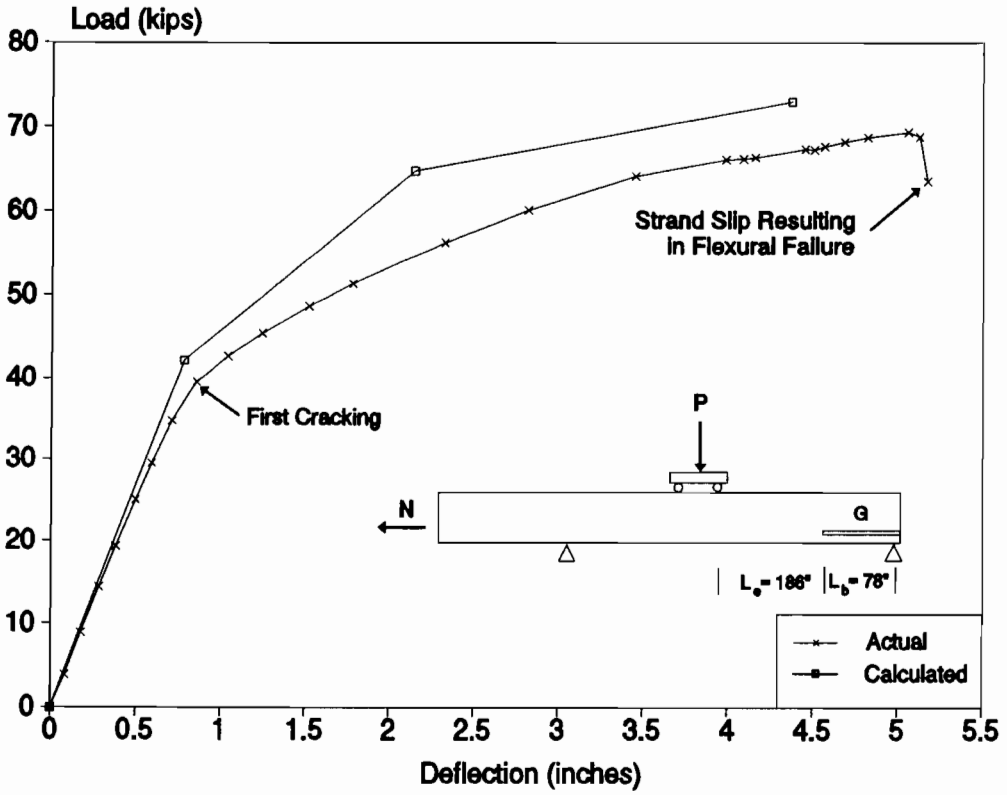

Figure 4.8 Load vs. Deflection, DB850-3B (G)

increase in load carrying capacity. At a load of 67.3 kips, a concrete strain of 0.003 inches/inch was measured in the top flange of the girder. At this point, strand B registered an end slip of 0.204 inches as shown by Figure 4.9.

The loading was continued because slight increases in the specimen's load carrying capacity were still being recorded. Crushing of the concrete occurred between the load points at approximately 69 kips and at a deflection of 5.25 inches. This corresponded to 95 and 125 percent of the calculated load and deflection, respectively.

Under the procedures developed for testing (Section 3.4.3), once crushing began, loading was stopped immediately but was not removed. After one to two minutes under full load, the girder erupted in a violent explosion. Apparently the limit of the section's ductility was reached at almost the same time crushing of the concrete occurred.

The explanation for the eruption was that the neutral axis of the cross section was positioned near the bottom of the top flange when crushing began. As crushing occurred, the neutral axis attempted to shift lower in the beam to include additional concrete in the compression zone. Unfortunately, the additional concrete was not available, resulting in the violent explosion.

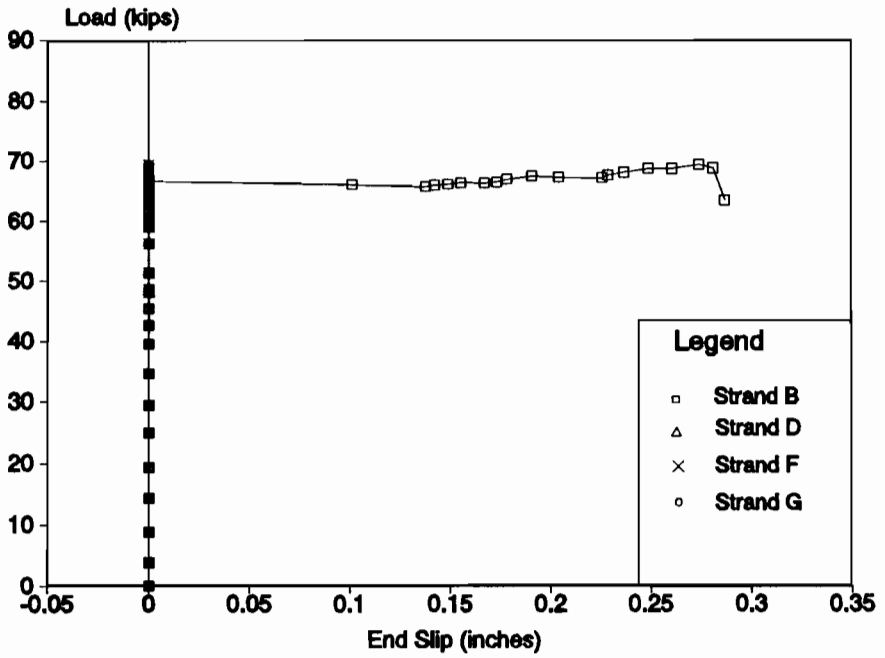

Figure 4.9 Load vs. End Slip, DB850-3B (G)

As a summary, test DB850-4B (G) reached 95 percent of the calculated ultimate flexural capacity. Although slight end slip was registered in strands B and G, a reduction in load capacity through general bond slip did not occur. Additionally, the deflection recorded under load exceeded the estimated deformations by 25 percent, thus providing adequate ductility. This test was defined as a flexural failure.

4.2.5 Test DB850-4A (G). Test DB850-4A (G) was performed on the north end of specimen DB850-4. The test was set up with an embedment length of 120 inches, 1.50 L_d, and is shown in Figure 4.10.

As expected, the girder behaved elastically until flexural cracking occurred at a load of 42 kips. The behavior is displayed by the load versus deflection plot shown in Figure 4.11. Failure of the specimen occurred when the concrete crushed between the load points at a load of 70.33 kips.

Figure 4.12 plots the load versus end slip for the test. It shows that strand B started slipping at a load of 16 kips and continued to slip to a maximum of 0.095 inches at failure. The slip is unusual because cracking did not occur in the debond/transfer zone. The end slip is also contrary to the data recorded by the strand strain gauges.

Figure 4.13 illustrates the load versus strain increase in the strands. Each strain gauge exhibits a linear behavior until the concrete cracking moment is exceeded at the corresponding gauge location. At that point, the increase in steel strain jumps dramatically to carry the tensile load released by the concrete. The strain continues to increase in the strand until failure occurs. This would indicate adequate bond development and would discount the general strand slip necessary to produce end slip. Also, if the strand had slipped, a dramatic loss in strand strain would have occurred. An example of this behavior is in Section 4.2.6, Figure 4.17.

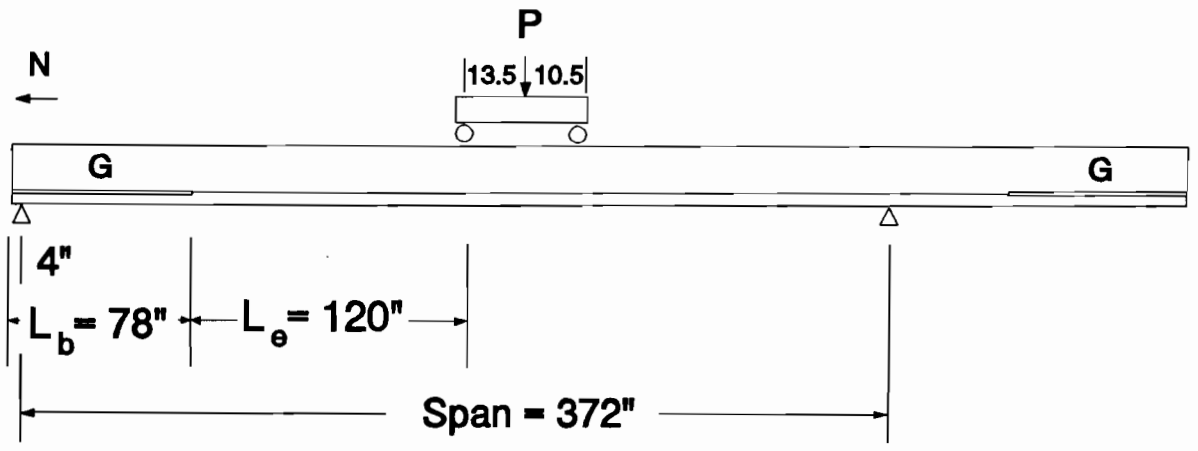

Figure 4.10 Test Setup for DB850-4A (G)

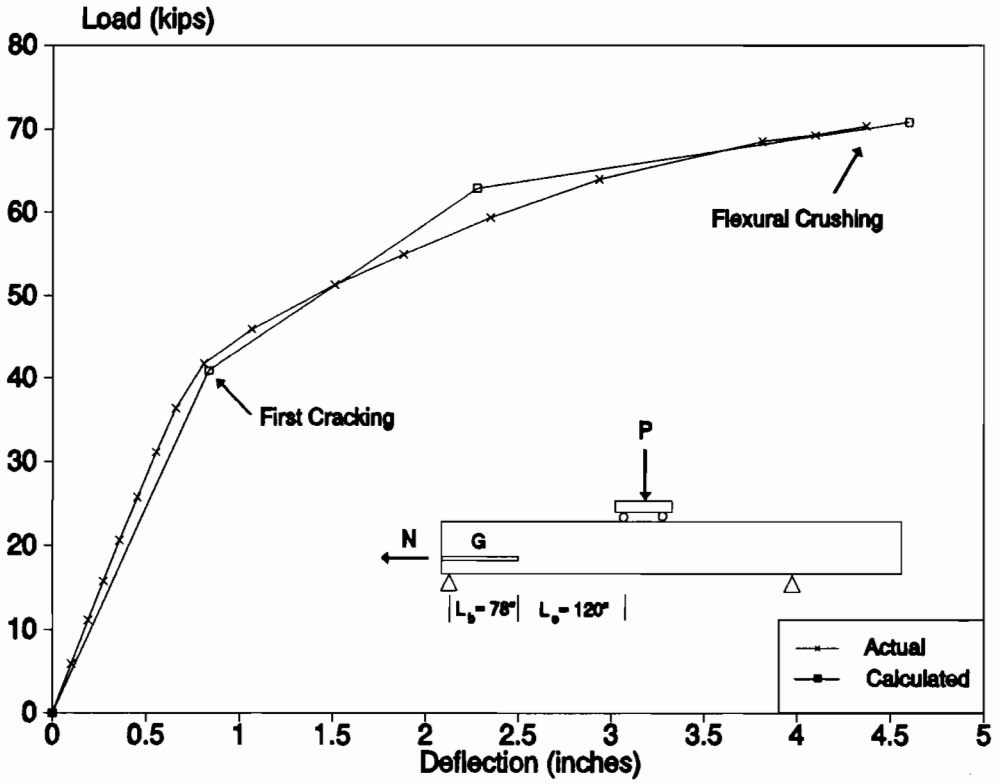

Figure 4.11 Load vs. Deflection, DB850-4A (G)

As displayed by Figure 4.11, the specimen achieved the ultimate flexural capacity and deflection calculated. The failure mode for this test was a flexural failure.

4.2.6 Test DB850-4B (G). Test DB850-4B (G) was performed on the south end of specimen DB850-4. The test was set up for an embedment length of 100 inches, 1.25 L_d, and is shown in Figure 4.14.

As depicted by Figure 4.15, the specimen behaved elastically until flexural cracking occurred at a load of 46 kips. At 71 kips, a crack formed near the debond/transfer zone at a distance of 108 inches from the end of the beam. The consequence was strand B immediately registered an end slip of 0.063 inches. Under additional loading, strand G also began to display end slip which is shown in Figure 4.16.

The strand slip was also recorded by the strain gauges mounted on the strands. Figure 4.17 displays the load versus strain increase in strand B. The strand shows an increase in strain until the load of 71 kips is reached. As the cracking occurred near the

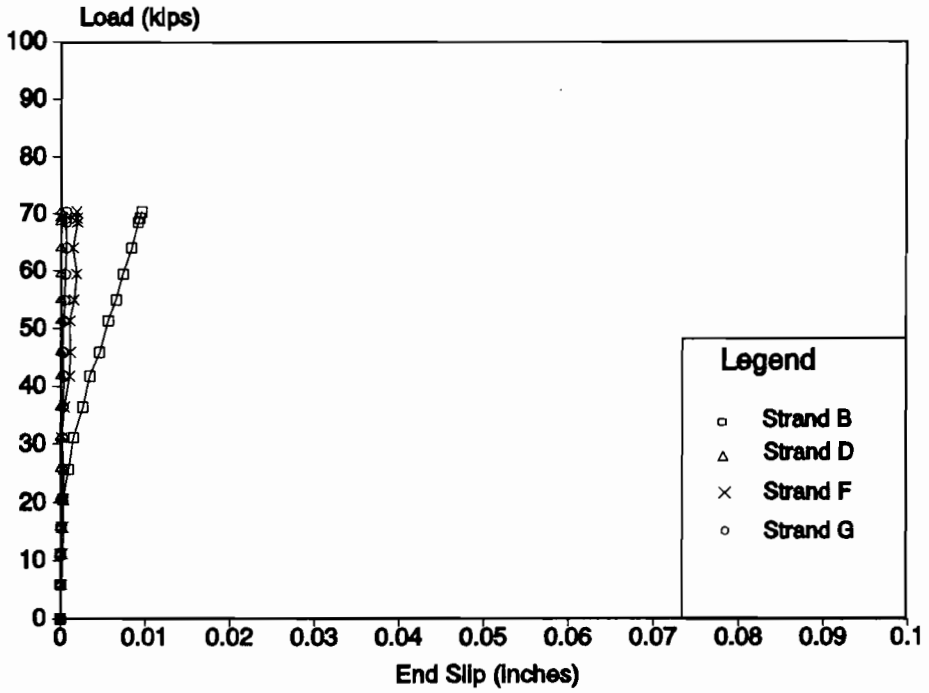

Figure 4.12 Load vs. End Slip, DB850-4A (G)

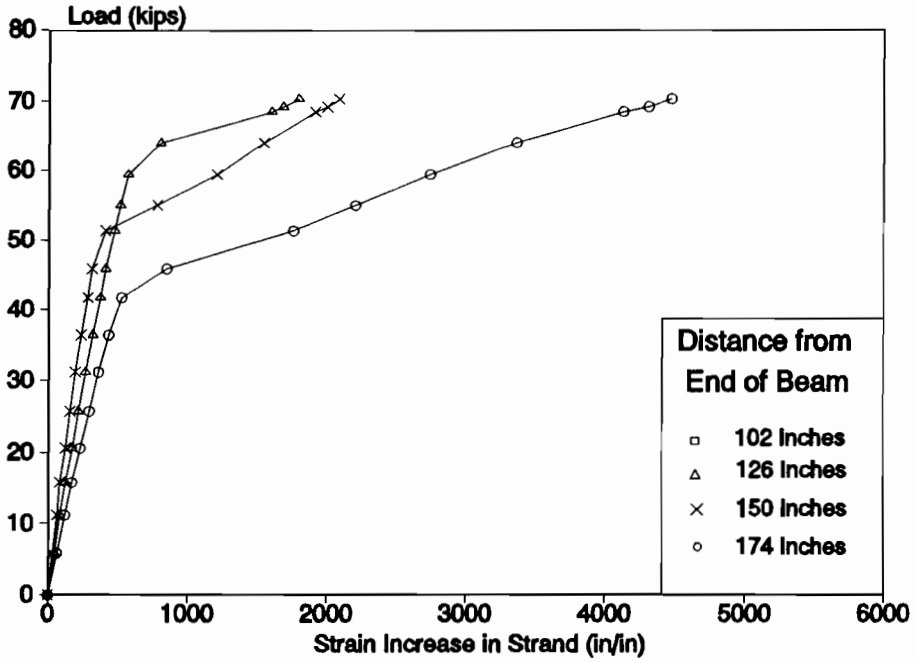

Figure 4.13 Load vs. Increase in Strand Strain, DB850-4A (G)

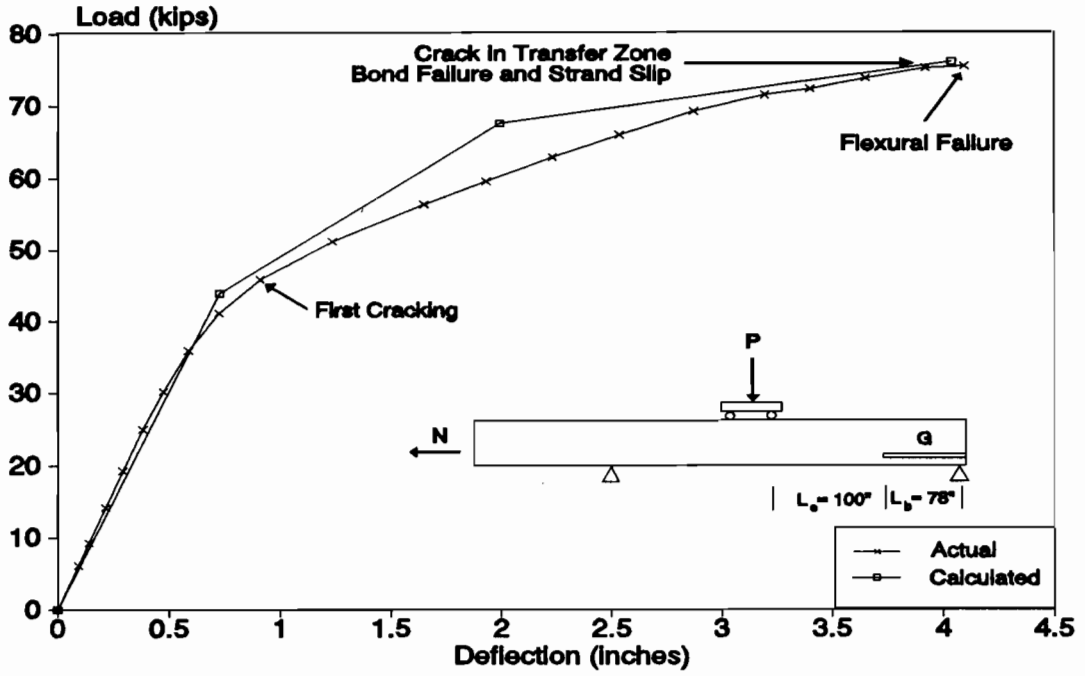

Figure 4.14 Test Setup for DB850-4B (G)

debond/transfer zone, an immediate loss in strain was registered. Under additional loading, the reduction of strain continued until failure occurred.

At 75 kips, additional flexural cracking developed at 95 inches, inside the debond/transfer zone. At a load of 75.4 kips (99 percent of ultimate), the loading was stopped. Strands B and G registered 0.24 and 0.13 inches of end slip, respectively. The specimen was returned to an unloaded condition in which a permanent deflection of 0.3 inches was recorded.

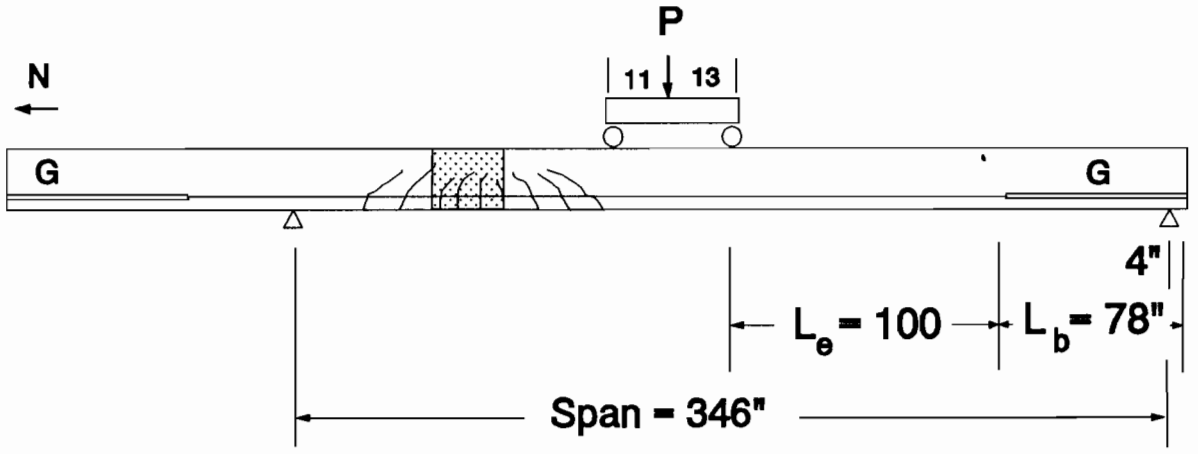

Figure 4.15 Load vs. Deflection, DB850-4B (G)

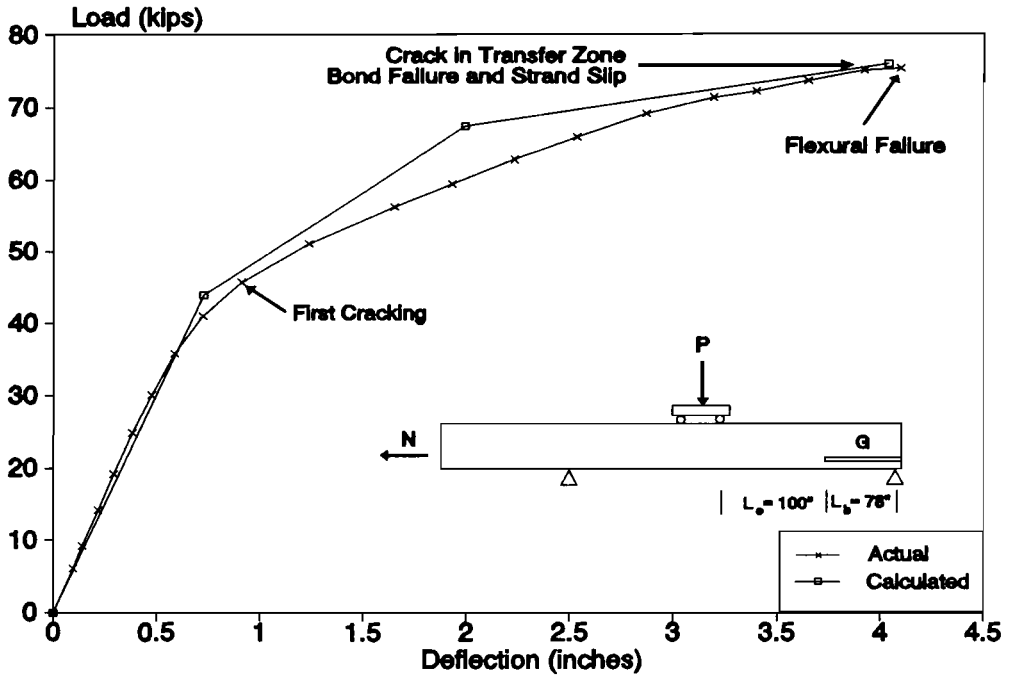

Figure 4.16 Load vs. End Slip, DB850-4B (G)

The specimen was then reloaded, in 10 kip intervals, to almost 60 kips. Figure 4.18 displays the load vs. deflection plot for both the initial and reload phases. Loading was stopped after additional strand slip occurred.

As a summary, test DB850-4B (G) reached 99 percent of the calculated ultimate flexural capacity. Although end slip was registered in strands B and G, a reduction in load capacity through general bond slip did not occur. This test was defined as a flexural failure.

It is important to note that, according to the prediction model, the load arrangement placed test DB850-4B (G) on the boundary line between bond failure and flexural failure. The 'borderline' behavior was also supported by the test data. The failure mode was a flexural failure that reached 99% of the calculated ultimate moment capacity and displayed adequate ductility. However, significant end slips were observed, on the order of 0.24 inches, which indicated bond failure was imminent.

4.2.7 Test DB850-5A (S). Test DB850-5A (S) was performed on the north end of specimen DB850-5. The specimen contained four suddenly debonded strands which were all terminated at 78 inches from the end of the beam. Designed as a companion to test DB850-4A (G), the test was set up to determine the influence of sudden versus gradual

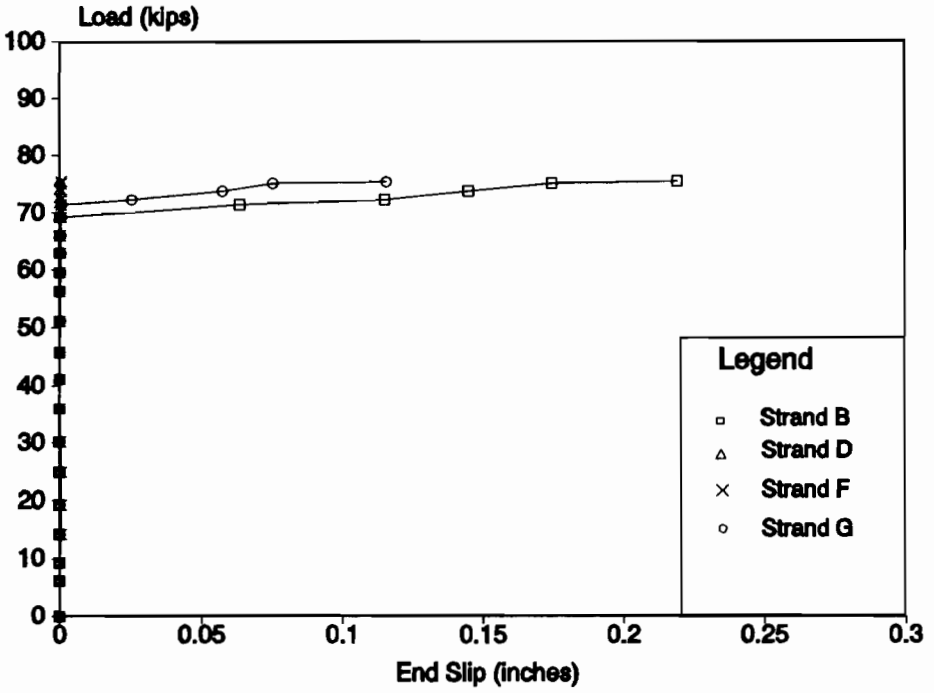

Figure 4.17 Load vs. Increase in Strand Strain, DB850-4B (G)

termination of debonding on the behavior of the girder. The setup is illustrated in Figure 4.19.

Figure 4.20 displays the load versus deflection plot for the test. The first flexural cracks developed between the load points at a load of 52 kips. Crack formation and deformation continued as additional load was applied. At 78 kips, a flexural crack formed in the debond/transfer zone at a distance of 81 inches. Immediate strand slips of 0.025, 0.015, and 0.022 were recorded for strands B, F, and G, respectively. Additional loading resulted in an increase in deflection of 0.3 inches with a slight loss in capacity of 0.1 kips (Figure 4.20). At this point, strands B, F, and G each displayed additional end slip of approximately 0.08 inches.

Further loading resulted in an increase in load carrying capacity to a maximum value of 81.2 kips. The average end slip at this point was 0.18 inches for the three strands as shown in Figure 4.21. As loading resumed, additional deformation ensued with further loss of load carrying capacity. Failure resulted by the crushing of the concrete directly beneath the north loading point at a load of 71.2 kips and a deflection of 4.6 inches. The results correspond to 88 percent of the calculated ultimate flexural capacity and 133 percent of the estimated deflection.

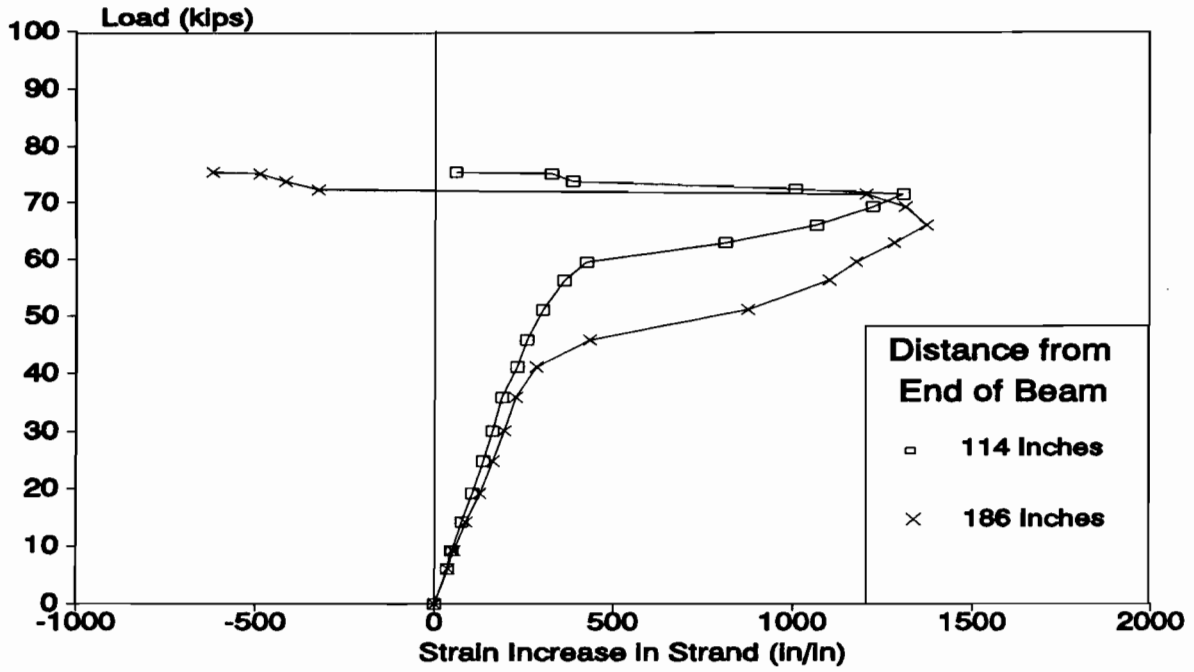

Figure 4.18 Load and Reload vs. Deflection, DB850-4B (G)

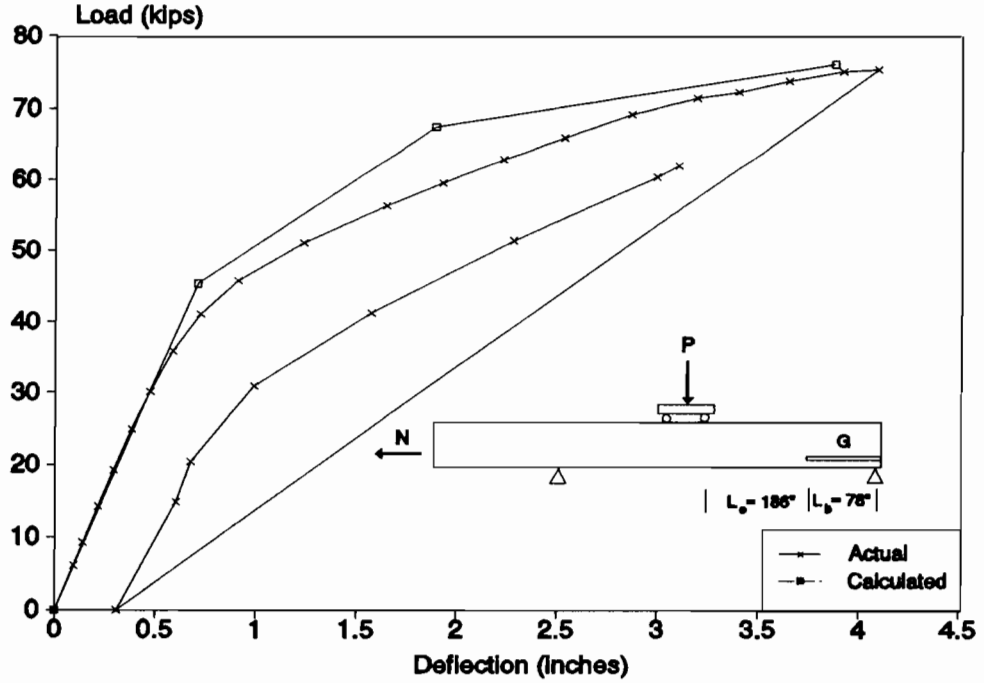

Figure 4.19 Test Setup for DB850-5A (S)

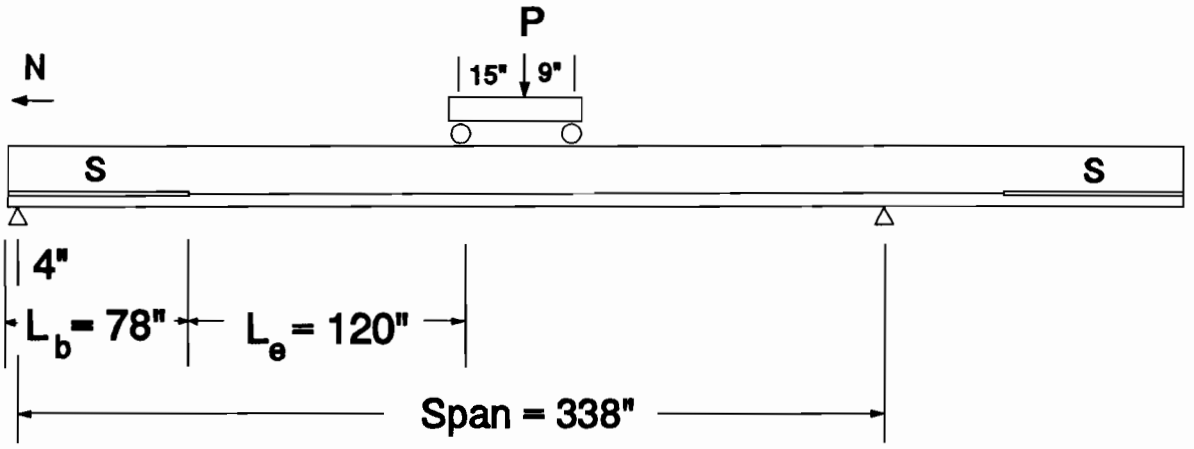

Figure 4.20 Load vs. Deflection, DB850-5A (S)

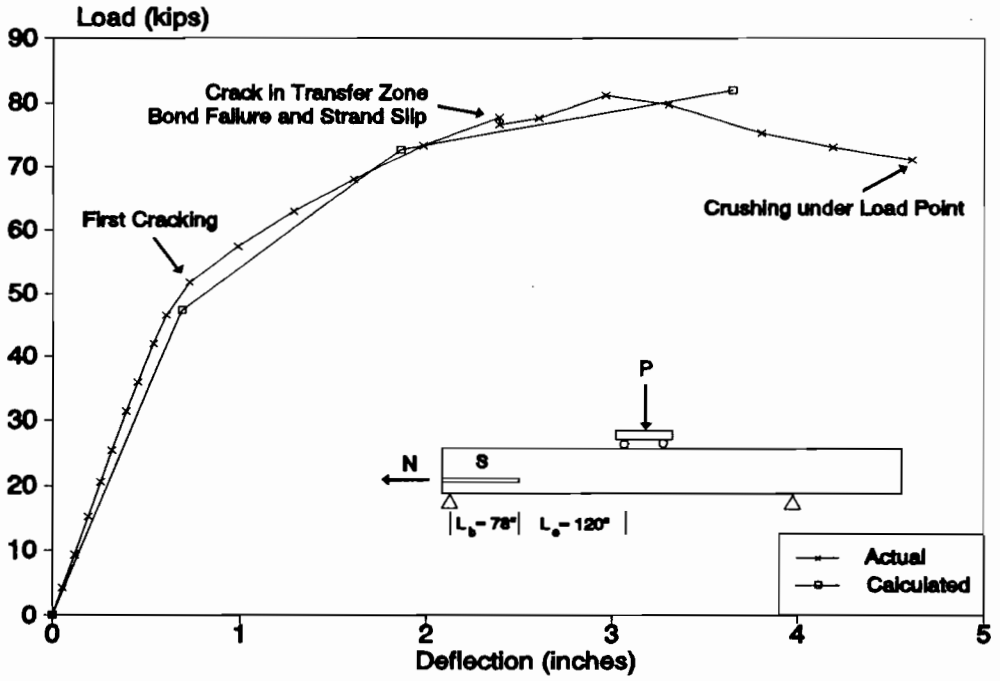

Figure 4.21 Load vs. End Slip, DB850-5A (S)

End slips of the debonded strands are displayed in Figure 4.21. Strands B, F, and G recorded a maximum slip at failure of 0.90, 0.772, and 0.745 inches, respectively. Upon visual inspection of the end of the beam, strand D also exhibited strand slippage of approximately the same magnitude. An electrical malfunction prevented accurate recording of the end slip measurements from strand D. It should be noted that all four debonded strands exhibited a general bond failure and end slip during the test. The failure mode for test DB850-5A (S) was defined as a bond failure.

4.2.8 Test DB850-5B(S). Test DB850-5B (S) was conducted on the south end of specimen DB850-5. It tested an embedment length of 120 inches, 1.50 L_d, and is shown in Figure 4.22.

Unlike the previous tests, test DB850-5B(S) did not exhibit linear elastic behavior. As illustrated in Figure 4.23, the amount of deformation per increment of applied load increased slightly until new flexural cracking occurred at 52 kips. Close inspection of the specimen determined that the flexural cracks in the damaged zone caused by test DB850-5A (S) had reopened. Because of the reopening of existing cracks, the load necessary to initiate first cracking was unable to be determined.

At a load of 71 kips, the specimen began crushing the concrete in the top fibers at a point directly beneath the north load point. Compressive failure occurred at an ultimate deflection of 3.4 inches without the measurement of end slip at the south beam end.

Notes recorded during the test observed that initially the point of maximum deflection was located near the center of the damaged zone. Upon loading, the point of

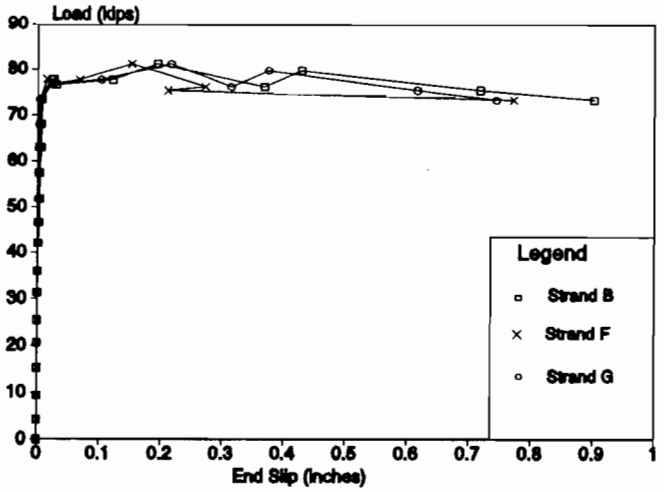

Figure 4.22 Test Setup for DB850-5B (S)

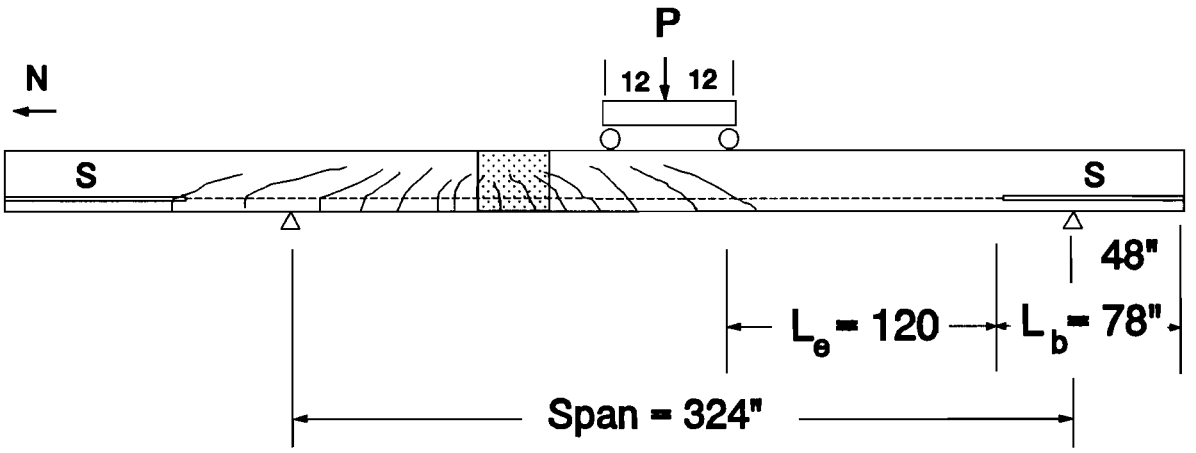

Figure 4.23 Load vs. Deflection, DB850-5B (S)

maximum deflection slowly moved southward until reaching the northern loading point. Compressive failure then occurred at 83 and 97 percent of the calculated ultimate flexural capacity and estimated deflection, respectively.

Since strand slip was not recorded at the south end, conclusions were that the strands had continued to slip in the north end of the beam. Since the behavior of test DB850-5B (S) was controlled by the damaged zone from the previous test, test DB850-5B (S) was declared invalid and is only included for completeness.

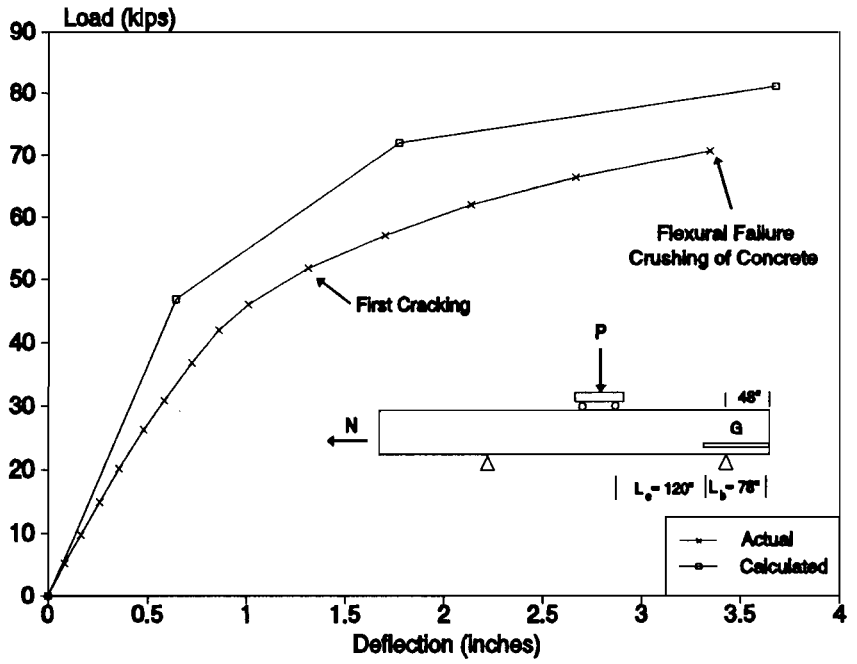

Figure 4.24 Test Setup for DB850-6A (S)

4.2.9 Test DB850-6A (S). Test DB850-6A (S) was conducted on specimen DB850-6. The specimen layout tested both ends of the specimen at an embedment length of 150 inches, 1.875 L_d. The test setup is illustrated in Figure 4.24.

The load versus deflection plot is shown in Figure 4.25. The girder behaved linear elastic until flexural crack formation at a load of 31 kips. As the load increased, deformations increased dramatically as the flexural stiffness of the section was decreased by cracking. At a load of 49.5 kips and a deflection of 4.8 inches, the LVDT's measuring deflection were readjusted to provide the necessary range needed to measure the estimated deflection of 6.6 inches.

At a load of 51.7 kips, a flexural crack formed in the northern debond/transfer zone at a distance of 78 inches from the end of the beam. Immediate end slip was recorded for all four debonded strands in the northern end. Further loading resulted in additional end slip and deflection with a minor drop in the load carrying capacity. The test was terminated at a load of 51.5 kips corresponding to a concrete strain in the top flange of 0.003 (Appendix B).

End slip measurements were recorded for the debonded strands on both ends of the beam. Figure 4.26 displays the load versus end slip for the north end of the girder. The end slips at failure measured 0.12, 0.11, and 0.10 inches for strands D, F and G, respectively. Strand B also exhibited end slip but sporadic measurement of increases and decreases throughout the test resulted in questionable data. The south end did not experience any measurable end slip.

Although the specimen reached 96 percent of the calculated ultimate flexural capacity, significant strand slip occurred after the formation of cracks in the debond/transfer zone. Because of the strand slip and the minor drop in load carrying capacity, test DB850-6A (S) was labelled as a bond failure.

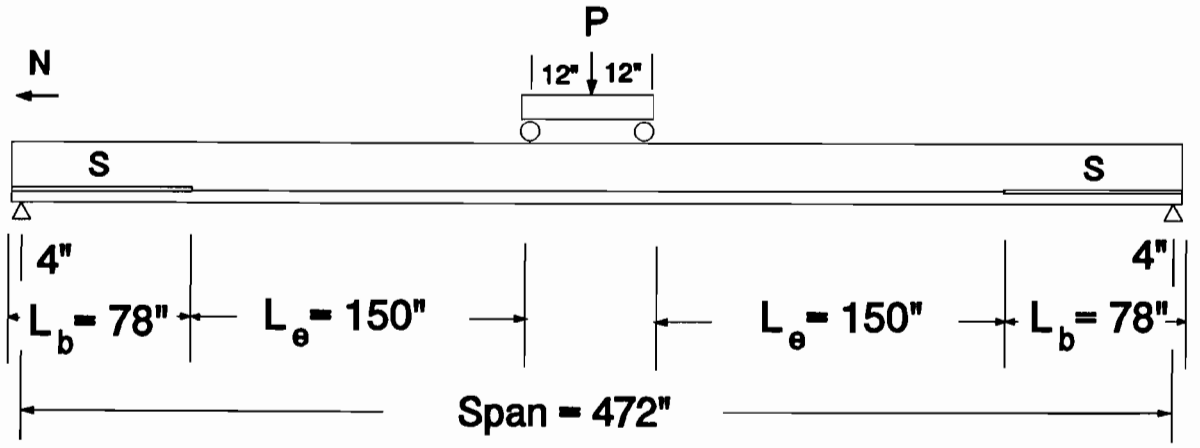

Figure 4.25 Load vs. Deflection, DB850-6A (S)

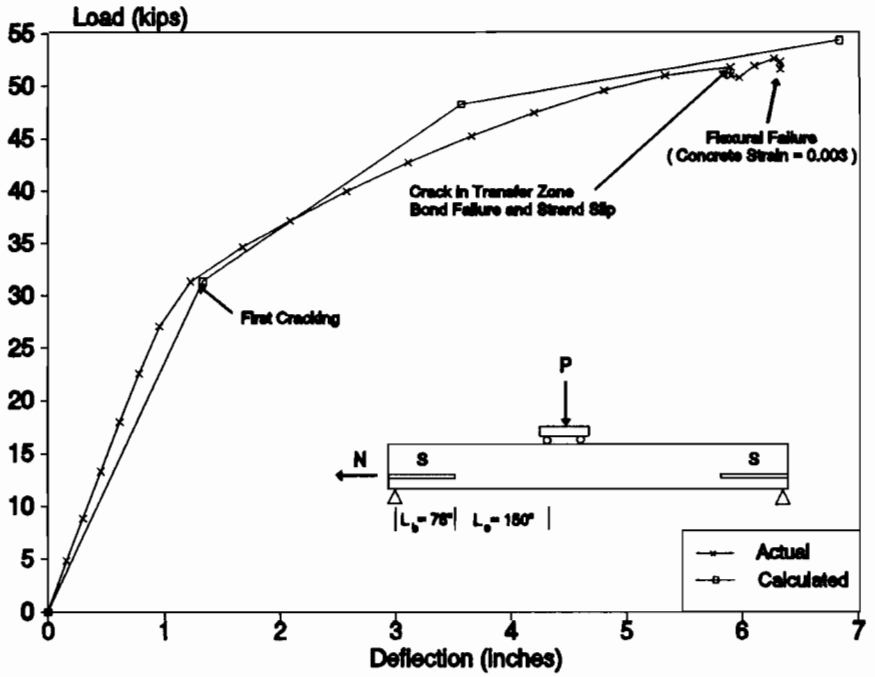

Figure 4.26 Load vs. End Slip, DB850-6A (S)

4.2.10 Test DB850-1A (G). Test DB850-1A (G) was performed on the north end of specimen DB850-1. The specimen contained eight strands, four of which were gradually debonded to 36 inches. The setup tested an embedment length of 84 inches, 1.05 L_d, and is illustrated in Figure 4.27.

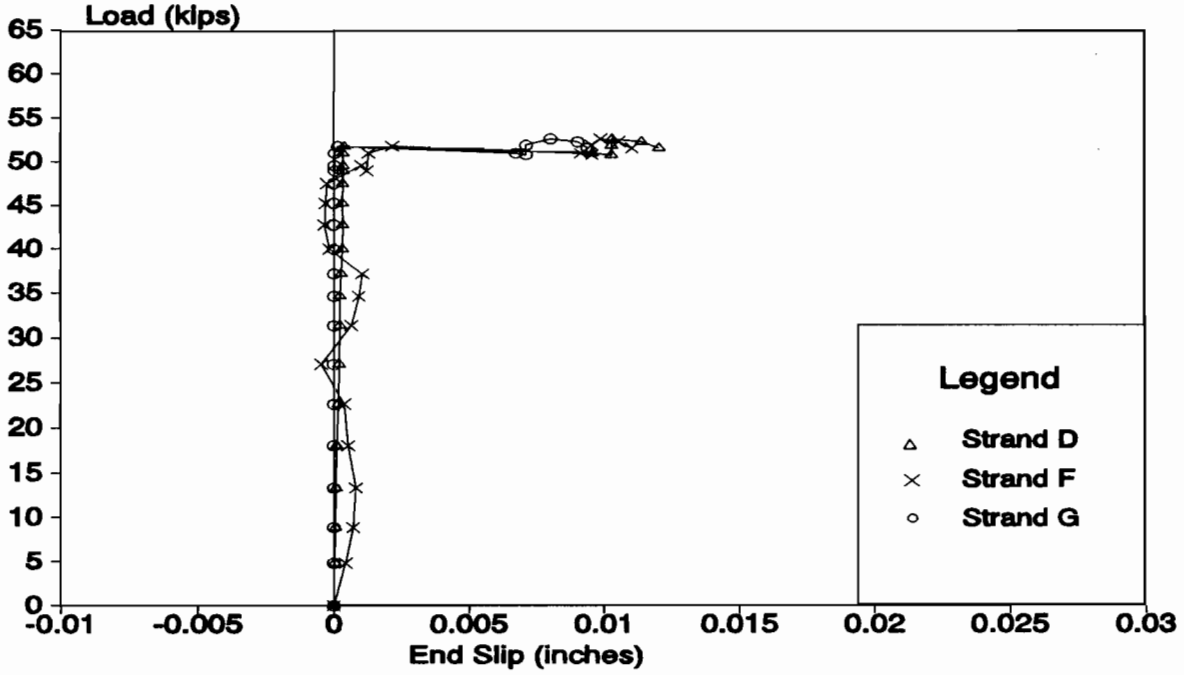

Figure 4.27 Test Setup for DB850-1A (G)

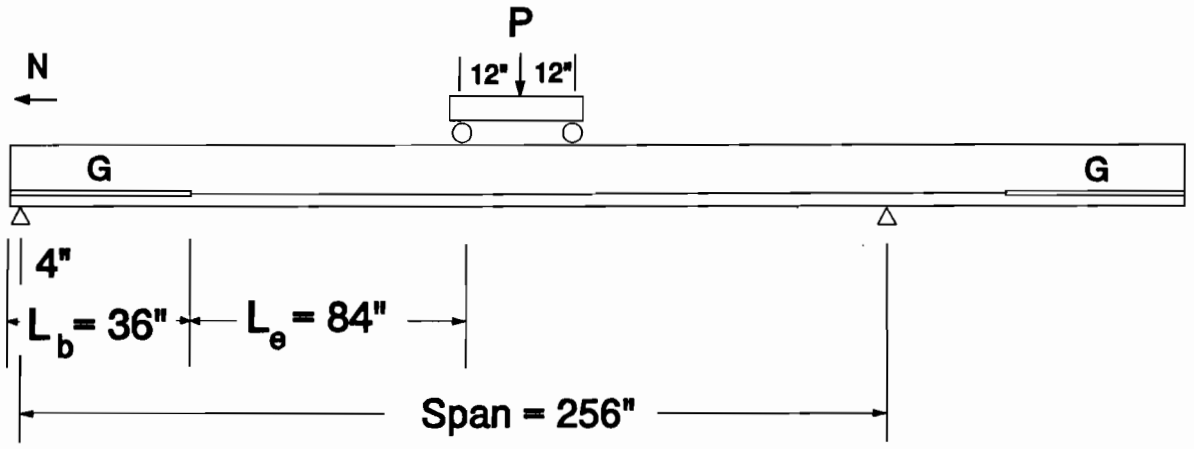

Figure 4.28 Load vs. Deflection, DB850-1A (G)

Figure 4.28 displays the load versus deflection plot for the test. Linearly elastic behavior was exhibited by the specimen until flexural cracking developed at a load of 61 kips. At this point, a negligible amount of end slip, 0.001 inches, was registered in strand B (Figure 4.29). Further loading resulted in additional deformation and flexural crack formation.

At a load of 88 kips, web shear cracking developed in the debond/transfer zone at a distance of 30 inches from the end of the beam. Immediate slip of all eight strands

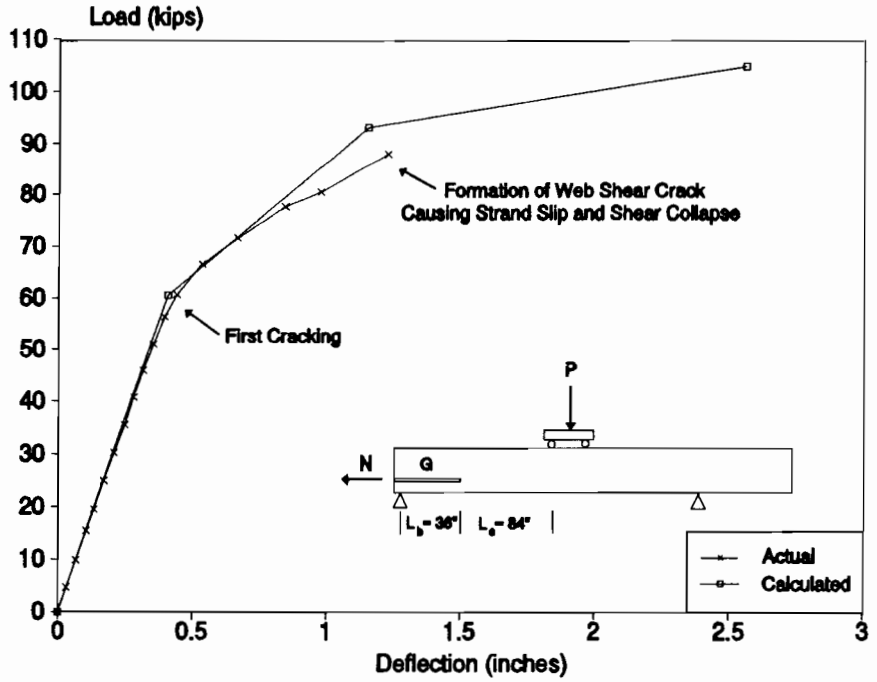

Figure 4.29 Load vs. End Slip, DB850-1A (G)

Figure 4.30 Web Shear Cracking, DB850-1A (G)

resulted in a total loss of prestress in the cross section. With the loss of prestress, the cracking penetrated the top flange and created a hinge. Excessive deformations then occurred before the load was removed. Figure 4.30 is a photograph illustrating the effects of the web shear cracking on the specimen.

Although the specimen's calculated ultimate flexural capacity was 105 kips, the girder's shear capacity was much lower (87.7 kips). Upon exceeding the web shear cracking strength of the specimen, web shear cracks formed in the debond/transfer zone and propagated through the cross section to the height of the steel. This resulted in a dramatic loss of prestress and a sudden, catastrophic failure. The failure was defined as a bond/shear failure.

4.2.11 Test DB850-1B (G). Test DB850-1B (G) was conducted on the south end of specimen DB850-1. The setup tested an embedment length of 84 inches, 1.05 L_d, and included the damaged zone created by the test DB850-1A (G). The test layout is presented in Figure 4.31.

Because test DB850-1A (G) failed catastrophically when web shear cracking occurred, an effort was made to control the extent of the cracking in test DB850-1B (G). Each side of the web of the girder was retrofitted with four steel plates. The plates allowed web shear cracking to form in the top portion of the web but prevented crack extension through the cross section to the height of the strands. The plates were attached to the web by the procedure outlined in Section 3.4.5 and is illustrated in Figure 3.13.

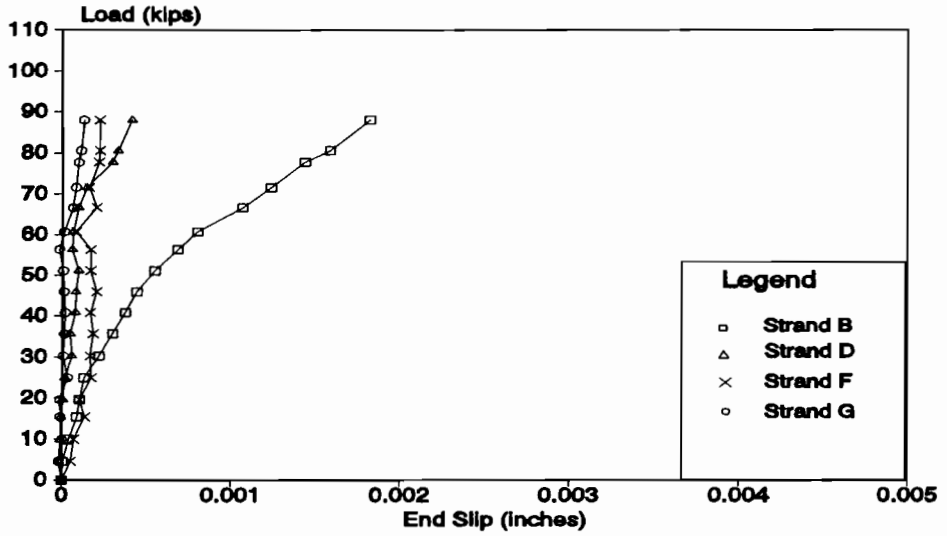

Figure 4.31 Test Setup for DB850-1B (G)

Because the damage at the north end of the girder was extensive, special modifications were completed to prevent further strand slip. Five sets of vertical, post-tensioned Dywidag bars were used to induce transverse prestressing into the damaged section to clamp the strands to prevent further slip. The exact procedure is described in Section 3.4.5 and the modification is displayed in Figure 3.14.

Once the repairs and retrofit were completed, the specimen was tested under the standard procedure. Figure 4.32 illustrates the load versus deflection plot for the test. The

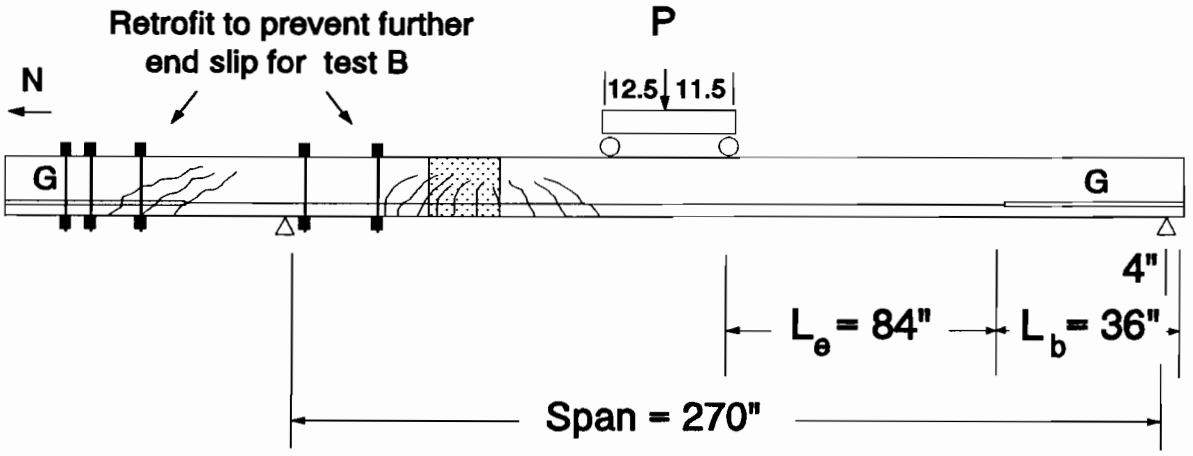

Figure 4.32 Load vs. Deflection, DB850-1B (G)

first flexural cracking occurred at a load of 56.5 kips between the load points. Further loading resulted in increased flexural cracking and deformations.

At a load of 80 kips, web shear cracking developed in the debond/transfer zone. However, these cracks were prevented from extending down to the level of the strands by the steel plate cladding. At this point, only minor amounts of end slip were recorded in the debonded strands.

As the load was increased to 82.5 kips, an additional web shear crack formed approximately 38 inches from the end of the beam. It too was prevented from propagating by the steel cladding. Increased loading resulted in additional flexural cracking and deflection without further web shear cracks.

At 92.6 kips, a web shear crack formed at 46 inches and penetrated through the vertical joint in the unwelded steel plates to the level of the strands. As was the case in DB850-1A (G), an immediate loss of prestress occurred and the beam failed suddenly at 94 percent of the ultimate flexural capacity.

Although web shear cracking developed at 80 kips, only minor amounts of end slip were recorded at this point. Figure 4.33 shows that significant amounts of slip were not recorded until the web shear crack penetrated the level of the strands.

The significance of test DB850-1B (G) is the order of events in which failure occurred. When the load exceeded the calculated shear capacity of the specimen, web shear cracks were formed in the debond/transfer zone. However, the cracks were prevented from reaching the level of the strands and the sudden failure displayed by DB850-1A (G) was avoided. Under additional loading, the specimen behaved in a flexural manner while web shear cracks continued to develop along the length of the specimen toward the load points.

When web shear cracking developed at the point of the unwelded plates, the crack was not contained and it propagated down to the level of the strands. The result was a destruction of bond between the strands and concrete and an immediate slip of all strands. It was clear that the web shear crack triggered the loss of prestress and the ultimate failure of the girder. Test DB850-1B (G) was defined as a bond/shear failure.

4.2.12 Test DB850-2A (G). Test DB850-2A (G) was performed on the north end of specimen DB850-2. The setup tested an embedment length of 76 inches, 0.95 L_d, and is illustrated in Figure 4.34.

Under the procedure outlined in Section 3.4.5, steel plates were attached to the web to control the propagation of the web shear cracking. Unlike test DB850-1B (G), the plates were welded into a unit before being epoxied into place.

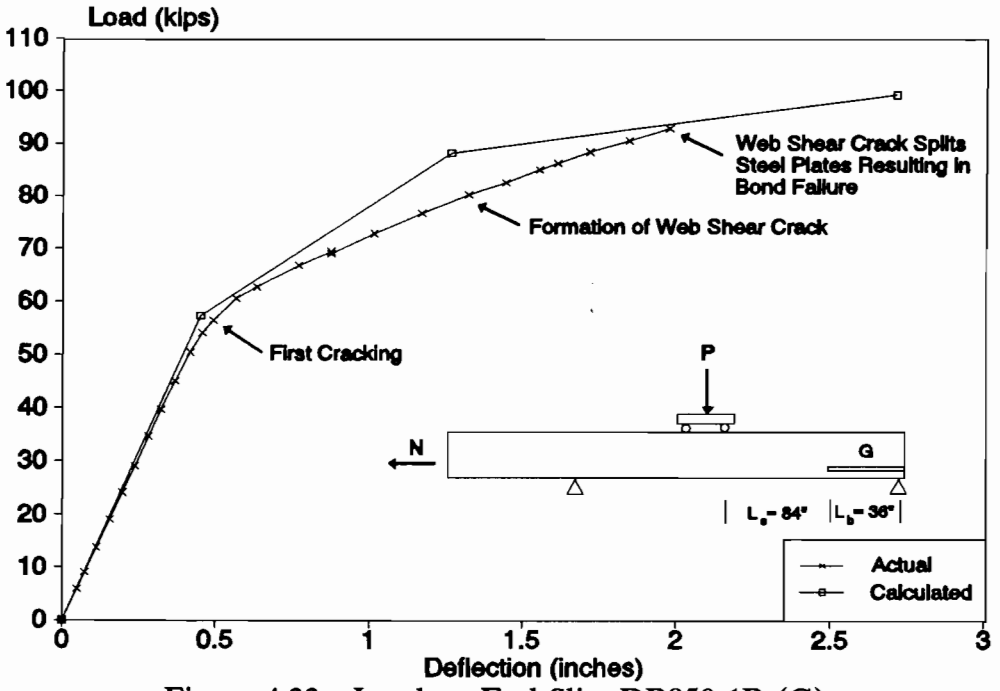

Figure 4.33 Load vs. End Slip, DB850-1B (G)

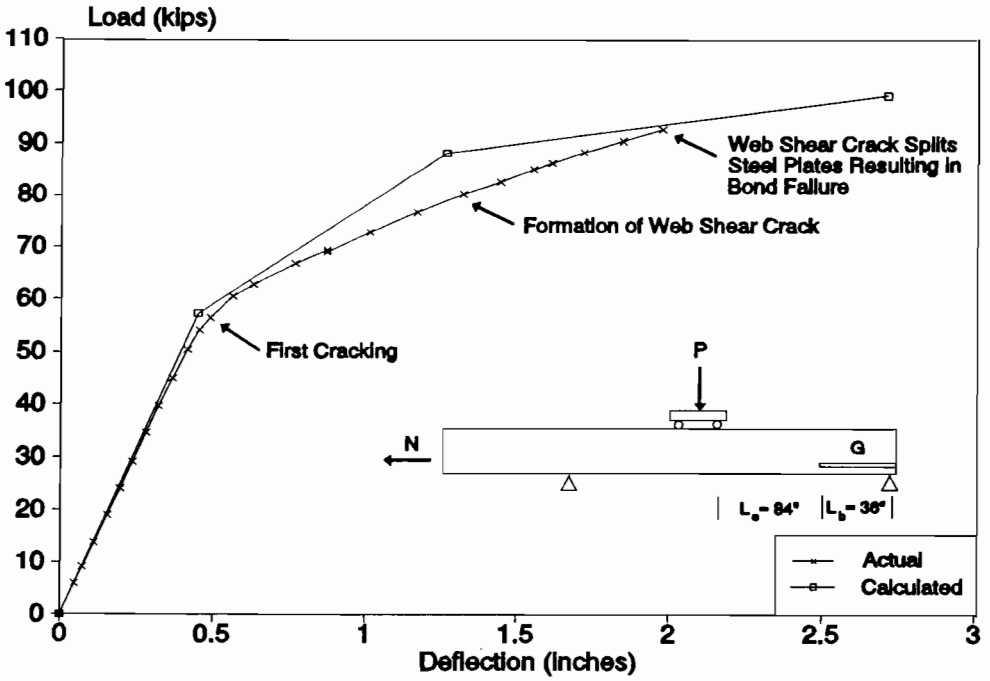

Figure 4.34 Test Setup for DB850-2A (G)

Figure 4.35 illustrates the load versus deflection plot for the test. At a load of 61 kips, flexural cracking occurred and continued to develop throughout the test. At 77 kips, web shear cracking occurred in the debond/transfer zone but was prevented from reaching the level of the strands. At 90 kips, a flexural crack formed at the end of the debond/transfer zone at a distance of 64 inches. Figures 4.36 and 4.37 depict the cracking at the north end of specimen DB850-2.

Also at a load of 90 kips, strands B and G registered end slips of 0.018 and 0.014 inches, respectively (Figure 4.38). Although further loading resulted in additional end slip for both strands B and G, an increase in load carrying capacity also occurred.

At 96 kips, web shear cracks formed in the chamfer region of the bottom flange (Figure 4.37). The cracking resulted in end slip in all eight strands and a loss of prestress. The load was immediately reduced to 63 kips to diminish the amount of damage. Final end slips of 0.35 and 0.31 inches were recorded in strands G and B, respectively. The other strands all measured an average end slip of 0.04 inches.

The maximum load of 96 kips corresponded to 92 percent of the calculated ultimate flexural capacity. The lower load and the significant amount of strand slip classify the test as a bond/shear failure.

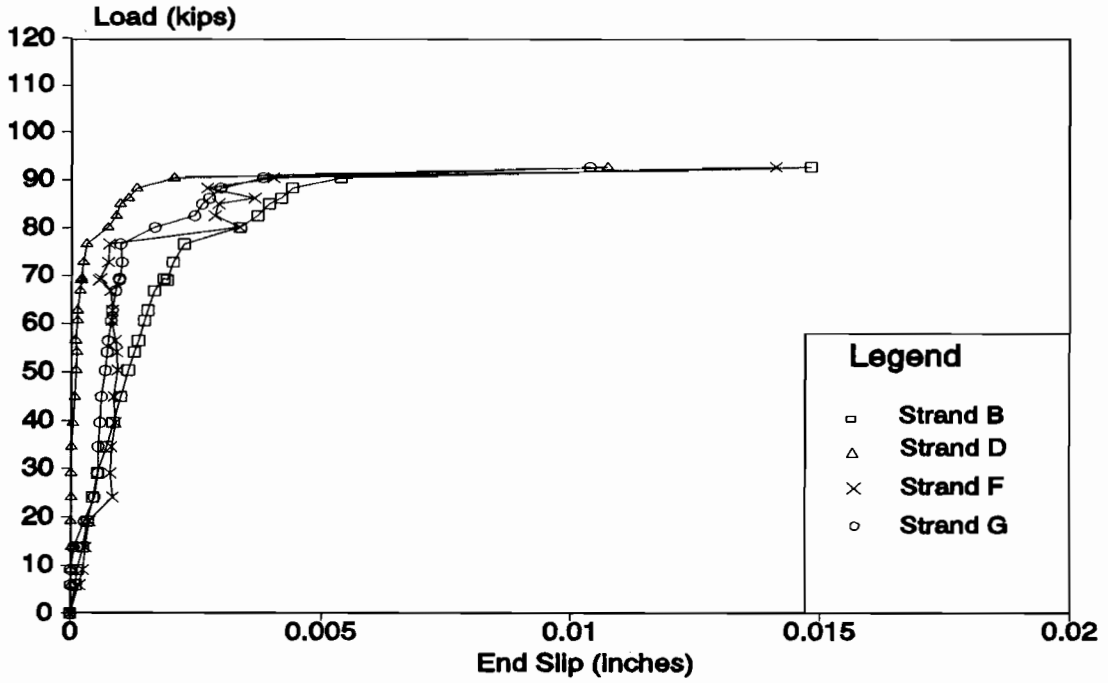

Figure 4.35 Load vs. Deflection, Test DB850-2A (G)

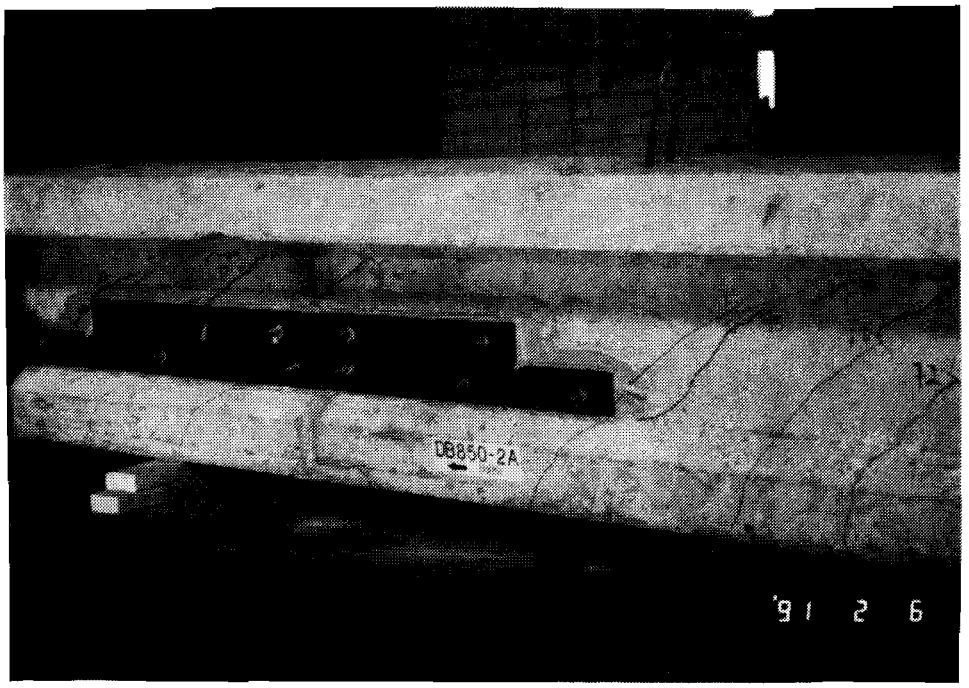

Figure 4.36 Flexural Cracking in the Debond/Transfer Zone, Test DB850-2A (G)

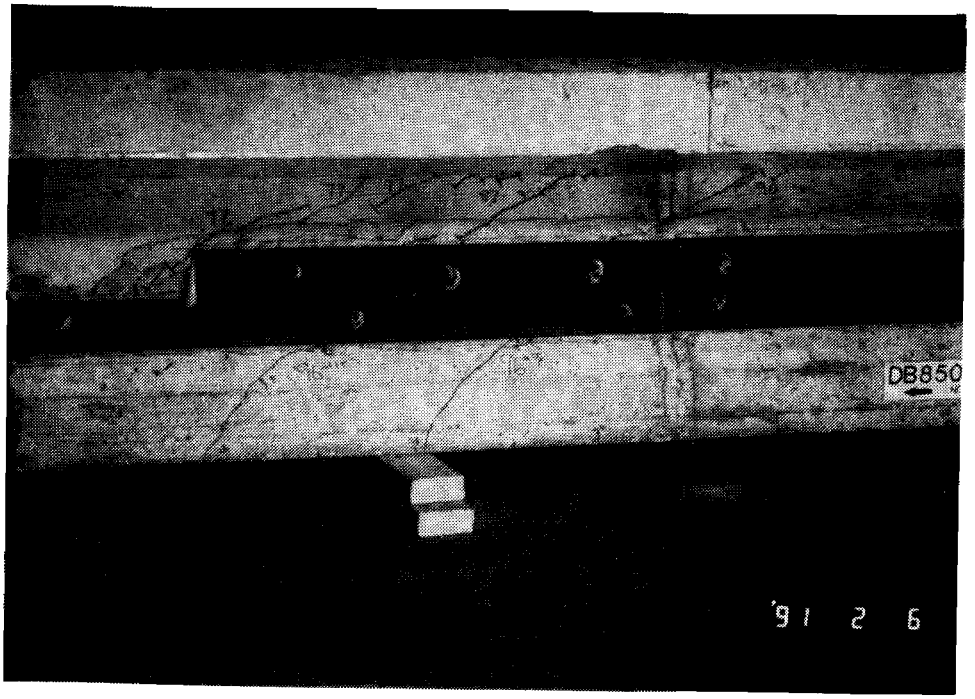

Figure 4.37 Web Shear Cracking, Test DB850-2A (G)

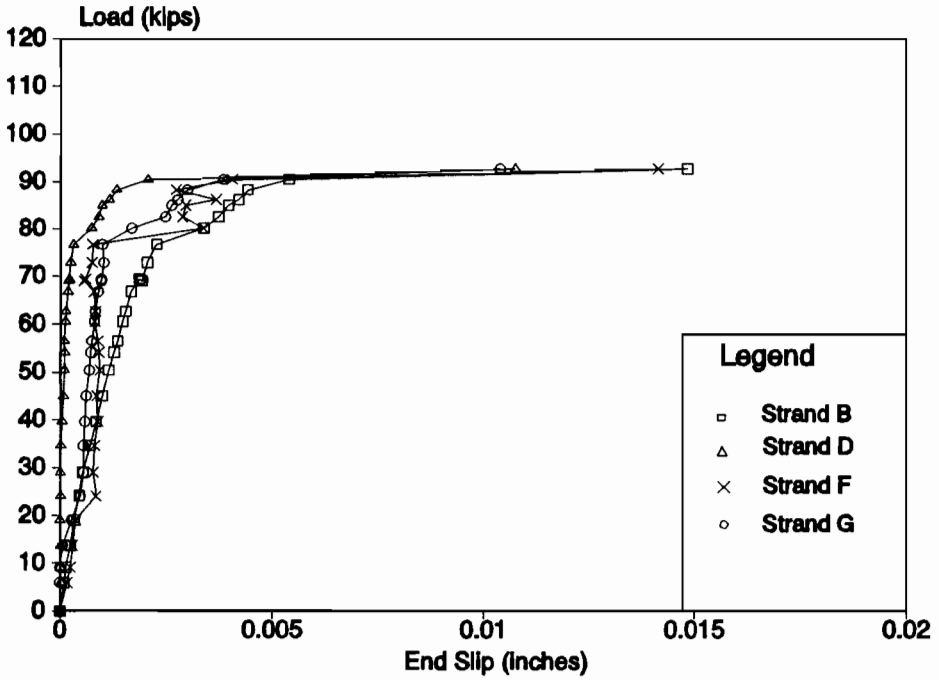

Figure 4.38 Load vs. End Slip, DB850-2A (G)

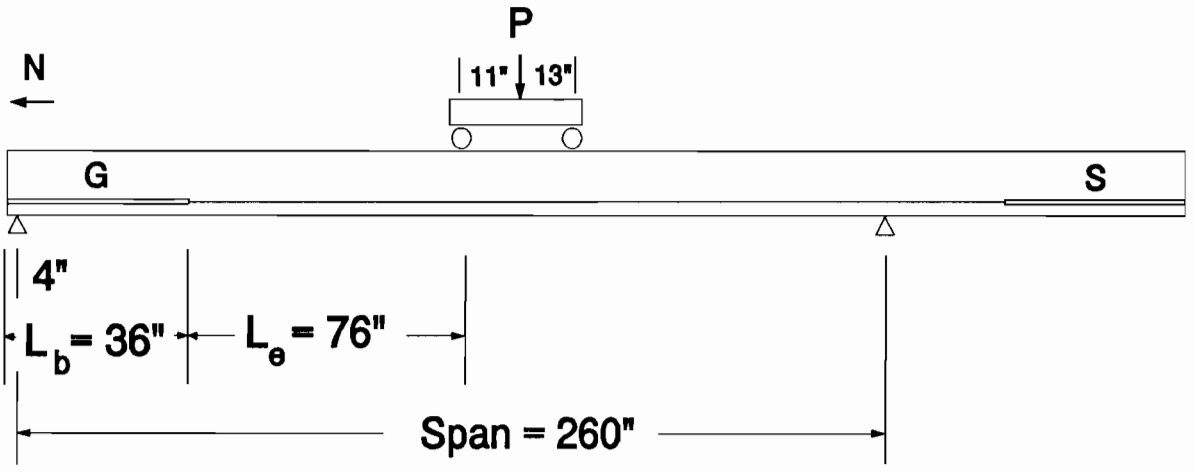

Figure 4.39 Test Setup for DB850-2B (S)

4.2.13 Test DB850-2B (S). Test DB850-2B (S) was performed on the south end of specimen DB850-2. The specimen contained eight strands, four of which were suddenly debonded to 36 inches. The setup was designed to test an embedment length of 88 inches, 1.10 L_d, and included the damaged zone created by test DB850-2A (G). The setup is presented in Figure 4.39.

By the procedure outlined in Section 3.4.5, specimen DB850-2 was repaired and retrofitted before testing the south end. To prevent further strand slip, two sets of vertical, post-tensioned Dywidag bars were positioned at a distance of 36 and 72 inches from the north beam end.

To control the propagation of web shear cracking, two steel plates were attached to each side of the web at the south end of the specimen. The plates permitted web shear cracking to develop but prevented the cracks from reaching the level of the strands. Once the repairs and retrofit were completed, the specimen was tested under the standard procedure. Figure 4.40 illustrates the load versus deflection plot for the test. Until flexural cracking occurred at a load of 61 kips, the girder behaved elastically. Further loading resulted in an increase in flexural cracking and deformations.

At a load of 79 kips, web shear cracking occurred in the debond/transfer zone but was prevented from reaching the level of the strands by the steel plate cladding. At 90 kips, the first end slip of 0.005 inches was measured in strand G. An increase in load of 3 kips, resulted in the formation of a flexural crack at a distance of 70 inches from the beam end, about 9 inches from the debond/transfer zone. No immediate effects from the crack could be determined except for some minor additional end slip by strand G.

As loading was resumed, a peak load of 93 kips and a deflection of 2.4 inches was reached before a flexural crack formed at the end of the debond/transfer zone at a distance of 57 inches. At this point, end slips of 0.052, 0.089 and 0.096 inches were registered in strands D, F and G, respectively (Figure 4.41). Under further loading, the load carrying capacity of the specimen remained approximately constant while an increase in deflection and strand slip was recorded. Figure 4.42 illustrates the cracking in the debond/transfer zone.

At a load of 92.6 kips and deflection of 2.6 inches, end slip was measured in four debonded strands and resulted in the termination of the test. End slips at the completion of testing were 0.003, 0.209, 0.264, and 0.169 inches for strands B, D, F, and G, respectively. Figure 4.41 depicts the load versus end slip for the four debonded strands.

After reaching the load carrying capacity plateau and while additional deformations were occurring, strand F displayed an unusual effect on the cross section. As it slipped, a 26 inch long, longitudinal crack formed in the concrete at the level of the strand. It extended from the point of termination of the debonding to the flexural crack that formed at the end of the debond/transfer zone. The crack can be viewed in Figure 4.43.

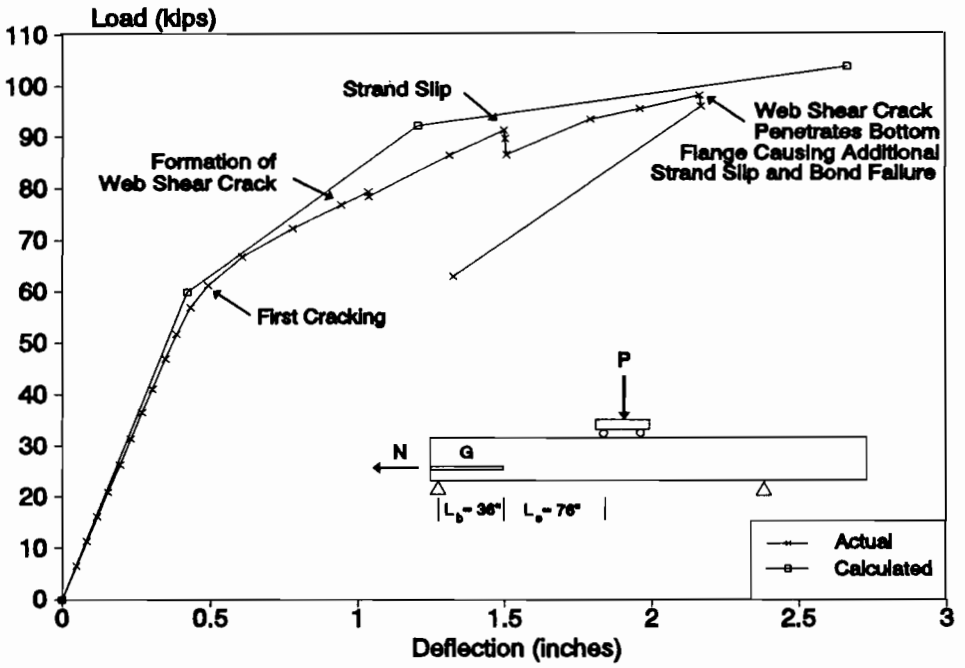

Figure 4.40 Load vs. Deflection, DB850-2B (S)

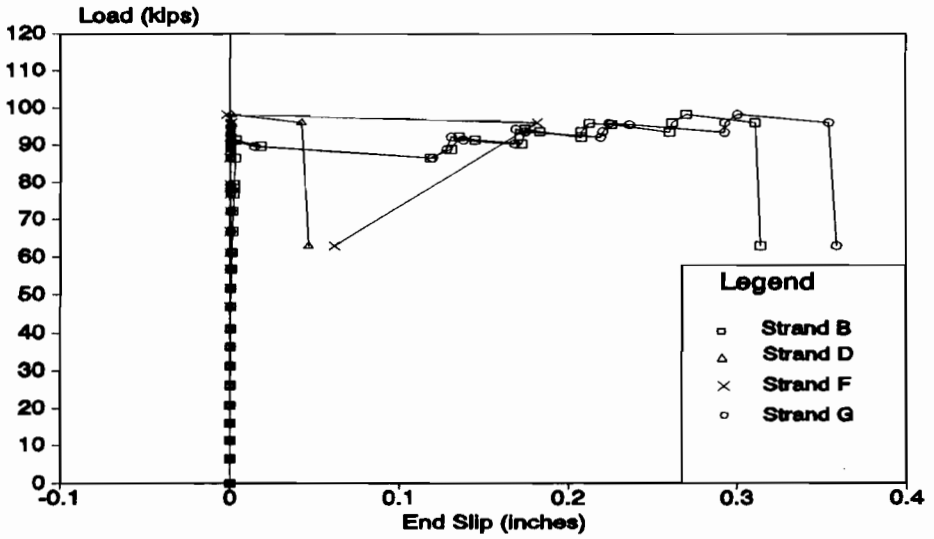

Figure 4.41 Load vs. End Slip, DB850-2A (S)

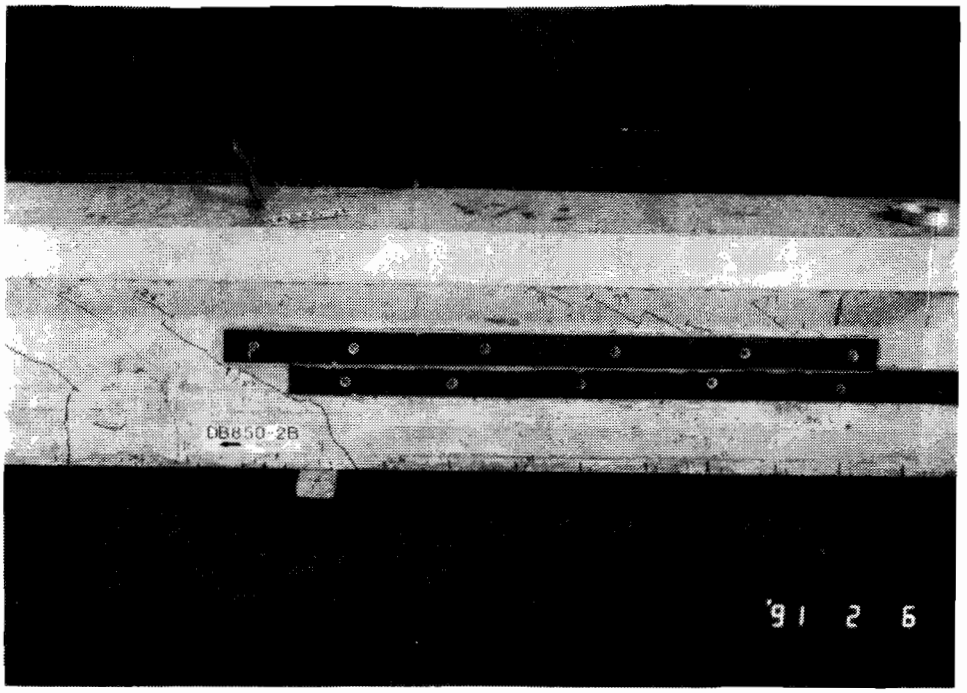

Figure 4.42 Flexural Cracking and Web Shear Cracking in the Debond/Transfer Zone Test DB850-2B (S)

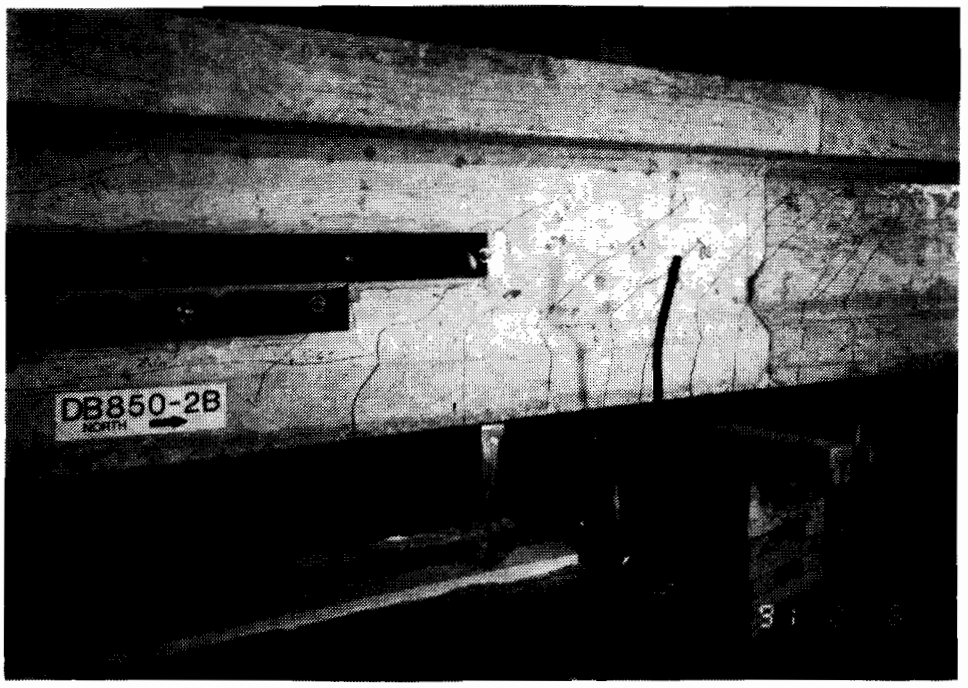

Figure 4.43 Bursting Crack Developed During Test DB850-2B (S)

Strand F was located outside the shear reinforcing cage and did not benefit from the effects of concrete confinement. Once it began to slip, a reduction of stress occurred in the strand near the beginning of the transfer zone resulting in an increase in the strand diameter. As the larger diameter strand tried to slip through the existing opening, it exerted a radial tensile force on the concrete surrounding it. The radial force exceeded the local tensile capacity of the concrete which resulted in the longitudinal bursting crack. Because the crack developed near the ultimate capacity while additional deformations were occurring, the crack was representative of a flexural bond failure.

The testing was completed at a load of 92.6 kips and a deflection of 2.6 inches corresponding to 93 percent of the calculated capacity. Since the load carrying capacity did not decrease with strand slip and adequate ductility was evident, the failure mode was defined as a flexural failure.

4.3 Summary of Test Results

The results for the tests described in Sections 4.2.3 through 4.2.13 are displayed in Table 4.1. The table summarizes the important variables and mode of failure for each test.

Although concrete strains were measured during each test, the data obtained was not used directly in the determination of failure mode. Instead, it was used to monitor the level of compressive strain in the concrete during testing. The level of strain indicated the relative position of the test to the ultimate failure state of 3000 microstrain as determined by the ACI code [2]. The plots of load versus concrete strain are included in Appendix B.

Table 4.1 Summary of Test Results

TEST NUMBER	EMBEDMENT (INCHES)	L_e / ACI L_d	MEASURED**		M_{cr} / M_{calc}	M_{ult} / M_{calc}	MODE OF FAILURE
			M_{cr}	M_{ult}			
DB850-1A (G)	84	1.05	3525	5104	1.00	0.84	BOND/SHEAR
DB850-1B (G)	84	1.05	3460	5671	0.98	0.93	BOND/SHEAR
DB850-2A (G)	76	0.95	3588	5622	1.02	0.92	BOND/SHEAR
DB850-2B (S)	88	1.10	3782	5783	1.08	0.95	FLEXURAL/BOND
DB850-3A (G)	80	1.00	3332	5358	0.95	0.88	BOND
DB850-3B (G)	108	1.35	3298	5787	0.94	0.95	FLEXURAL
DB850-4A (G)	120	1.50	3580	6038	1.02	0.99	FLEXURAL
DB850-4B (G)	100	1.25	3663	6028	1.04	0.99	FLEXURAL
DB850-5A (S)	120	1.50	3568	5590	1.02	0.92	BOND
DB850-6A (S)	150	1.875	3509	5851	1.00	0.96	BOND

** Units of inch-kips

4.4 Summary of Typical Failure Modes

During the testing of the specimens, the mode of failure could be categorized as either a flexural, flexural/bond, or a bond/shear failure. Brief descriptions of each type of failure follows with references to the specific tests.

4.4.1 Flexural Failure Mode. A typical flexural failure is illustrated by test DB850-4A (G), Section 4.2.5. As the girder was loaded, it behaved linear elastic until flexural cracking developed between the load points. Additional loading induced further deformations and flexural cracking along the length of the girder. The failure occurred when the concrete crushed between the load points near the calculated ultimate flexural capacity. Tests DB850-3B (G) and DB850-4B (G) are also examples of a flexural failure.

4.4.2 Flexural/Bond Failure Mode. An example of a flexural/bond failure is test DB850-5A (S), Section 4.2.8. As the girder was loaded, it too behaved linear elastic until flexural cracking developed. However, the difference between a flexural failure and a flexural/bond failure was that flexural cracking developed in the debond/transfer zone and end slip of the debonded strands occurred. As additional loading was applied, the strands continued to slip resulting in a loss of prestress. The reduction in prestress resulted in a dramatic decrease in the load carrying capacity of the specimen.

The failure normally occurred at the lower capacity when either the concrete crushed between the load points or reached a compressive strain of 0.003 inches/inch. Although the specimen typically exhibited an increase in the ductility, a sudden, catastrophic collapse would have occurred if the loading had been a gravity load instead of hydraulic. Tests DB850-3A (G) and DB850-6A (S) also exhibited this type of failure.

Test DB850-2B (S), Section 4.2.13, was a unique case of the flexural/bond failure mode. Significant strand slip did not occur until the specimen had nearly reached the ultimate capacity and was continuing to accept deformations without increasing the capacity. Unlike the other flexural/bond failures, the specimen did not experience the sudden decrease in load carrying capacity. Instead, it failed in a flexural mode indicating that the test was on the border between the flexural and flexural/bond failure modes.

4.4.3 Bond/Shear Failure Mode. A bond/shear failure mode was illustrated by test DB850-1A (G), Section 4.2.10. During the test, the specimen also behaved linear elastic until flexural cracking developed. Upon further loading, the specimen behaved in a flexural mode until the web shear capacity of the specimen was exceeded in the debond/transfer zone. At that point, web shear cracking developed in the web and penetrated the cross section to the level of the strands. An immediate loss of prestress by the strands in the web allowed further propagation of the cracks through the cross section. The result was an immediate, total loss of prestress of all eight strands and a sudden, catastrophic collapse.

CHAPTER FIVE

DISCUSSION OF RESULTS

In Chapter four, the data for each test was reviewed. This chapter discusses the test results and their influence on the behavior of the tests. Discussions concerning gradual versus sudden debonding, ACI code provisions, and the adequacy of the prediction model are also presented.

5.1 Moment Capacity

A strain compatibility analysis was used to determine the moment- curvature relationship for the girder's cross section. From the analysis, the cracking moment and the ultimate flexural capacity of the cross section was determined. The assumptions and calculations for the analysis are included in Appendix C.

The calculated cracking moment was based on a maximum concrete tensile strength of $7.5\sqrt{f_c'}$. Table 5.1 displays the values obtained during the actual testing of the specimens. As shown by the table, the values determined experimentally correlate very closely with the calculated value.

Table 5.1 - Test Results of Cracking and Ultimate Moments

TEST NUMBER	MEASURED (inch-kip)		M_{cr} /	M_{ult} /	FAILURE
	M_{cr}	M_{ult}	M_{calc}	M_{calc}	MODE
DB850-1A (G)	3525	5104	1.00	0.84	B/S
DB850-1B (G)	3460	5671	0.98	0.93	B/S
DB850-2A (G)	3588	5622	1.02	0.92	B/S
DB850-2B (S)	3782	5783	1.08	0.95	F/B
DB850-3A (G)	3332	5358	0.99*	0.98*	B
DB850-3B (G)	3298	5787	0.97*	1.03*	F
DB850-4A (G)	3580	6038	1.02	0.99	F
DB850-4B (G)	3663	6028	1.04	0.99	F
DB850-5A (S)	3568	5590	1.02	0.92	B
DB850-6A (S)	3509	5851	1.00	0.96	B

B = Bond F = Flexural S = Shear

* DB850-3 had slightly different cross-section

Table 5.1 also displays the moment achieved by each test before failure occurred. The flexural failures were within five percent of the calculated ultimate moment while the bond type failures were within sixteen percent. This clearly indicates that the load carrying capacity of the cross section approaches the ultimate flexural capacity regardless of the type of failure.

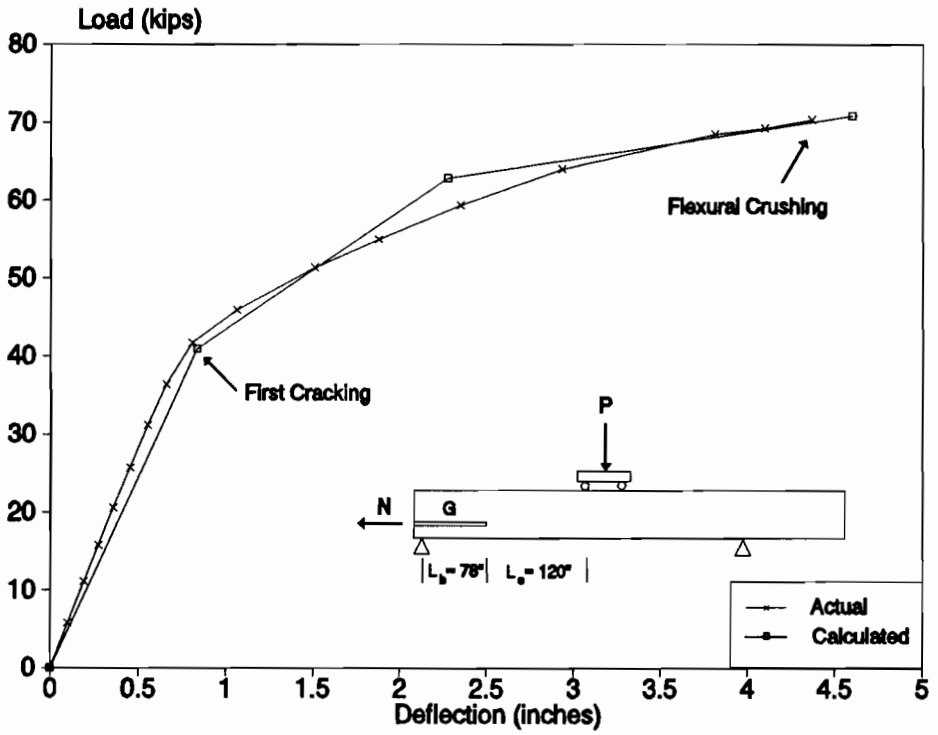

Figure 5.1 Flexural Failure, DB850-4A (G)

As Figure 5.1 illustrates, the ability to accurately calculate the cracking moment and ultimate capacity of a cross section is possible. The accuracy is important because the prediction model of cracking and bond failure is based on the analytical values. The accuracy of the analysis determines the accuracy and usefulness of the prediction model.

5.2 Effect of Cracking

During testing, two types of cracks influenced the behavior of the specimen, flexural cracking and web shear cracking. Although both were predictable, there was significant difference in the effect each had on the tests.

5.2.1 Flexural Cracking. Flexural cracking typically occurred when the tensile stresses in the concrete exceeded $7.5\sqrt{f'_c}$. Cracking first developed between the load points in the region of pure flexure. As additional loading was applied, flexural cracks formed progressively toward the supports. If cracking did not occur in the debond/transfer zone, the beam behaved as predicted by the estimated load vs. deflection curve. An example is test DB850-4A (G) which resulted in a flexural failure.

However, if flexural cracking developed in the debond/transfer zone, strand slip occurred. Strand slip resulted in a loss of prestress and in the reduction of the flexural capacity of the specimen. The new capacity was dependent upon the number of strands slipping and the level of prestress maintained by those strands. Behavior of the test depended on the load at which the strand slip or flexural cracking occurred.

If flexural cracking developed at a relatively low load in comparison to the ultimate load, the specimen continued to accept additional load and deformation. Eventually, the specimen failed in a flexural mode at a lower capacity. Figure 5.2 illustrates this type of failure.

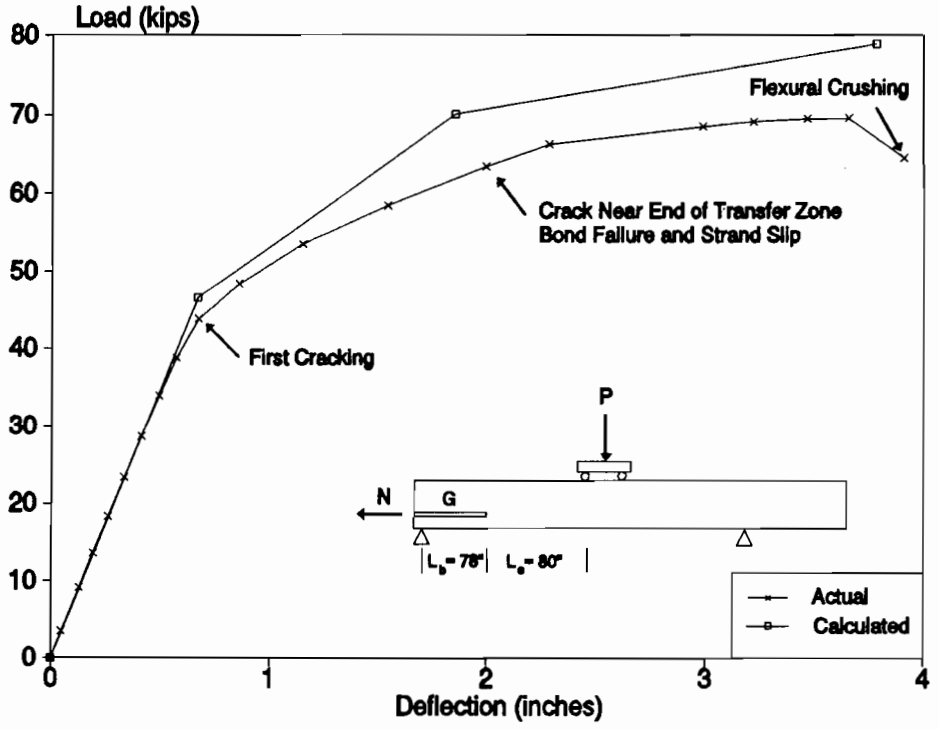

Figure 5.2 Flexural Behavior of Test DB850-3A (G)

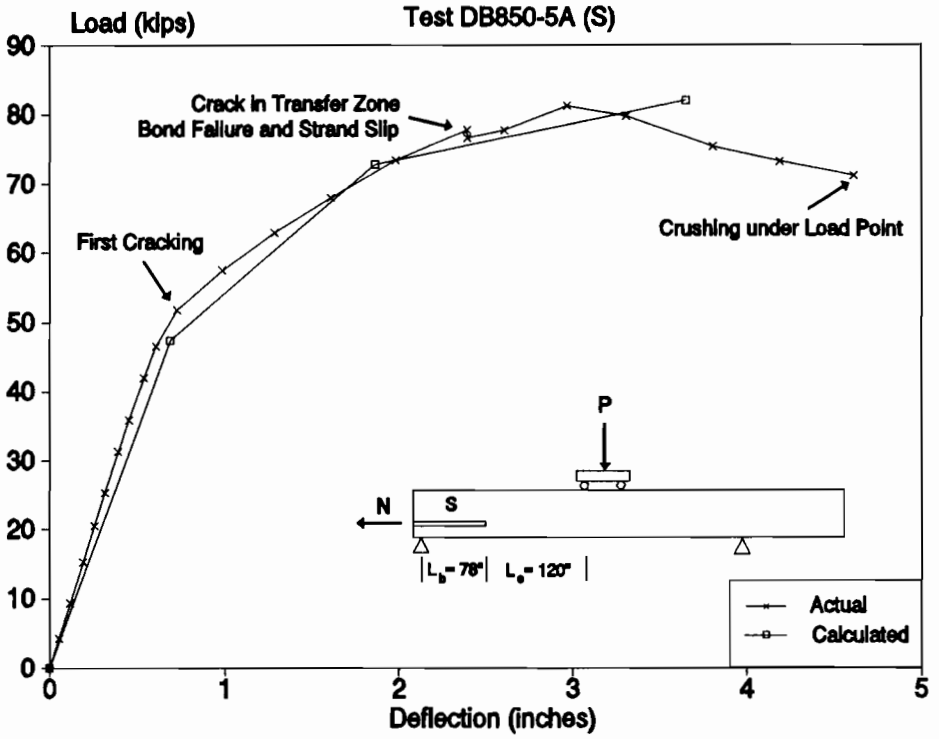

Figure 5.3 Flexural Behavior of Test DB850-5A (S)

Figure 5.3 displays the behavior of the test when cracking occurs in the debond/transfer zone at a relatively high load in comparison to the ultimate load. Initially, the specimen experienced an immediate, but slight, decrease in capacity. With additional loading, the beam recovered and experienced an increase in both capacity and deflection. However, the increase in the capacity was soon lost as subsequent slip of the strands occurred. Further loading resulted in increased deflections and reduced capacity. The specimen ultimately failed in compression at a lower flexural capacity. It should be noted that if the applied load had been a gravity based loading, a sudden, catastrophic collapse of the specimen would have occurred.

If cracking in the debond/transfer zone developed at, or near, the ultimate load of the specimen, the slight decrease in capacity resulted in a compressive failure of the concrete. DB850-2B (S) and DB850-4B (G) were both examples of this type of flexural failure.

The effect of flexural cracking in the debond/transfer zone on the behavior of the specimen is dependent on the amount of load present when cracking occurs. If cracks form at, or near, the ultimate state, the effect is minimal. However, if flexural cracking occurs earlier, the effect under gravity loading could be catastrophic.

Table 5.2 - Test Results of Web Shear Capacity

TEST NUMBER	MEASURED CRACKING LOAD (KIPS)	MEASURED LOAD / CALCULATED LOAD
DB850-1A (G)	44.0	1.09
DB850-1B (G)	42.4	1.05
DB850-2A (G)	41.8	1.04
DB850-2B (S)	40.9	1.01

5.2.2 Web Shear Cracking. Initiation of web shear cracking occurs when the maximum principal tensile stress of the section exceeds the concrete tensile capacity. Previous research determined that the maximum tensile stress required for cracking was $4\sqrt{f_c'}$ [10]. The tests completed on specimens' DB850-1 and DB850-2 also exhibited a close correlation to that value. Table 5.2 illustrates the data obtained from the testing.

The tests also provided an insight into the behavior of debonded specimens under the influence of web shear cracking. During the testing of DB850-1A (G) (Section 4.2.10), the appearance of web shear cracking was immediately preceded by minor amounts strand slip (0.003 inches). At 88 kips, web shear cracking occurred, producing a loss of prestress and sudden collapse of the beam. Although a failure resulted, the cause of the failure was unclear because the order in which strand slip and web shear cracking had occurred was unable to be determined.

However, the order of events was determined during the testing of DB850-1B (G), Section 4.2.11. At 80 kips, web shear cracking developed in the debond/transfer zone but was prevented by the external plates from reaching the level of the strands. Unlike test DB850-1A (G), a sudden collapse did not ensue. Further loading resulted in additional deformation, flexural cracking, and web shear cracking. Figure 5.4 is a photograph displaying the cracking in the debond/transfer zone.

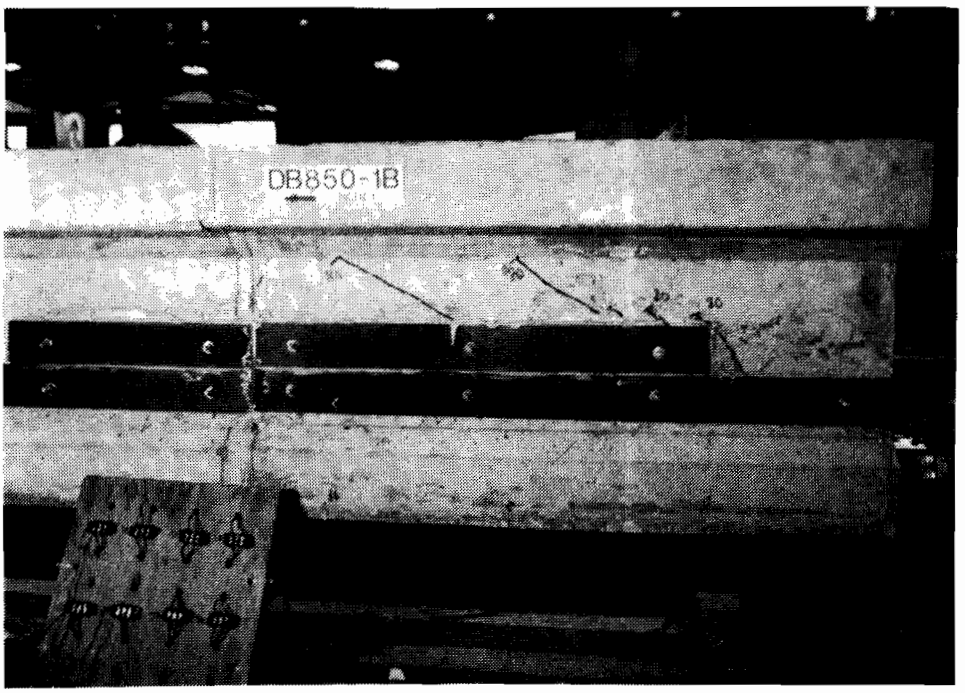

Figure 5.4 Web Shear Cracking in Debond/Transfer Zone

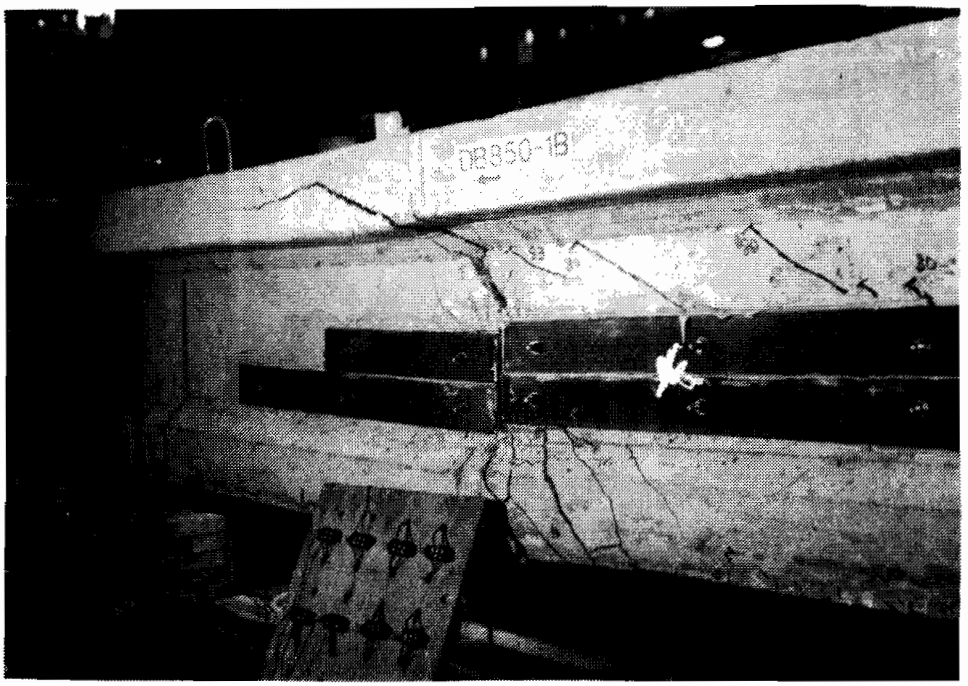

Figure 5.5 specimen Collapse from Web Shear Cracking

At a load of 92.6 kips, web shear cracking developed in the region containing the vertical construction joint of the steel plating. The crack penetrated through the unwelded joint to the level of the strands, resulting in immediate end slip and loss of prestress. In this test, the determination was clear that web shear cracking precipitated the total bond failure and beam collapse. Figure 5.5 is a photograph displaying the web shear crack responsible for the failure of test DB850-1B (G).

Although the formation of web shear cracking was predicted to control the behavior, test DB850-2B (S) proved that a flexural failure mode could be achieved. As in the previous tests, web shear cracking occurred but was controlled by the external steel plates. Additional loading produced further deformation and cracking and resulted in the achievement of a flexural failure.

The failure mode of specimens under web shear cracking was a sudden, catastrophic failure. When web shear cracking occurred, the initial strand slip was registered by strands in or near the web of the girder. The resulting loss of prestress allowed the propagation of web shear cracks causing additional strand slip. The progression led to a bond failure in all strands, a total loss of shear strength, and sudden collapse. Although test DB850-2B (S) was a flexural failure, it is evident that the failure occurred only because the web shear cracks were prevented from reaching the level of the strands. The formation of web shear cracking should be prevented in specimens with debonded strands.

5.3 Effect of End Slip

As described in Section 3.1.1, end slip will occur when the wave of high bond stress caused by flexural cracking reaches the transfer zone. As bond slip occurs, the stress is increased in the immediate vicinity of the crack. The increase results in a decrease in the strand diameter due to Poisson's effect. As the diameter is reduced, the frictional resistance is lowered which causes a general bond slip.

As the strand slips, it tries to rotate along the helical path formed in the concrete. However, the rotation is resisted by frictional resistance and mechanical interlock in the transfer zone. This causes increased tangential hoop tensile stresses in the concrete in the transfer zone as the strand tries to pull through the existing opening.

The effect is illustrated in Figure 5.6. A bursting crack of approximately 26 inches formed in the concrete at the level of the strand. The crack formed during an increase in deflection from 2.4 inches to 2.64 inches near the conclusion of test DB850-2B (S). The crack corresponds to a measured end slip of 0.6 inches.

Although end slip suggests a general bond failure and loss of prestress, the effect is not necessarily a failure. Frictional resistance and mechanical interlock will continue to carry significant amounts of flexural load. Although DB850-5A (S) had recorded end slips

Figure 5.6 Bursting Crack Developed During Test DB850-2B (S)

of approximately 0.2 inches in the debonded strands, it continued to exhibit increased load carrying capacity until further slip occurred. As most of the tests displayed slippage in the debonded strands, it was determined that minor amounts of end slip could occur during a flexural failure and not significantly influence the behavior.

However, major amounts of end slip normally resulted in bond failure and large decreases in load carrying capacity. An example is found in test DB850-3A (G). Strand slip occurred at an early stage in the loading and resulted in a reduction of capacity. The girder continued to accept load until a flexural failure occurred at 80 percent of the predicted load. The average recorded slip for strands B and G was 0.6 inches.

While the consequence of end slip alone resulted in lower flexural capacity, the formation of web shear cracks and concurrent end slip was catastrophic. The loss of prestress, caused by the strand slip, reduced the shear capacity of the section which led to further cracking and additional strand slip. The sudden progression produced a total bond failure, loss of prestress, and a catastrophic collapse of specimen. Web shear cracking in the debond/transfer zone should be prevented to avoid the possibility of bond failure and subsequent beam failure.

In these tests, bond failure could not be exactly defined in terms of end slips. Instead, bond failure is defined by a reduction in a beam's capacity directly caused by a loss of strand anchorage. Beams that failed in bond demonstrated an inability to obtain flexural

capacity and/or an inability to sustain loads through large deformations (ductility). In these tests, the pretensioned strands demonstrated the ability to continue to develop bond stresses even while the strands were slipping. In some cases, mostly bond/shear failures, small amounts of end slip, 0.003 inches to 0.01 inches, were enough to create the mechanism that initiated bond failure. In these cases, the bond slips increased greatly at failure and slips were generally quite large, in excess of 0.25 inches. In other cases, particularly with debonded strands, end slips were measured as large as 0.1 inches without causing bond failure. In these cases, the strands were able to develop additional anchorage even though the strands were slipping through the concrete.

5.4 Gradual versus Sudden Termination of Debonding

In order to determine the effect of gradual versus sudden debonding on the behavior of the specimens, beams DB850-5 and DB850-6 were fabricated with suddenly debonded strands at both ends. Also, the south end of DB850-2 contained suddenly debonded strands. Once testing had been completed on gradually debonded girders, DB850-3 and DB850-4, test DB850-5A (S) was set up as a companion test to match the embedment length of the flexural failure, DB850-4A (G).

During test DB850-5A(S), cracking developed in the debond/transfer zone at 95 percent of the predicted load producing strand slip. Although the girder maintained the applied loading during additional deformations, additional strand slip eventually caused the girder to fail in flexure at 84 percent of the calculated load. The test was defined as a bond failure.

Test DB850-6A (S) was set up with an embedment length of 150 inches (1.875 L_d) after failure occurred at 120 inches (1.5 L_d) in the previous test. As testing proceeded, flexural cracking again developed in the debond/transfer zone leading to slip of all four suddenly debonded strands. This test was also defined as a bond failure.

Figure 5.7 illustrates the reason behind the various types of failures. The figure displays the applied moment versus cracking moment for the two types of specimens. It also exhibits the test setup for all three of the tests that were discussed. As shown, the gradual debonding allows a larger portion of the effective prestress to be transferred to the specimen closer to the end resulting in a higher cracking moment. The higher cracking moment capacity allowed DB850-4A (G) to develop the full flexural capacity without the development of cracking in the debond/transfer zone.

In the case of the suddenly debonded strands, the cracking moment remains constant until transfer occurs for the debonded strands. This results in a lower cracking moment in the debond/transfer zone. Both DB850-5A (S) and DB850-6A (S) required a larger cracking moment to develop the full capacity of the cross section. The outcome was the formation of cracking in the debond/transfer zone and strand slip. In order to prevent

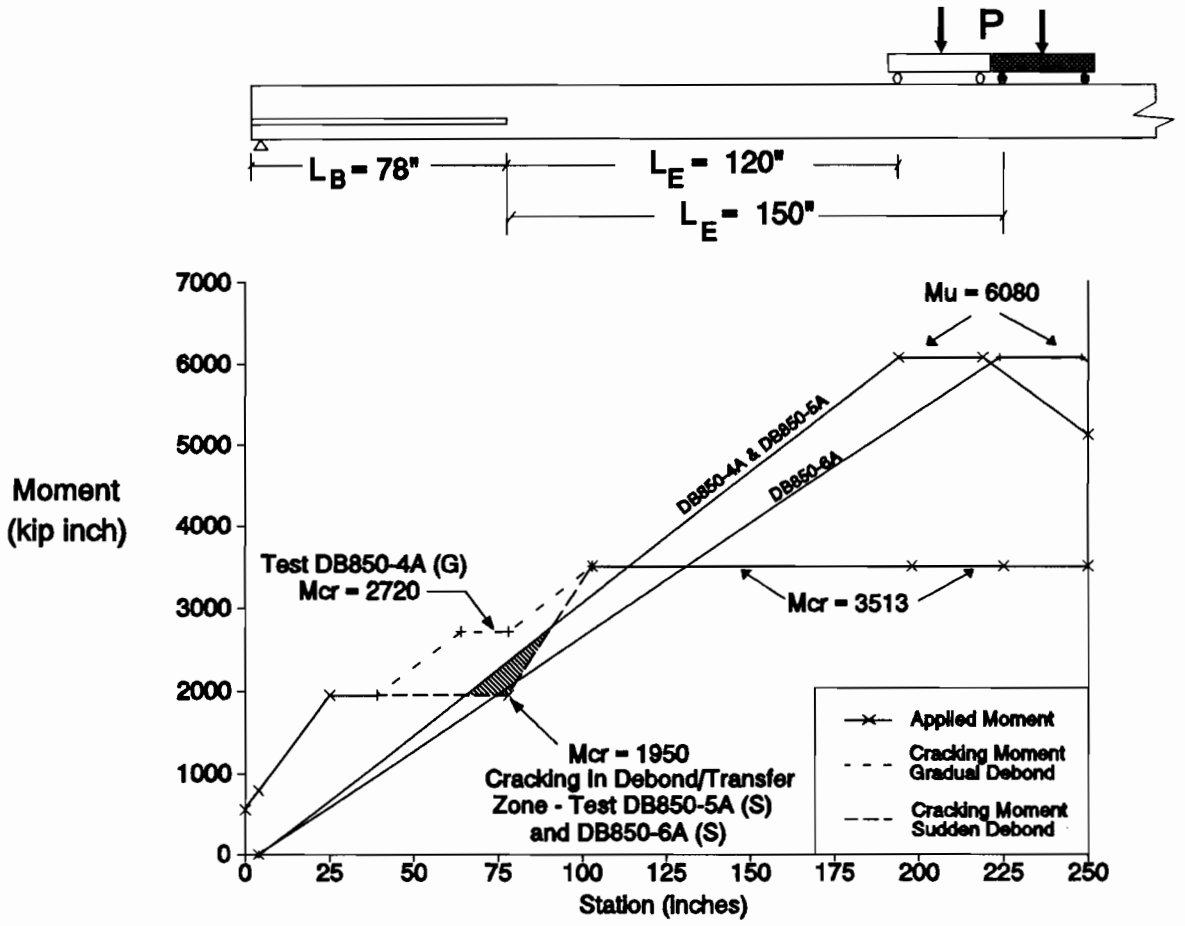

Figure 5.7 Applied Moment vs. Cracking Moment

cracking in the debond/transfer zone, an estimated embedment length of 166 inches (2.075 L_d) would be required. This is an increase of 66 percent over the length required for a gradually debonded specimen, (L_e = 100 inches, 1.25 L_d).

The effects of suddenly debonding strands versus gradually debonding strands is evident. In comparison to gradual debonding, the sudden termination of strands results in a lower cracking moment in the debond/transfer zone . The amount of difference is dependent upon the length of debonding and the number of strands of strands involved. Because end slip normally accompanies cracking in the debond/transfer zone, the lower cracking moment could be the difference between a flexural failure mode or a bond failure mode in specimens with debonded lengths.

5.5 Development Length

The development length code provisions are presented in Section 2.2. For strand extending to the end of the member, the calculated development length required is 80 inches for 0.5 inch diameter strand. For debonded 0.5 inch strand, the required development length is 160 inches.

Figure 5.8 illustrates the development lengths determined experimentally for 0.5 inch diameter debonded strand. As shown, the development length was determined to be 84 inches for strand debonded to a maximum length of 36 inches. For strands gradually debonded to a length of 78 inches, the development length was determined to be 100 inches. These lengths correspond to 0.525 L_d and 0.625 L_d, respectively, and indicate that the code provisions are extremely conservative.

The development length could not be determined from the data obtained for specimens containing suddenly debonded strands. However, an estimate, based on the two bond failures and the prediction model, predicts a development length of 166 inches is required. This corresponds to 1.0375 L_d which suggests that the code is slightly unconservative.

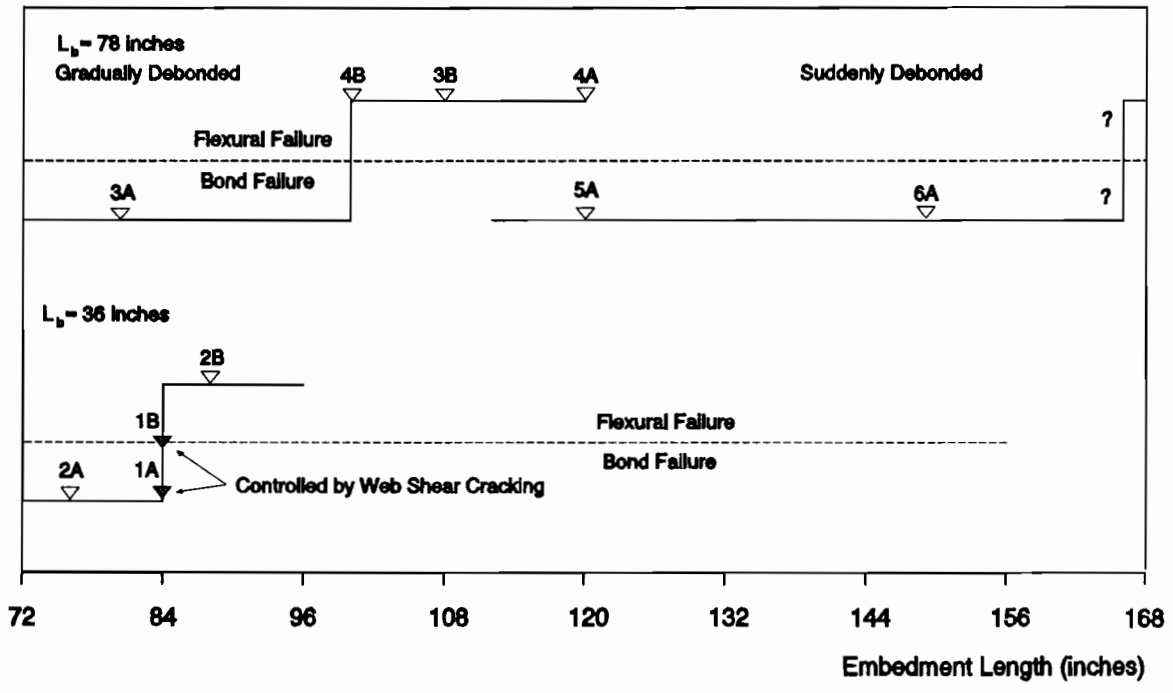

Figure 5.8 Development Length of Tests

These results indicate that the current ACI code provision inaccurately predicts the required length necessary to develop the full flexural capacity of a member containing debonded strands. The three different development lengths demonstrate that a constant value for all cases of debonding for a particular strand is unreasonable and can be highly inaccurate. Instead, the code provision should also account for the cross sectional properties, the percentage of strands debonded, and the length of the debonding. The conclusion is that the code requirement is inconsistent with the demonstrated behavior of specimens containing debonded strands and should be changed.

5.6 Prediction Model

The prediction model of cracking and bond failure was discussed in Section 3.1.1. It was based on the theory that bond failure would occur if cracking developed in the debond/transfer zone of a specimen. The model accounted for loading conditions, cross sectional properties, length of debonding and the percentage of strands debonded. A graphical presentation of the model is found in Figure 5.9.

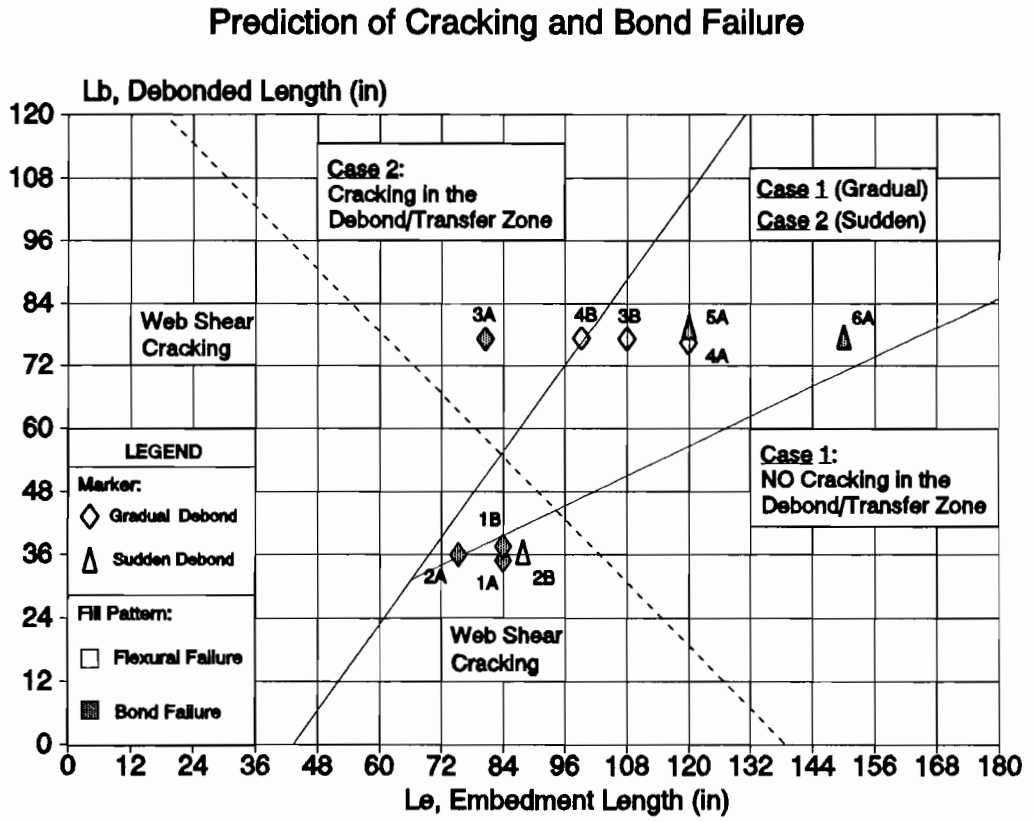

Figure 5.9 Overlay of Test Results on Prediction Model

The results for the tests are also displayed on Figure 5.9. The accuracy of the model was very good when compared to the failures experienced by the specimens containing debonded lengths of 78 inches. An example of the accuracy was test DB850-4B (G). The tested embedment length placed the specimen on the border between case 1 and case 2. This meant that flexural cracking could occur before the flexural capacity of the section was achieved. During the test, flexural cracking formed in the debond/transfer zone at 99 percent of the predicted load. However, the specimen demonstrated additional capacity and failed in a flexural mode at 99.5 percent of the predicted load.

In viewing the data from the specimens containing debonded lengths of 36 inches, the prediction model was also very accurate. Although the model predicted a flexural failure for all four tests, it also suggested that web shear cracking could influence the outcome. As indicated in the figure, the first three tests experienced a bond failure. The failure occurred when web shear cracking developed in the debond/transfer zone and caused strand slip. The only flexural failure resulted when the web shear cracking was prevented from propagating into the level of strands.

In general, the prediction model reliably predicted the cracking in the debond/transfer zone of the specimens. Since strand slip and bond failure are directly related to cracking, the model also displayed a high correlation between the predicted and the observed failure modes. The significance is that the prediction model could be used in a design application to determine the embedment length necessary to develop the full flexural capacity of a beam.

CHAPTER SIX

SUMMARY AND CONCLUSIONS

6.1 Summary

This thesis presents the results from the fourth phase of an ongoing investigation into the behavior of prestressed concrete beams containing debonded strands. This phase examined the behavior of specimens containing debonded strands subjected to static loading. Eleven tests were conducted on six specimens containing 0.5 inch diameter strands. Each specimen contained eight strands, four of which were debonded at each end.

The experimental program focused on the influence of cracking, length of debonding, debonding termination points, and strand embedment length on the flexural capacity of the specimens. An analytical model was developed to predict the failure mode of each test. During testing, the required data was obtained using load cells, strand strain gauges, LVDT's and a DEMEC mechanical strain gauge.

Following the presentation of the data, the test results were discussed in relation to the primary variables. Further discussions presented a comparison of the data to current code provisions and to the prediction model.

6.2 Conclusions

During the course of the investigation, a number of variables were studied to determine their influence on the behavior of specimens containing debonded strands. The conclusions drawn from the observed behavior are presented below:

1. The formation of flexural cracking in the debond/transfer zone of the debonded strands leads to bond failure and general slip of the strands. The result is a loss of prestress and a reduction in the ultimate flexural capacity of the specimen.

2. The effect of the formation of web shear cracking in the debond/transfer zone at the level of the strands, is an immediate, catastrophic collapse. Unlike flexural cracking, web shear cracking affects all strands and should be prevented.

3. Sudden termination of strand debonding results in a lower cracking moment in the debond/transfer zone in comparison to a gradually debonded companion specimen. Because strand slip normally accompanies flexural cracking in the debond/transfer zone, a lower cracking moment in this zone could result in a bond failure instead of a ductile flexural failure. Unless calculations determine it to be satisfactory,

termination of strand debonding of multiple strands at the same point should not be considered.

4. The occurrence of small amounts of strand slip does not, by itself, indicate a general bond failure. For the failure to occur, the slip must occur in conjunction with a decrease in the load carrying capacity for the specimen.

Also during the investigation, an analytical model was developed to predict cracking in the debond/transfer zone and the resulting bond failure. To determine the validity of the model, the results of the experimental program were compared to the predicted results. From the comparison, the following conclusions were reached:

1. The ability to accurately calculate the cracking moment and the flexural capacity of a specimen is possible.

2. The prediction model reliably predicts cracking in the debond/transfer zone. Since strand slip and bond failure are directly related to cracking, the model also predicts the failure mode for the specimen.

3. The current code provision is inconsistent with the demonstrated behavior of specimens containing debonded strands. Changes should be considered that incorporate the additional affects of loading conditions, length of debonding, and cross sectional properties. However, before a code provision is suggested, it is recommended that consideration should be given to fatigue and the influence it also has on the behavior of beams with debonded strands.

APPENDIX A

STEEL AND CONCRETE MATERIAL PROPERTIES

This appendix presents the material properties for both the steel strand and concrete used in the experimental program. Figure A1 displays the stress-strain relationship furnished by Florida Wire and Cable for the prestressing strand. The strand measured 0.5 inches in diameter, and was a low-relaxation, seven-wire prestressing strand.

Table A1 presents the concrete mix design and Table A2 gives concrete cylinder strengths at various times. Figures A2 through A6 demonstrate the concrete compressive strength versus elapsed time. A total of five casts were completed for the six girder specimens.

Table A1 Concrete Mix Design

Material	Quantity
Type I Cement	611 pounds/cubic yard
Water	290 pounds/cubic yard
Course Aggregate (Gravel)	1680 pounds/cubic yard
Fine Aggregate (Sand)	1355 pounds/cubic yard
Master Builders 761-N Admixture	37.0 ounces/cubic yard

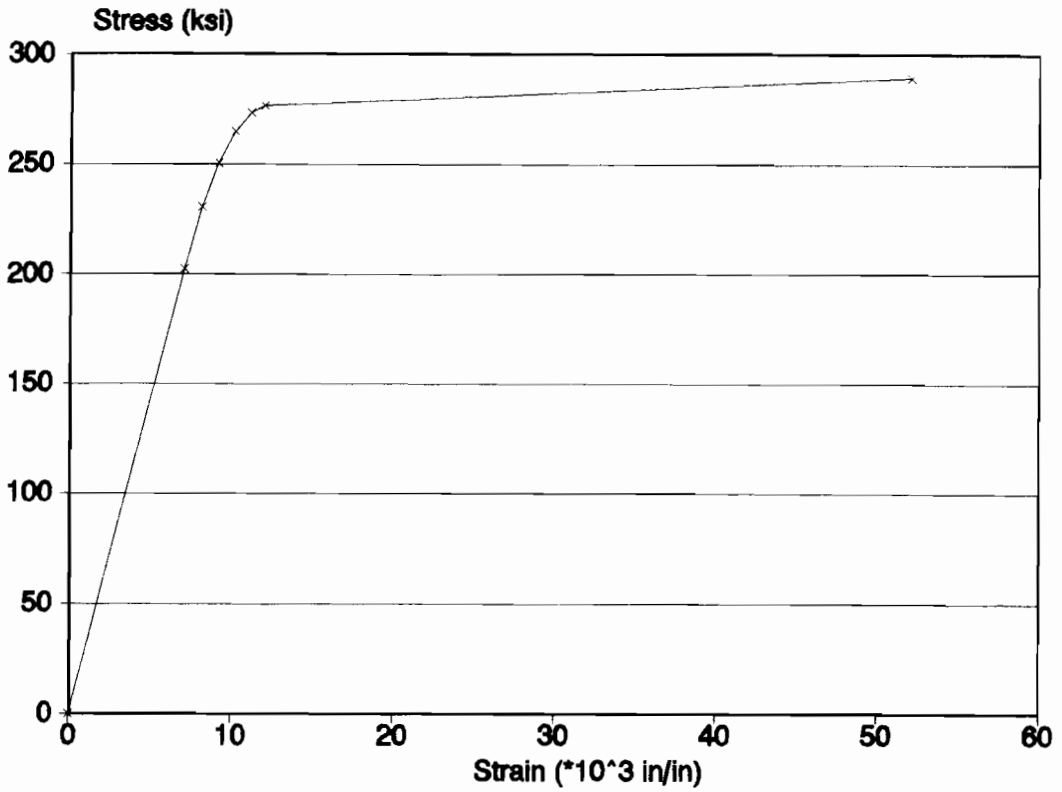

Figure A1 0.5-inch Diameter Strand

Table A2
CONCRETE CYLINDER STRENGTHS

BEAM	RELEASE (2 days)	28 DAYS	@ FLEXURAL TEST
DB850-1	4640	6560	7010
DB850-2	4640	6560	7010
DB850-3	5080	6250	6610
DB850-4	5800	6320	7370
DB850-5	5580	6320	7460
DB850-6	5150	6880	6940

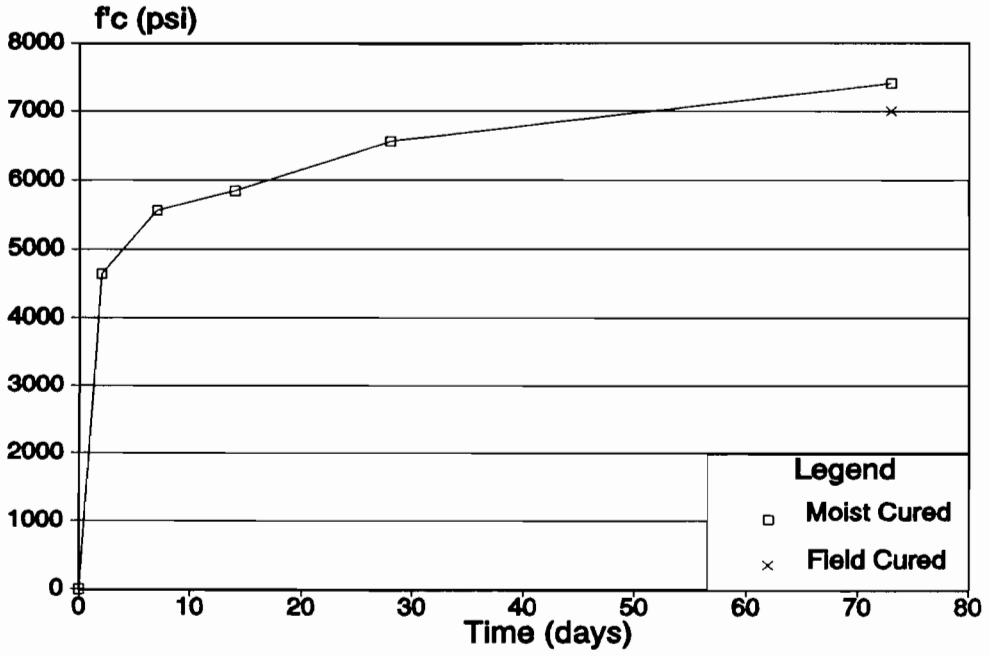

Figure A2 - Beams DB850-1 and DB850-2

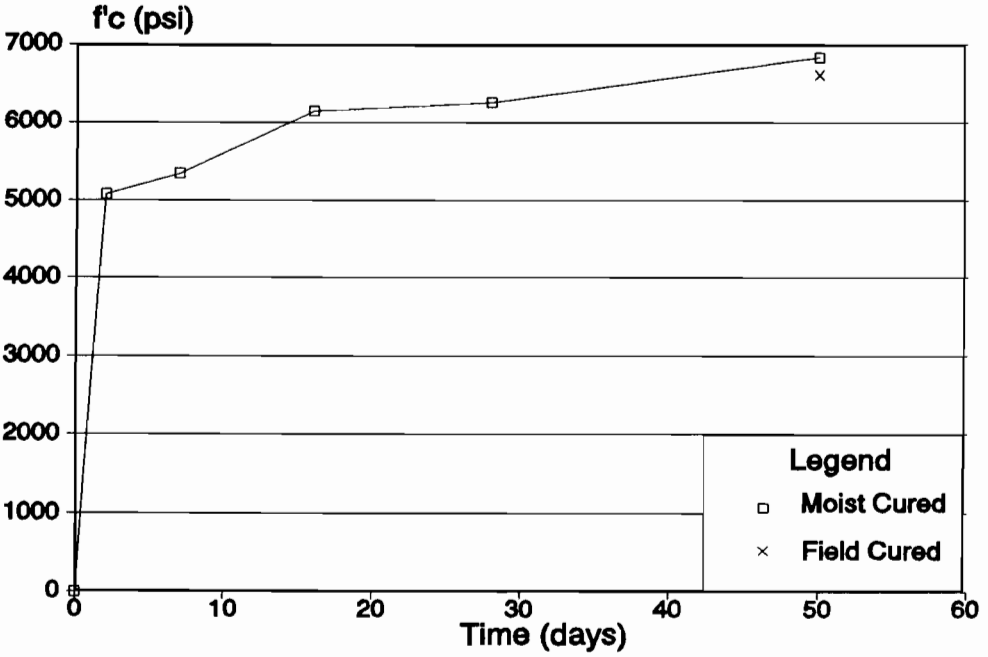

Figure A3 - Beam DB850-3

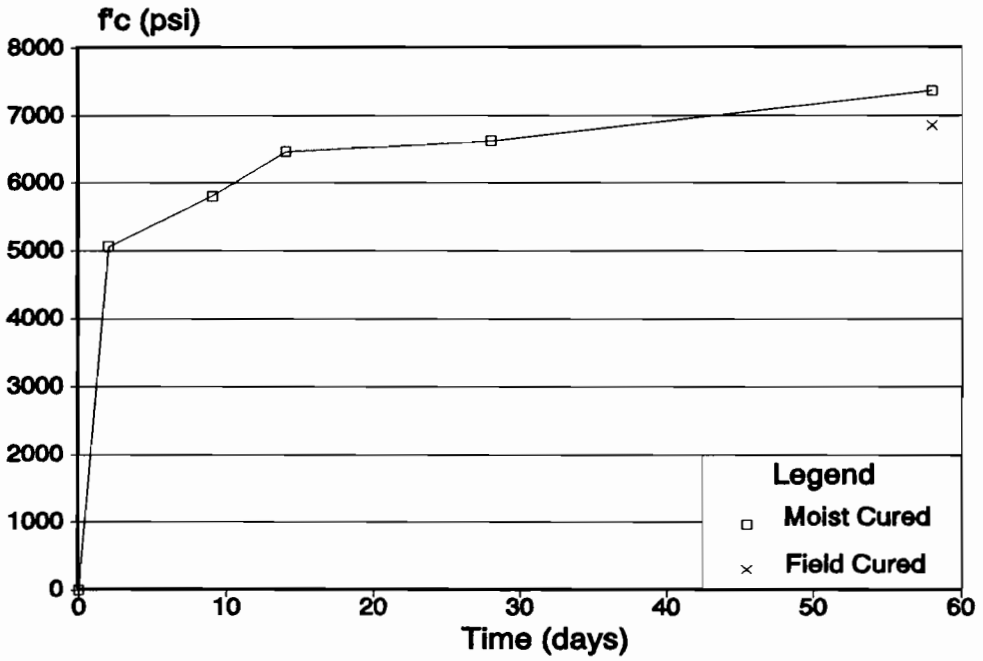

Figure A4 - Beam DB850-4

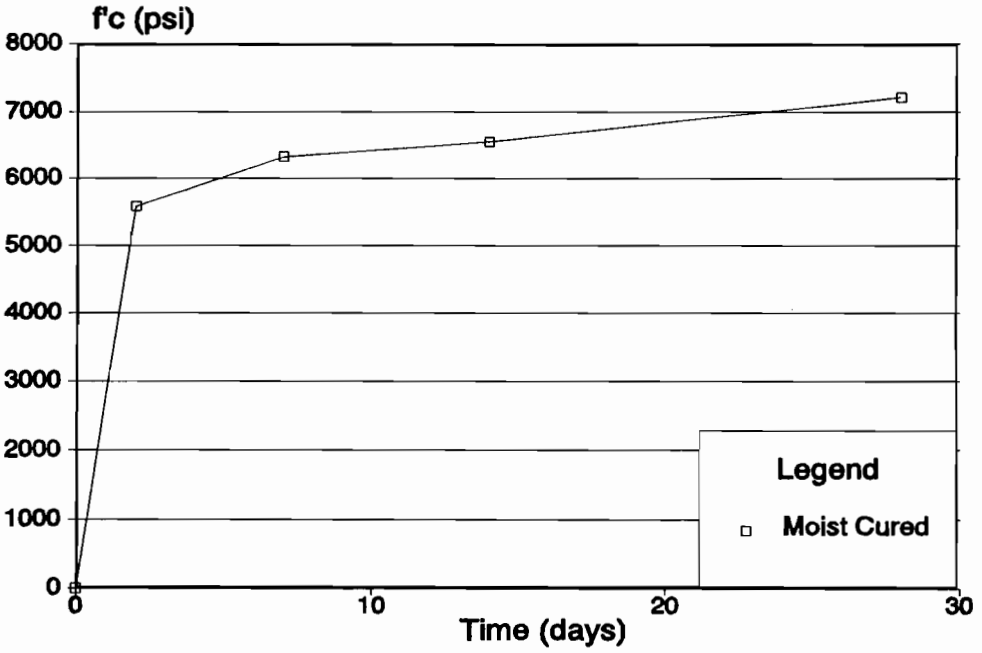

Figure A5 - Beam DB850-5

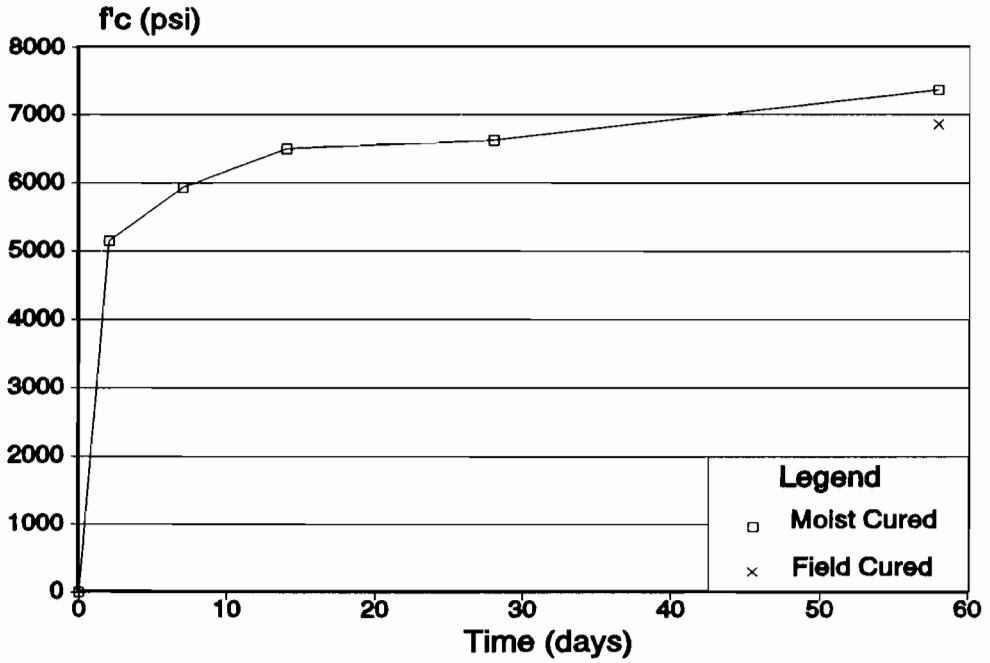

Figure A6 - Beam DB850-6

APPENDIX B

LOAD VERSUS CONCRETE COMPRESSIVE STRAIN

This appendix presents the average extreme fiber strain vs. applied load for all ten tests. The data was obtained using the DEMEC mechanical gauge. The measurements plotted are an average strain recorded over four, eight-inch gauge lengths located between the two load points.

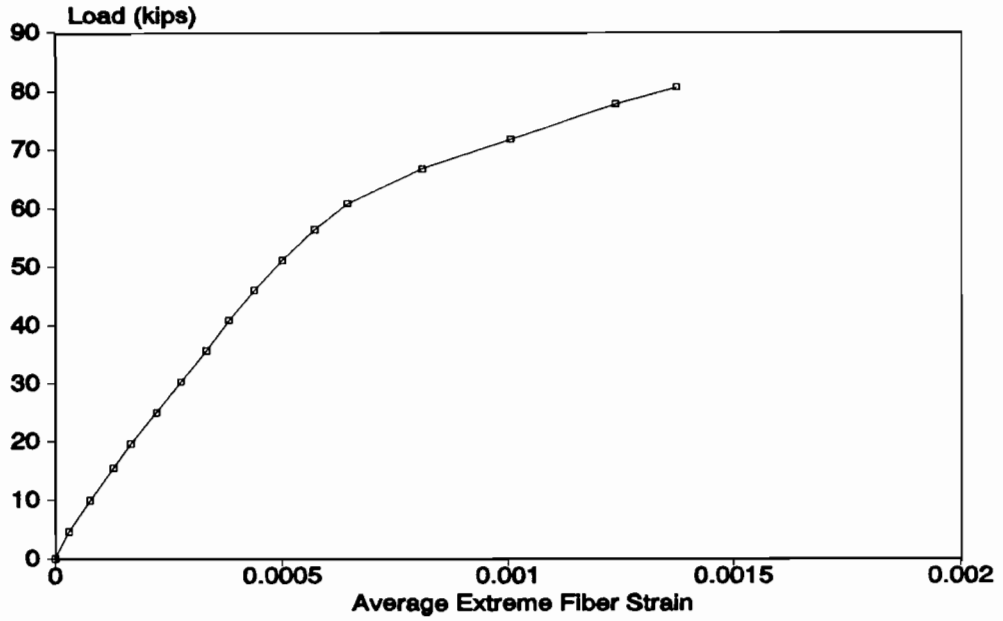

Figure B1 - Test DB850-1A (G)

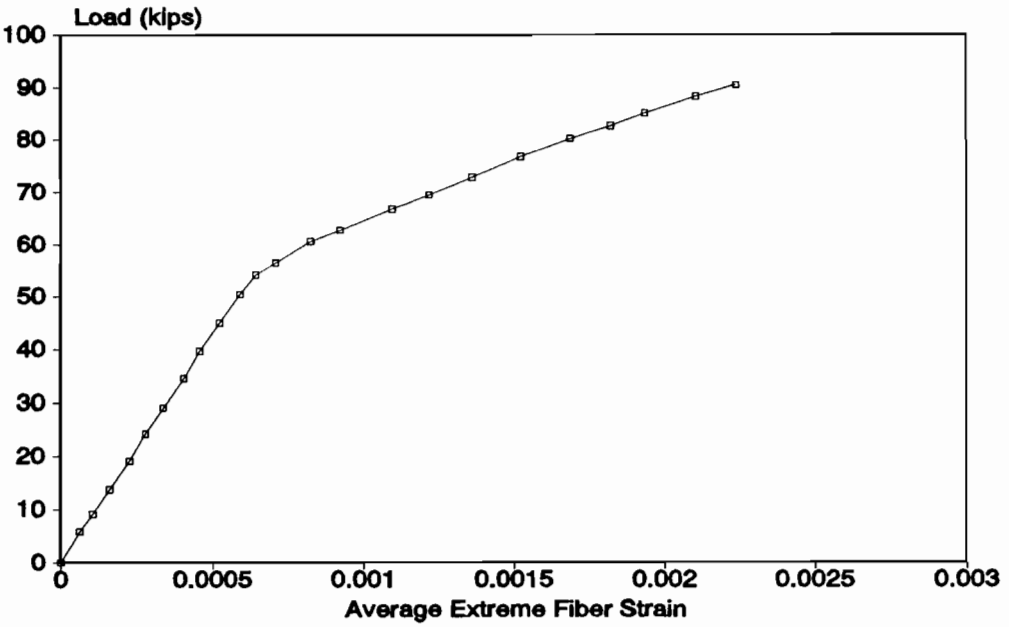

Figure B2 - Test DB850-1B (G)

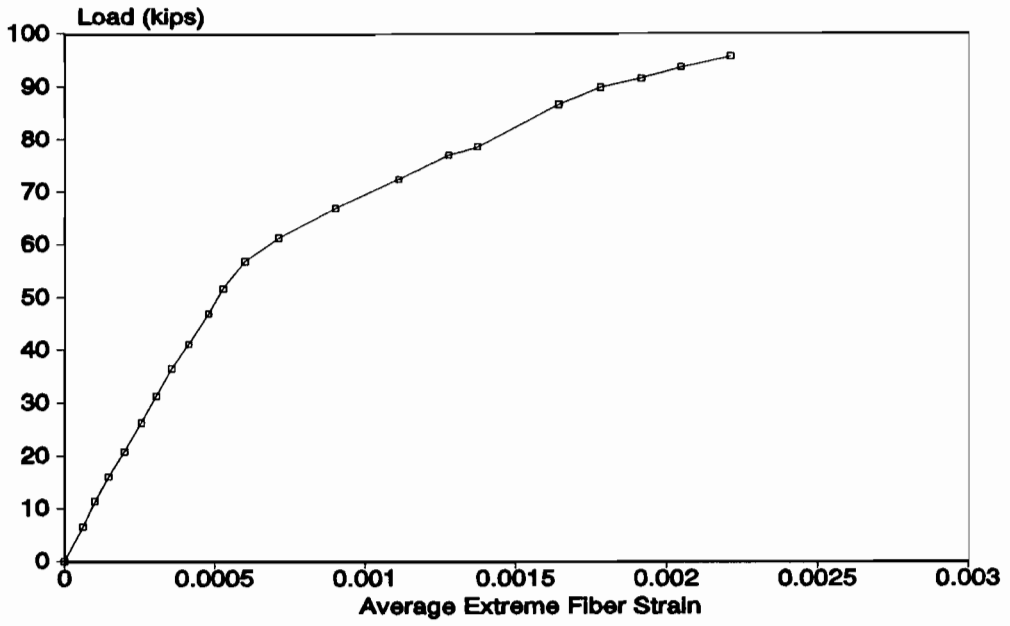

Figure B3 - Test DB850-2A (G)

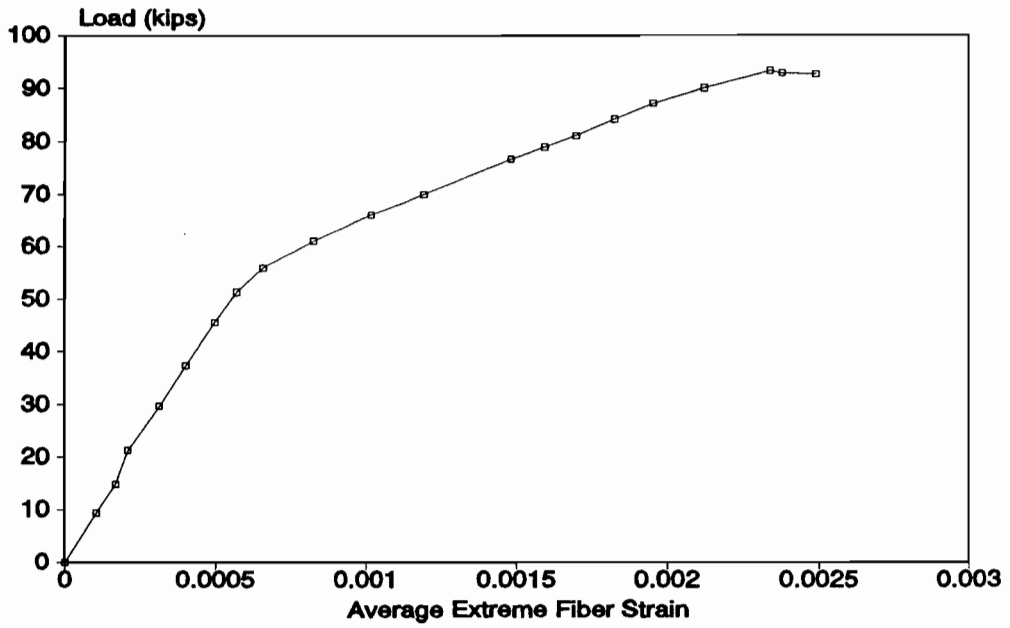

Figure B4 - Test DB850-2B (S)

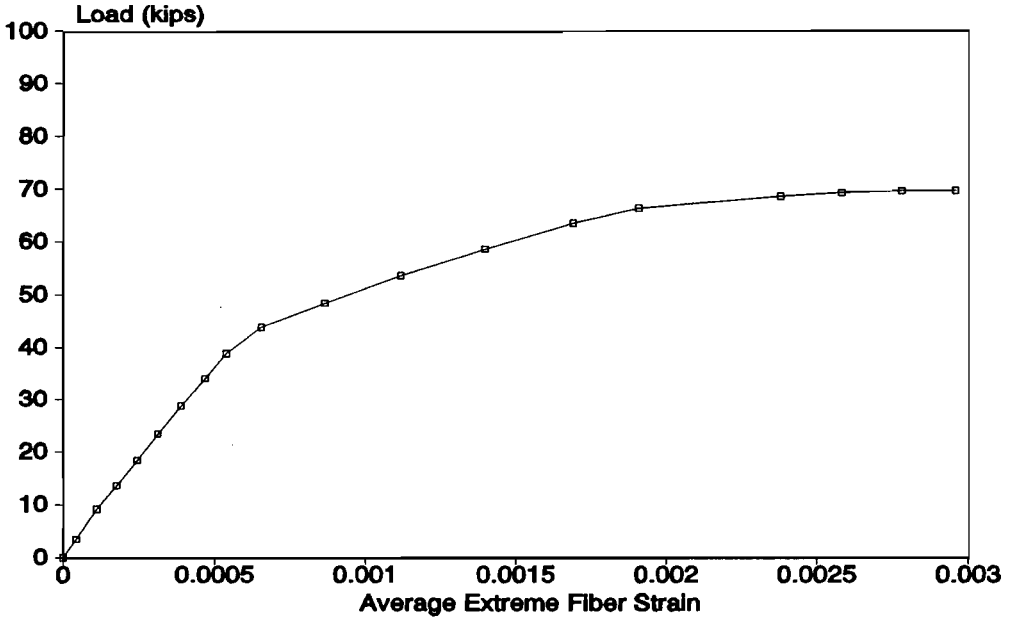

Figure B5 - Test DB850-3A (G)

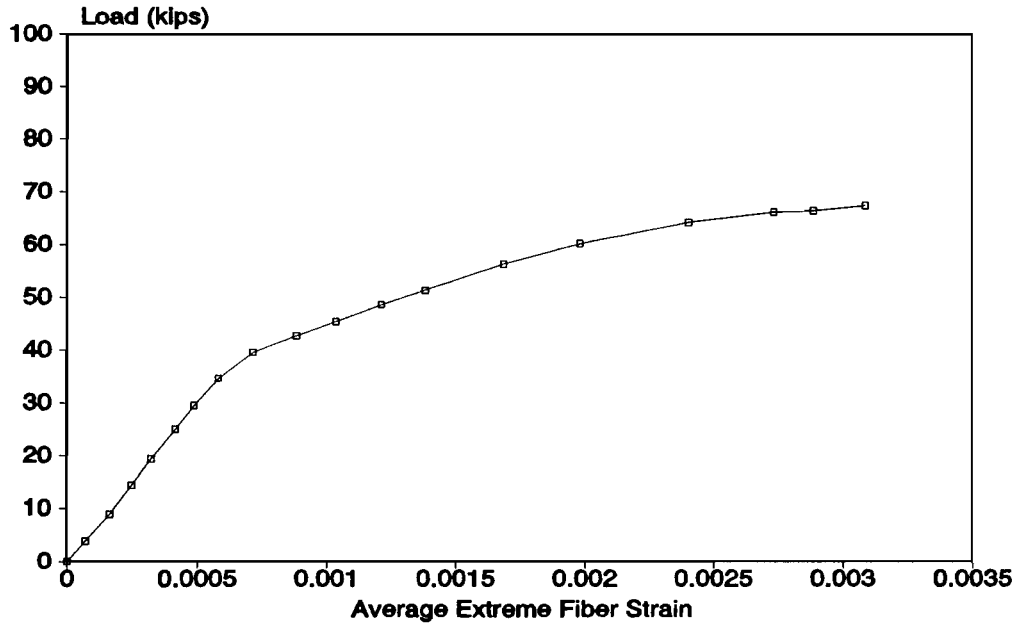

Figure B6 - Test DB850-3B (G)

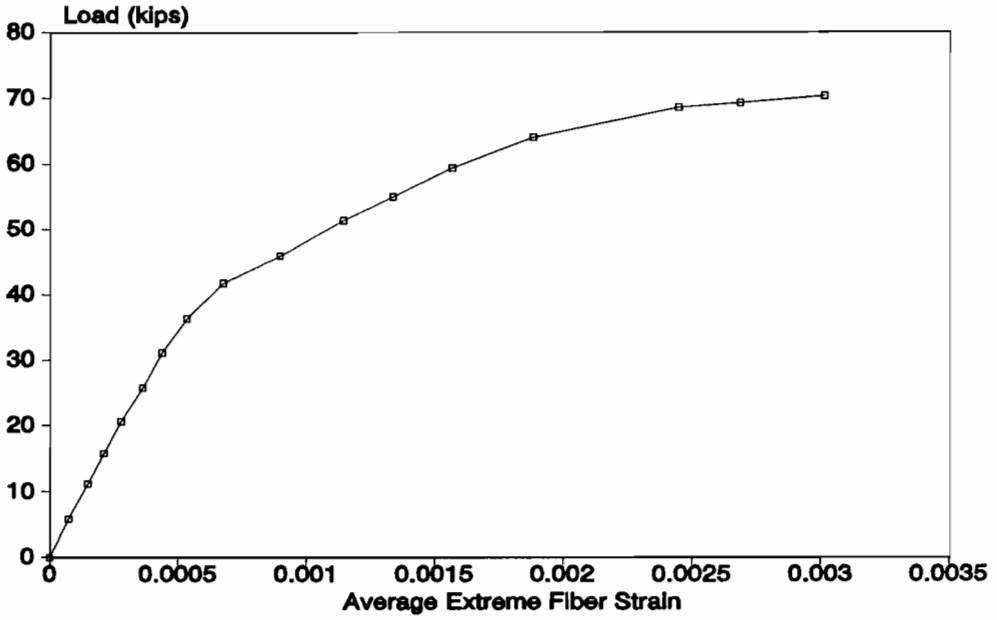

Figure B7 - Test DB850-4A (G)

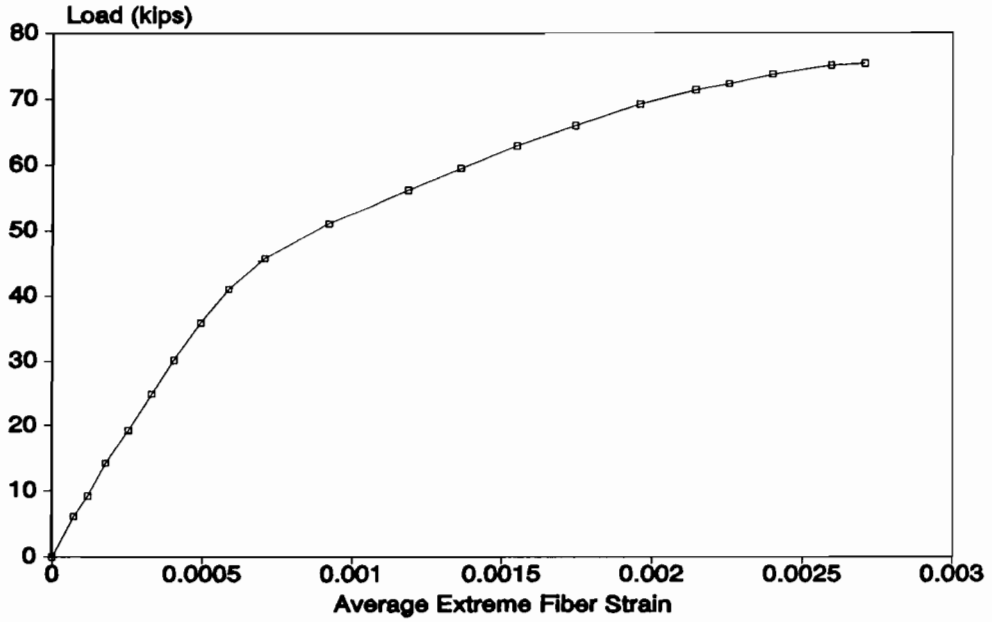

Figure B8 - Test DB850-4B (G)

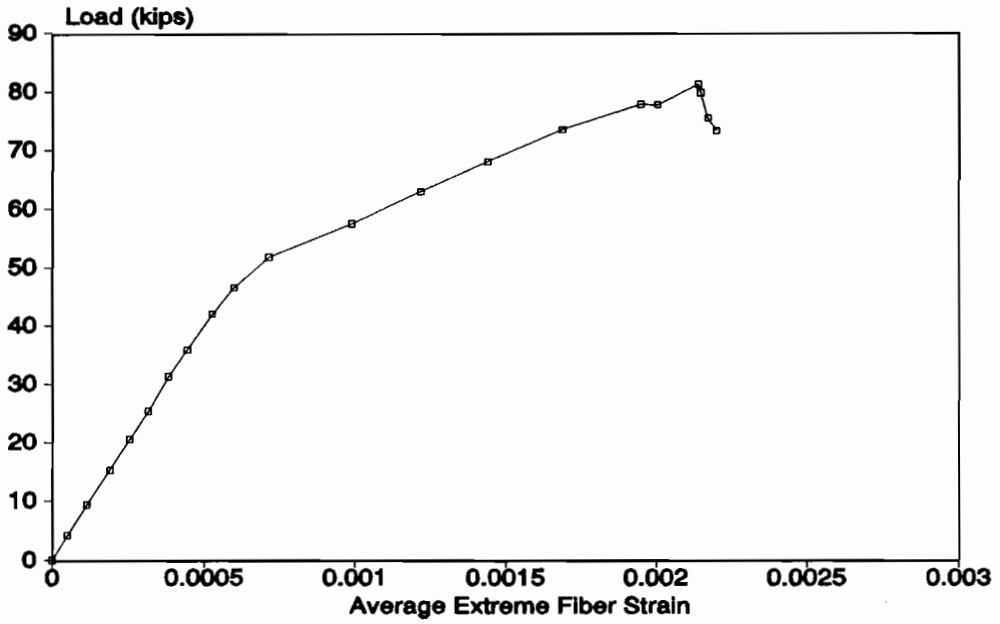

Figure B9 - Test DB850-5A (S)

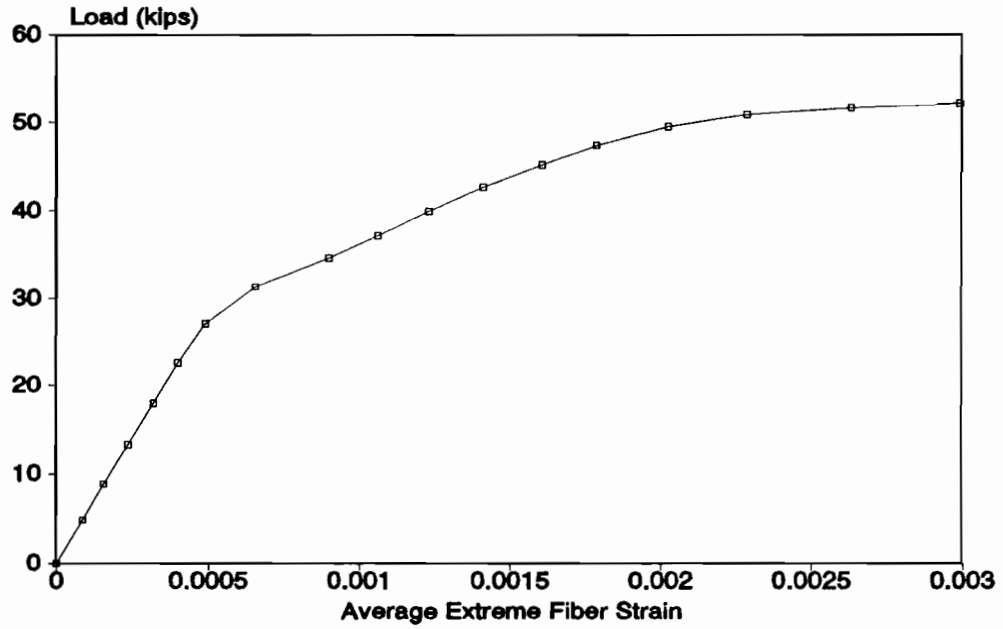

Figure B10 - Test DB850-6A (S)

APPENDIX C

MOMENT VERSUS CURVATURE RELATIONSHIP

The moment versus curvature relationship was derived for the specimens based on strain compatibility. It is displayed in Figure C1. The predicted load versus deflection curves, plotted on test load vs. deflection graphs, were based on Figure C1.

C.1 Effective Prestress

To derive the moment versus curvature relationship, it was necessary to determine the level of effective prestress at the time of testing. To determine the level of force after initial tensioning and seating losses, the elongation measurement for each strand was divided by the initial length of the strand. This value was then multiplied by the modulus of elasticity for the strand to obtain the level of stress. An example calculation of the average elongation is shown below:

$L_{elongation} / L_{initial} * E_s + 10.4$ ksi = Total Strand Stress

Average Elongation	=	5.48 inches
Strand Length	=	840 inches
Average Strand Strain	=	0.006524 in/in
Modulus of Elasticity (E_s)	=	$28.6 * 10^3$ ksi
Stress in the Strand due to Elongation	=	186.6 ksi
Initial Stress Before Measurements	=	10.4 ksi
Average Stress in All Strands	=	197.0 ksi

From the time of initial strand stressing until the specimen was actually tested, a time period of 50 to 70 days occurred. In this time, the amount of stress in the strand was reduced by a series of losses including transfer, creep and shrinkage. The losses were estimated using the general method described by the PCI Committee for calculating prestress losses [10,15]. The technique estimated the losses in two time intervals: from initial stressing to transfer, and from transfer to the time of testing.

The calculations completed are shown below:

Initial calculations:

f'_{ci} = 5000 psi; E_{ci} = 4030 ksi

f'_c = 6000 psi; E_c = 4415 ksi

f_{pu} = 289.5 ksi; E_s = 28600 ksi

Volume/Surface area = 2.62: SSF* = 0.9; SCF* = 0.9

UCR = 95 - 20 E_c / 10^6 ≥ 11; UCR = 11

USH = 27000 - 3000 E_c / 10^6 ≥ 12 ksi; USH = 13.742

* values obtained from tables listed in Appendix D of reference 10.

Initial Tensioning and Transfer:

Relaxation:

RET = f_{st} {[log $24t_2$ - log $24t_1$] / 45} * [f_{st} / 0.9f_{pu} - 0.55]

t_1 = 1/24, t_2 = 2, f_{st} = 197 ksi, f_{pu} = 289.5

RET = 1.52 ksi

Elastic Shortening at Transfer:

M_G = 492.5 inch-kip

f_c = 492.5 * 9.1 / 12083 = 0.371 ksi

Assume ES = 16.1 ksi

f_{si} = 180.9 ksi; Po = 180.9 * 1.224 = 221.4 kips

f_{ct} (due to Po) = 221.4 / 197 + 221.4 * $(9.1)^2$ / 12083 = 2.641 ksi

f_{ct} = 2.641 - 0.371 = 2.27

ES = f_{ct} * E_s / E_c = 16.1 ksi ✓ok with assumption

Total losses:

$$TL = 16.1 + 1.52 = 17.62 \text{ ksi}; \quad f_{st} = 179.4 \text{ ksi}$$

From Transfer to Testing at 60 Days:

Relaxation:

$$RET = f_{st} \{[\log 24t_2 - \log 24t_1] / 45\} * [f_{st} / 0.9f_{pu} - 0.55]$$

$$t_1 = 2, \; t_2 = 60, \; f_{st} = 179.4 \text{ ksi}, \; f_{pu} = 289.5$$

$$RET = 0.82 \text{ ksi}$$

Creep:

$$CR = UCR * SSF^{*} * PCR^{*} * f_{ct} = 11 * 0.9 * 0.45 * 2.27 = 10.1 \text{ ksi}$$

Shrinkage:

$$SH = USH * SSF^{*} * PSH^{*} = 13.742 * 0.9 * 0.55 = 6.8 \text{ ksi}$$

Total losses:

$$TL = 0.82 + 10.1 + 6.8 = 17.72; \quad f_{st} = 161.7 \text{ ksi}$$

The effective prestress at the time of testing was calculated to be 161.7 ksi. However, for simplicity, a value of 160 ksi was used in the calculations for the moment versus curvature relationship.

C.2 Moment versus curvature relationship

The moment versus curvature relationship calculations were based on the following considerations [10]:

1. $f'_c = 6000$ psi and $f_{st} = 160$ ksi.

2. In the uncracked section, changes in strain in the steel and concrete after bonding are assumed to be the same.

3. The stress-strain curve provided in Appendix A was used for the prestressing strand.

4. The strains are distributed linearly over the depth of the beam.

5. The stress-strain relationship for the concrete used the Secant Modulus approach:

$$\epsilon_0^2 - 4(\epsilon_{50} * \epsilon_0) + 2\epsilon_{50}^2 = 0$$

After solving for ϵ_0, hand calculations were performed to determine initial curvature and the curvature associated with the cracking moment. The points after cracking were determined by a computerized trial and error procedure.

The procedure assumed a position for the neutral axis for a given concrete strain. The compressive concrete load was then found using the following equation:

$$C_c = b * c^2 * (f'_c) * (\Phi / \epsilon_0) * [1 - (\Phi c) / (3\epsilon_0)]$$

The level of tensile load in the steel was then checked. If the tensile load (T) did not approximately match the compressive load (C_c), a new position for the neutral axis was chosen. The procedure continued until $T=C_c$ and the corresponding moment was calculated. The ultimate moment represents an extreme fiber strain in the concrete of 0.003 in/in. Figure C1 illustrates the moment versus curvature relationship.

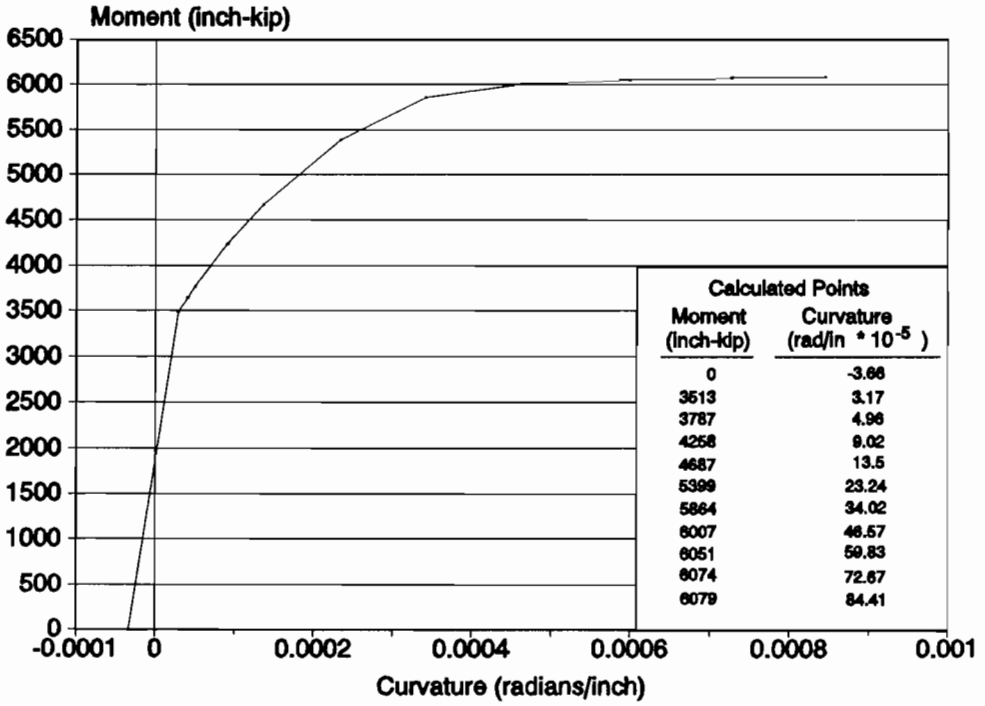

Figure C1 - Moment vs. Curvature Relationship

APPENDIX D

PREDICTION MODEL CALCULATIONS

This appendix presents the calculations performed in developing the prediction model for cracking and bond failure. Bruce W. Russell, a Ph. D. candidate responsible for the completion of the overall investigation, developed the prediction model [16].

D.1 Assumptions

In developing the prediction model, a number of assumptions were made. They are as follows:

1) Transfer length of 0.5 inch diameter strand is 25 inches.

2) In a suddenly debonded specimen, flexural cracking occurs at the cracking moment of the debonded region at the termination point of the debonding (point A).

3) In a gradually debonded specimen, cracking occurred when M_{cr} of the entire section was achieved at the end of the debond/transfer zone (point B).

4) Until cracking, concrete behaves as elastic, isotropic material.

5) $f_c' = 6000$ psi.

6) The flexural tensile capacity of the concrete was equal to $7.5\sqrt{f_c'}$.

7) For web shear calculations, the inclined tensile capacity of the concrete was equal to $4\sqrt{f_c'}$.

D.2 Prediction Model Calculations:

The prediction model consisted of three separate calculations. The calculations involved the embedment length versus debond length relationships for both the suddenly and gradually debonded cases and also the value of the web shear capacity of the specimen. The calculations are presented below:

Suddenly Debonded Relationship:

The relationship between embedment length and the debonded length is illustrated in Figure D.1 and is represented by equation 1:

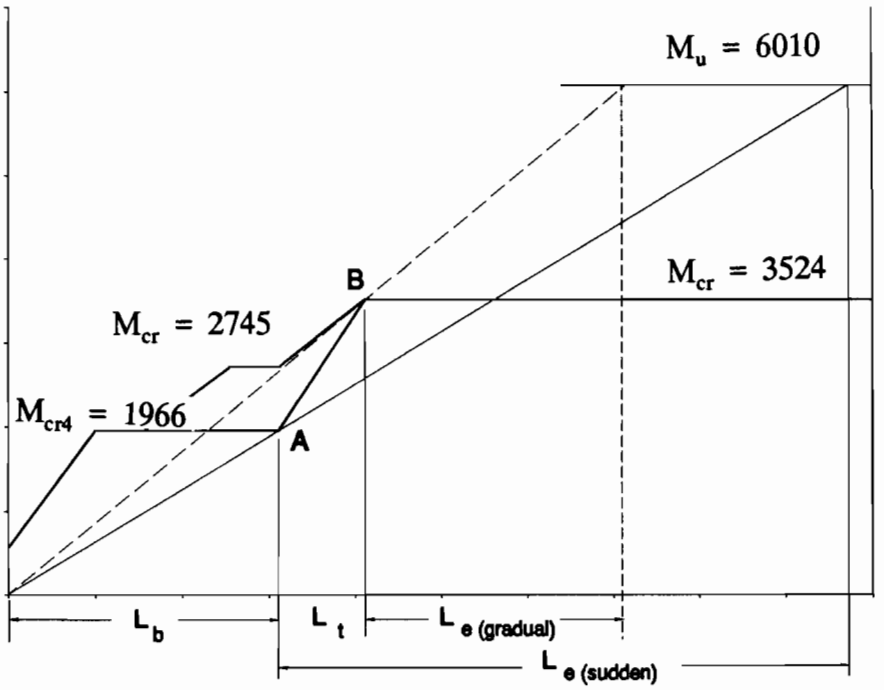

Figure D.1 Relationship Between L_e and L_b

$$\frac{M_{cr4}}{L_b} = \frac{M_{ult}}{L_b + L_e} \tag{1}$$

The equation is simplified by substituting the values 1966 and 6010 inch-kips for M_{cr4} and M_{ult}, respectively. It is represented by equation 2.

$$L_b = 0.486\, L_e \tag{2}$$

The significance of equation 2 is that if $L_b > 0.486\ L_e$, cracking will occur in the debond/transfer zone resulting in a bond failure.

Gradually Debonded Relationship:

The relationship between embedment length and the debonded length is illustrated in Figure D.1 and is represented by equation 3:

$$\frac{M_{cr}}{L_b + L_t} = \frac{M_{ult}}{L_b + L_e} \tag{3}$$

The equation is simplified by substituting the values 3524 and 6010 inch-kips and 25 inches for M_{cr}, M_{ult}, and L_t, respectively. The new representation is shown by equation 4.

$$L_b = 1.42\ L_e - 60.4 \tag{4}$$

The significance of equation 2 is that if $L_b > 1.369\ L_e - 59.27$, cracking will occur in the debond/transfer zone resulting in a bond failure.

Web Shear Capacity:

Web shear capacity was computed as the shear force resulting in a principal tensile stress of $4\sqrt{f_c'}$ at the centroidal axis of the specimen. The critical cross section has only four strands active in prestressing the concrete; f_{ce} is computed from the prestress force of four strands. The resulting equation is shown by equation (5).

$$\frac{v_s\ I\ b_w}{Q} \tag{5}$$

where

$$v_s^2 = \left(4\sqrt{f_c'} + \frac{f_{ce}}{2A_c}\right)^2 - \left(\frac{f_{ce}}{2A_c}\right)^2$$

The values of the variables used are shown below:

f_{se}	= 152 ksi	A_s	= 197 inches^2	f_{ce}	= 472 psi
f_c'	= 6000 psi	b_w	= 4.5 inches		
d	= 19.5 inches	Q	= 713 in^3		

The result was that web shear cracking will occur at a shear of $V_{cw} = 40.3^k$ kips. By dividing the ultimate flexural capacity by the web shear capacity, a relationship was derived for embedment length versus debond length. The relationship is displayed in equation (6).

$$L_e = L_b - 149.1 \text{ in.} \tag{6}$$

All three sets of calculations are summarized on Figure D.2.

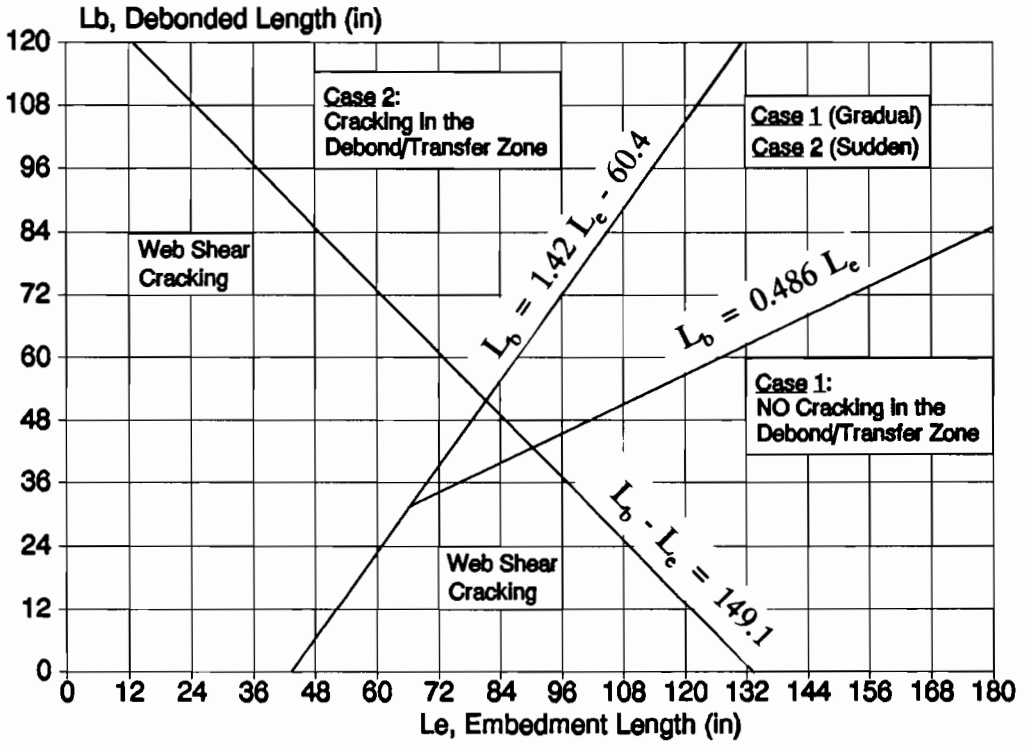

Figure D.2 Development of Prediction Model of Cracking and Bond Failure

APPENDIX E

NOTATION

This appendix contains the definitions of the symbols used throughout this thesis.

b	---	width of top flange (inches)
b_w	---	width of web (inches)
c	---	position of neutral axis measured from top of section (inches)
CR	---	loss of prestress due to creep of concrete over time (ksi) [10]
d	---	distance from extreme compression fiber to centroid of longitudinal tension reinforcement (inches)
d_b	---	strand diameter (inches)
ϵ_0	---	concrete strain corresponding to 28 day concrete strength
ϵ_{50}	---	concrete strain corresponding to 50% of 28 day concrete strength
f'_c	---	compressive strength of concrete at 28 days (psi)
f'_{ci}	---	initial concrete compressive strength at transfer (psi)
f_{ps}	---	stress in prestressed reinforcement at nominal strength (ksi)
f_{pu}	---	ultimate tensile strength of prestressing strand (ksi)
f_{se}	---	effective stress in prestressed reinforcement after allowance for all prestress losses (ksi)
f_{si}	---	stress in prestressing reinforcement immediately after transfer (ksi)
f_{st}	---	stress in prestressing steel at time t (ksi)
ksi	---	kilopounds per square inch
L_b	---	length of debonding (inches)
L_d	---	development length (defined in Section 2.1) (inches)

L_e	---	distance from end of the longest debonded length to the point of maximum moment (inches)
L_{flex}	---	flexural bond length (inches)
L_t	---	transfer length of prestressing strand (inches) -- Assumed to be 25 inches for 0.5 inch diameter strand.
M_{calc}	---	ultimate moment calculated by strain compatibility
M_{cr}	---	moment causing flexural cracking to occur in section (inch-kip)
M_G	---	moment due to loads present at the time of transfer (inch-kip)
PCR	---	amount of creep over a specified time interval [10]
psi	---	pounds per square inch
PSH	---	amount of shrinkage over a specified time interval [10]
RET	---	loss of prestress due to steel relaxation over a specified time interval [10]
SCF	---	factor that accounts for the effect of size and shape of a member on creep of concrete [10]
SH	---	loss of prestress due to shrinkage of concrete over time (ksi)
SSF	---	factor that accounts for the effect of size and shaped of a member on concrete shrinkage [10]
UCR	---	ultimate loss of prestress due to creep of concrete, (psi per psi of compressive stress in the concrete) [10]
USH	---	ultimate loss of prestress due to shrinkage of concrete, (psi)
V_{cw}	---	web shear capacity of specimen (kips)
Φ	---	curvature

BIBLIOGRAPHY

1. Aboutaha, Riyad, "Shear Strengthening of Pretensioned Prestressed Concrete Composite Flexural Members," Department of Civil Engineering, The University of Texas at Austin, 1990.

2. ACI Committee 318, "Building Code Requirements for Reinforced Concrete, (ACI 318-83)." American Concrete Institute, Detroit, MI, 1983.

3. ACI Committee 318, "Commentary on Building Code Requirements for Reinforced Concrete (ACI 318-83)." American Concrete Institute, Detroit, MI, 1983.

4. "Compilation of ASTM Standards Relating to Sand and Gravel and Concrete," National Ready Mixed Concrete Association, Publication No. 137, March 1988.

5. Dane, J., III, and Bruce, R. N., Jr., "Elimination of Draped Strands in Prestressed Concrete Girders," Civil Engineering Department, Tulane University. Submitted to the Louisiana Department of Highways, State Project No. 736-01-65, Technical Report No. 107, 1975.

6. Ghosh, S. K. and Fintel, M. "Development Length of Prestressing Strands, Including Debonded Strands, and Allowable Stresses in Pretensioned Members, PCI Journal, September-October 1986, pp.38-57.

7. Horn, D. G., and Preston, H. K., "Use of Debonded Strands in Pretensioned Bridge Members," PCI Journal, July-August 1981, pp. 42-58.

8. Janney, J. R., "Nature of Bond in Pretensioned Prestressed Concrete," ACI Journal, Proceedings V. 50, No.9, May 1954, pp. 717-736.

9. Kaar, P. H., and Magura, D. D., "Effect of Strand Blanketing on Performance of Pretensioned Girders," PCI Journal, V. 10, No. 6, December 1965, pp. 20-34.

10. Lin, T. Y., and Burns, N. H., Design of Prestressed Concrete Structures, Third Edition, John Wiley and Sons, 1981.

11. Lutz, B. A., "Measurement of Development Length of 0.5 Inch and 0.6 Inch Diameter Prestressing Strand in Fully Bonded Concrete Beams," Department of Civil Engineering, The University of Texas at Austin, 1991.

12. Malik, R., "Measurement of Transfer Length of 0.5 Inch and 0.6 Inch Diameter Prestressing Strand in Single Strand Specimens," Department of Civil Engineering, The University of Texas at Austin, 1990.

13. Prestressed Concrete Institute, PCI Design Handbook - Precast and Prestressed Concrete, Third Edition, PCI, Chicago, IL, 1985.

14. Rabbat, B. G., Kaar, P. H., Russell, H. G., and Bruce, R. N., Jr., "Fatigue Tests of Pretensioned Girders with Blanketed and Draped Strands," PCI Journal, July-August 1979, pp. 88-114.

15. "Recommendations for Estimating Prestress Losses," Report of PCI Committee on Prestress Losses, J. Prestressed Concrete Institute, Vol. 20, No. 4, July-August, 1975, pp.43-75.

16. Russell, B. W., Burns, N. H., and Kreger, M., "Development Length and Flexural Bond Behavior of AASHTO-Type Girders with Fully Bonded and Blanketed Strand," Technical Memo 1210-3, Center for Transportation Research, The University of Texas at Austin, March 1991.

17. Unay, I. O., Russell, B. W., Burns, N. H., Kreger, M., "Measurement of Transfer Length of Prestressing Strands in Prestressed Concrete Specimens, " Report 1210-1, Center for Transportation Research, The University of Texas at Austin, March 1991.